2011

ERYTHROPOIESIS IN THE ABSENCE OF ADULT HEMOGLOBIN

Shanrun Liu
University of Alabama at Birmingham

ERYTHROPOIESIS IN THE ABSENCE OF ADULT HEMOGLOBIN

By

SHANRUN LIU

THOMAS M. RYAN, COMMITTEE CHAIR
CHRISTOPHER A. KLUG
ANUPAM AGARWAL
CHING-YI CHEN
TIM M. TOWNES

A DISSERTATION

Submitted to the graduate faculty of The University of Alabama at Birmingham,
in partial fulfillment of the requirements for the degree of
Doctor of Philosophy

BIRMINGHAM, ALABAMA

2011

ERYTHROPOIESIS IN THE ABSENCE OF ADULT HEMOGLOBIN

SHANRUN LIU

BIOCHEMISTRY AND MOLECULAR GENETICS

ABSTRACT

The mammalian erythrocyte is a highly specialized blood cell that differentiates via an orderly series of committed progenitors in the bone marrow in a process termed erythropoiesis. During erythroid development, hemoglobin synthesis increases from early erythroid progenitors to mature enucleated red blood cells (RBCs). Although hemoglobin is the most extensively studied protein in history, the role, if any, that hemoglobin plays in erythroid development remains obscure. In this study, I ask the question what happens during erythropoiesis in the absence of hemoglobin. I demonstrate that my original hypothesis that excess free heme would accumulate in the absence of globin chain production resulting in the early death of erythroid progenitors is incorrect. To test this hypothesis, mouse embryos and embryonic stem (ES) cells that have all their adult α and β globin genes deleted (Hb Null) are generated and the Hb Null ES cells are used to produce Hb Null chimeric mice. I demonstrate that Hb Null embryos are extremely anemic, have a defect in their primitive erythropoiesis, and die in midgestation. Surprisingly, in Hb Null chimeric mice all stages of nucleated definitive erythroid development is normal, and Hb Null erythroid cells can even enucleate and form reticulocytes. Furthermore, the level of total heme in Hb Null erythoblasts is dramatically reduced. In chimeric mice the number of Hb Null reticulocytes is reduced more than 90%. Expression of the heme binding protein, human myoglobin, in Hb Null erythroid cells does not prevent reticulocyte loss. Bone marrow transplantation of donor Hb Null

derived hematopoietic cells into lethally irradiated wild type mice results in reconstituted mice with pure Hb Null derived erythropoietic tissues and up to 1% Hb Null reticulocytes in the peripheral blood. These data suggest that hemoglobin reduction in erythroid cells unlikely causes free heme level elevation. This novel Hb Null model provides a unique experimental system to test future hypotheses on the role played by hemoglobin in erythroid cell enucleation, cytoskeleton maturation, and heme and iron regulation.

Keywords: hemoglobin, erythropoiesis, heme regulation, EKLF, thalassemia

DEDICATION

This thesis is dedicated to my parents, Jiansheng Liu and Yuehua Li, who have given me

so much unconditional love that is better than any words can describe.

This thesis is also dedicated to my wife, Jing Wang, who has always stood by me,

supported me and inspired me.

ACKNOWLEDGMENTS

TABLE OF CONTENTS

LIST OF TABLES

LIST OF FIGURES

LIST OF ABBREVIATIONS

ALAS	5-aminolevulinate synthase
BFU-Es	burst-forming unit-erythroid
CFU-Es	colony-forming unit-erythroid
CMPs	common myeloid progenitors
DBA	Diamond-Blackfan anemia
E	embryonic day
EB	embryoid body
EGFP	enhanced green fluorescent protein
EKLF	Erythroid Krüppel-like Factor
EM	electron microscopy
EpoR	erythropoietin receptor
ES	embryonic stem cell
ES-EP	embryonic stem cell-derived erythroid progenitor
FACS	fluorescence activated cell sorting
FLVCR	feline leukemia virus subgroup C receptor
FPN1	ferroportin1
FSC	forward scatter
GMPs	granulocyte/monocyte-restricted progenitors
GR	gap-repair

Gyp	A glycophorin A
Hb	hemoglobin
Hb Null	homozygous adult α and β hemoglobin gene knockout
HO	heme oxygenase
HR	homologous sequences
HRI	heme-regulated eIF2α kinase
HS	DNase I hypersensitive site
HSC	hematopoietic stem cells
Hygro	hygromycin resistance gene
IREs	iron-responsive elements
IRPs	iron-regulatory proteins
Kan	kanamycin resistance gene
LCR	locus control region
MCHC	mean corpuscular hemoglobin concentration
MEL	murine erythroleukemia
MEP	megakaryocytic-erythroid progenitor
Neo	neomycin resistance gene
PCR	polymerase chain reaction
PHNNEC	pure Hb Null nucleated erythroid cells
PPOX	protoporphyrinogen oxidase
RBC	red blood cell
RFP	red fluorescence protein
ROS	reactive oxygen species

SSC   side scatter

TK   herpes simplex virus thymidine kinase gene

TO   thiazole orange

XLSA   X-linked sideroblastic anemia

INTRODUCTION

The mammalian erythrocyte is a highly specialized blood cell that differentiates via an orderly series of committed progenitors in the bone marrow in a process termed erythropoiesis. In mice and humans, erythropoiesis has been well characterized into "primitive" and "definitive" stages according to their developmental origin, morphology and globin chains expressed. Murine primitive erythropoiesis initiates around embryonic day 7 (E7) in the yolk sac blood islands[1,2] generating large and nucleated primitive erythrocytes that express embryonic α (ζ) and β (βH1and εY) globin chains[3]. These primitive erythrocytes are gradually replaced by smaller enucleated definitive erythrocytes that arise from the fetal liver beginning around E9.5[4]. Definitive erythrocytes begin to exit the fetal liver into the circulation between E11.5 and 12.5, becoming the predominant erythroid cells in the fetal blood by E14.5 and into adult life[5]. Definitive erythroid cells produce adult α (α1 and α2) and β (β^{major} and β^{minor} or β^s and β^t) globin chains[3,6,7]. After birth, the site of hematopoiesis shifts to the bone marrow. Adult definitive erythrocytes are derived from hematopoietic stem cells (HSC) in the bone marrow after a series of asymmetric cell divisions. The first committed erythroid progenitors are called burst-forming unit-erythroid (BFU-Es) because of their ability to generate large colonies *in vitro* in defined semisolid media with erythroid cytokines[8,9]. BFU-Es give rise to colony-forming unit-erythroid (CFU-Es)[10,11] which undergo several mitotic divisions and differentiate to four sequential stages of erythroblasts, including

1

pro-, basophilic, polychromatic and orthochromatic erythroblasts[12] (Figure 1). Erythroblasts progressively decrease in size, accumulate hemoglobin, condense their nuclei and finally enucleate to form reticulocytes (Figure 1). Reticulocytes reside in the bone marrow for several days where they degrade their cytosolic organelles and mature their cytoskeleton before exiting the bone marrow into the peripheral blood. Reticulocytes can be identified in the circulation by the continued presence of cytoplasmic RNA until they become fully mature red blood cells (RBCs) after about 2 days when all the RNA is degraded. RBCs represent approximately 25% of the total number of cells of the body and normal bone marrow erythropoiesis generates about 1% of the body's total RBCs daily.

In mature erythrocytes, over 95% of the cytosolic protein is hemoglobin, a tetramer composed of two α and two β globin chains, that is responsible for transporting oxygen throughout the body. In order to cope with the enormous mechanical and metabolic stress encountered in the blood vessels, erythrocytes possess marvelous properties to maintain their cellular deformability and stability. Erythrocyte viscosity, mainly determined by hemoglobin content, is one of the key factors contributing to those properties[13]. Another determinant is the unique red cell cytoskeleton that is a hexagonal latticework formed by spectrin tetramers associated with F-actin, adducin, tropomodulin, tropomyosin, and dematin. The RBC cytoskeleton is connected to the cell membrane integral proteins, such as band 3 and glycophorin, via either an ankyrin-based or protein 4.1R-based macromolecular complexes[13-16].

There is substantial evidence showing that hemoglobin can interact with the erythrocyte membrane[17-19] and this interaction may be important for the maintenance of RBC

flexibility. Specifically, hemoglobin can promote spectrin tetramer formation by excluding water from spectrin and thus increasing the effective concentration of spectrin, and also by its electrostatic interaction with spectrin[20]. Also, deoxyhemoglobin may interact with actin and tubulin present in the cytoskeleton within nucleated erythroid cells through its polyanion-binding nature[21]. Furthermore, numerous studies have shown an interaction between hemoglobin and band 3, a major erythroid membrane protein[22-25], and recent data revealed that deoxyhemoglobin can bind to residues 12-23 of band 3[26]. During the final steps of erythrocyte enucleation and maturation, the hemoglobin content continues to increase as the cytoskeleton is radically changed and remodeled in order to meet the shear stress demands in the circulation[27-32]. Interactions between hemoglobin and the maturing cytoskeleton raise the possibility that besides functioning as an O_2 carrier, hemoglobin may play a critical role in erythrocyte development/maturation. One possible way to investigate this possibility is to study developing erythroid cells in the absence of hemoglobin.

Hemoglobin is a hemoprotein. Each α and β chain contains a heme prosthetic group that provides the binding site for O_2. Heme is a ferrous iron-protoporphyrin IX complex, and is essential for all living aerobic organisms. In erythroid cells, heme also positively regulates hemoglobin expression by blocking DNA binding of transcriptional repressor Bach1[33], and by inactivating the translational inhibitor of heme-regulated eIF2α kinase (HRI)[34]. Heme deficiency can cause a variety of erythroid diseases, such as X-linked sideroblastic anemia (XLSA)[35] and erythropoietic protoporphyria[36]. However, in excess, free heme is also toxic, due to its potential to generate reactive oxygen species (ROS) via the iron-mediated Fenton reaction[37]. Erythroid cells regulate cytosolic free heme level by

balancing heme biosynthesis which is controlled by iron absorption[38], heme utilization by hemoglobin, heme degradation by heme oxygenase (HO)[39], and heme export out of cytoplasm by the heme exporter, feline leukemia virus C receptor (FLVCR)[40] (Figure 2). Owing to its great abundance, hemoglobin is the major force for the detoxification of free heme in erythrocytes. Previous studies have shown that inhibition of globin synthesis in reticulocytes can lead to an increase in free heme in both the cytosol and mitochondria[41,42]. The contribution of HO in erythroid cells is probably not critical since the differentiation of murine erythroleukemia (MEL) cells is associated with a reduction in HO mRNA levels[43]. Of note, FLVCR deficiency blocks erythroid development at the proerythroblast stage, resembling human Diamond-Blackfan anemia (DBA)[44]. Moreover, DBA familial association studies have independently identified several different mutated ribosomal proteins that were linked to the anemia in DBA[45-47]. Hence, it was proposed that delayed hemoglobin translation could result in a relative increase in free heme causing oxidative stress and hemolysis to erythroid progenitors and the anemic phenotype in DBA[44,48] (Figure 2). The availability of an experimental erythroid model system that is devoid of all globin chains could rigorously test whether excess intracellular heme would be toxic to erythroid progenitors.

In erythroid cells, a deficiency of either α or β globin chains of hemoglobin results in α or β thalassemia, respectively. The severe forms of α and β thalassemia are Bart's hydrops fetalis syndrome and Cooley's anemia (also called β-thalassemia major), respectively[49]. In Bart's hydrops fetalis syndrome, the fetus lacks all α globin genes. Functional embryonic hemoglobins, hemoglobin Gower 1 ($\zeta_2\varepsilon_2$) and hemoglobin Portland ($\zeta_2\gamma_2$), are responsible for oxygen delivery in early gestation. A hemoglobin switch from embryonic

4

hemoglobin to fetal hemoglobin ($\alpha_2\gamma_2$) occurs around 8 weeks of gestation. Due to the absence of α globin chains, fetal hemoglobin cannot be produced and excess γ globin chains form Bart's hemoglobin (Hb Bart's), a γ globin tetramer (γ_4)[50]. Hb Bart's is non-functional and relatively unstable, and can precipitate and cause shortened life span of erythroid cells. Fetuses with Bart's hydrops fetalis become hydropic in the 2nd and 3rd trimester and die *in utero* or shortly after birth. In Cooley's anemia, the adult β globin production is absent or greatly diminished. Fetal hemoglobin $\alpha_2\gamma_2$ can support fetuses to survive after birth until γ globin is switched off and adult hemoglobin, HbA ($\alpha_2\beta_2$), and minor adult, HbA2 ($\alpha_2\delta_2$), are expressed thereafter. In the absence of β globin chains, the unpaired excess α globin chains aggregate and precipitate causing deleterious effects to the erythrocyte membrane and cytoskeleton[51,52]. In Cooley's anemia, erythroid progenitor cells die in the bone marrow (ineffective erythropoiesis) and β thalassemic RBCs lyse in the peripheral blood (intravascular hemolysis). Patients suffering from this disorder require regular blood transfusions for survival beginning early in their second year of life.

In this dissertation using mouse models of α and β thalassemia[53-56], I generate mouse embryos and erythroid cells with all of the adult hemoglobin genes (α and β) deleted. As these erythroid cells cannot produce any adult hemoglobin, I have labeled them "Hb Null". These Hb Null embryos and Hb Null erythroid cells provide a model system for studying the most severe form of compound thalassemia that is devoid of both α and β globin chains. Rare Hb Null embryos may occur in nature from the progeny of parents with compound α and β globin thalassemia minor; though, these fetuses have not been described, likely because they do not survive long *in utero* due to extreme anemia.

I hypothesize that hemoglobin is not only important for O_2 delivery, but also important for erythroid development. In the absence of adult hemoglobin, I predict that Hb Null embryos will die early *in utero* due to extreme anemia. Hb Null primitive erythropoiesis will be compromised, since adult α globin chains are normally expressed in primitive erythroid cells. Additionally, developing Hb Null definitive erythroid cells will be blocked at the early erythroid progenitor stage from the toxicity of excess unbound free heme generated by the absence of globin chains.

To test these hypotheses, I studied Hb Null erythropoiesis *in vitro* and *in vivo*. In Chapter 1 I investigated Hb Null primitive and definitive erythropoiesis *in vivo* in developing fetuses produced by crossbreeding genetically engineered globin gene knockout mice. Because Hb Null embryos died early in development making it impossible to follow all stages of definitive erythroid cells, Hb Null ES cell lines (m$\alpha^{0/0}$m$\beta^{0/0}$) were generated for study. In Chapter 2, I describe the generation of Hb Null ES cell lines from Hb Null embryos. These Hb Null ES cells were used to produce Hb Null definitive erythroid cells in an *in vitro* culture system (Chapter 2). To study definitive Hb Null derived erythroid cells *in vivo*, I injected Hb Null ES cells into wild type mouse blastocysts and produced Hb Null chimeric mice (Chapter 3). In order to follow Hb Null erythroid cells in chimeras, the erythroid specific transcriptional factor, Erythroid Krüppel-like Factor (EKLF), was tagged with enhanced green fluorescent protein (EGFP) in Hb Null ES cells, and EGFP-EKLF Hb Null chimeric mice were produced and analyzed (Chapter 3). However, EKLF is only expressed in nucleated erythroid cells, and all enucleated erythroid cells are negative for its expression. In order to follow enucleated Hb Null erythroid cells in chimeras, a red fluorescence protein, mCherry, was targeted to downstream of the mouse

β^{major} globin promoter in Hb Null EGFP-EKLF ES cells, and mCherry Hb Null chimeric mice were produced and analyzed (Chapter 4). Due to the interference of wild type erythroid cells in chimeras, Hb Null erythroid cells cannot be examined in situ in tissues like spleen or bone marrow. In an attempt to generated adult mice with pure Hb Null erythroid cells, I sorted Hb Null HSCs and transplanted them into lethally irradiated wild type mice. Hb Null erythroid development in these transplanted mice was analyzed (Chapter 5). To examine the role of free heme toxicity in Hb Null erythroid development (Chapter 6), the non-erythroid heme binding protein, human myoglobin, was tagged with mCherry and knocked into the mouse β globin locus driven by the mouse β^{major} globin promoter in Hb Null ES cells. Hb Null erythroid cells expressing human myoglobin were analyzed in chimeric mice. Additionally, factors involved in heme and iron regulation were examined at the transcriptional level in Hb Null erythroid cells and compared with wild type erythroid cells (Chapter 6).
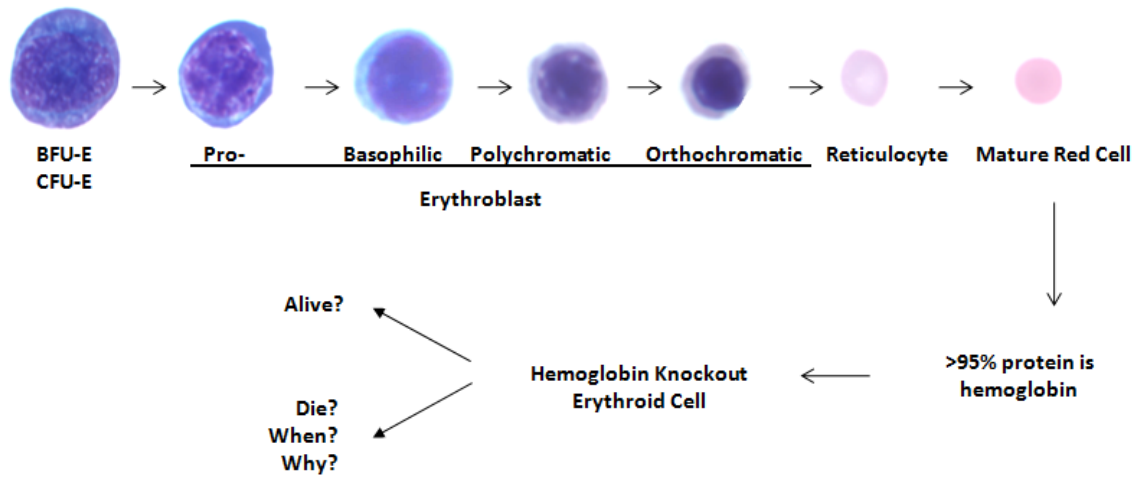
Figure 1. Different stages of erythroid cells. The first committed erythroid progenitor is BFU-E. In bone marrow, BFU-Es differentiates to CFU-Es. CFU-Es differentiate to four successive erythroblasts, including proerythroblasts, basophilic erythroblasts, polychromatic erythroblasts and orthochromatic erythroblasts. Orthochromatic erythroblasts enucleate and form reticulocytes. Reticulocytes then enter peripheral blood and terminally mature to red blood cells. In mature red cells, over 95% protein is hemoglobin, consisting of two α chains and two β chains. Each globin chain contains a heme prosthetic group. In this project, I ask the question that in the absence of hemoglobin, how erythroid cells develop, whether they can still be alive or they will die, and if they die, at what developing stage and why they die.
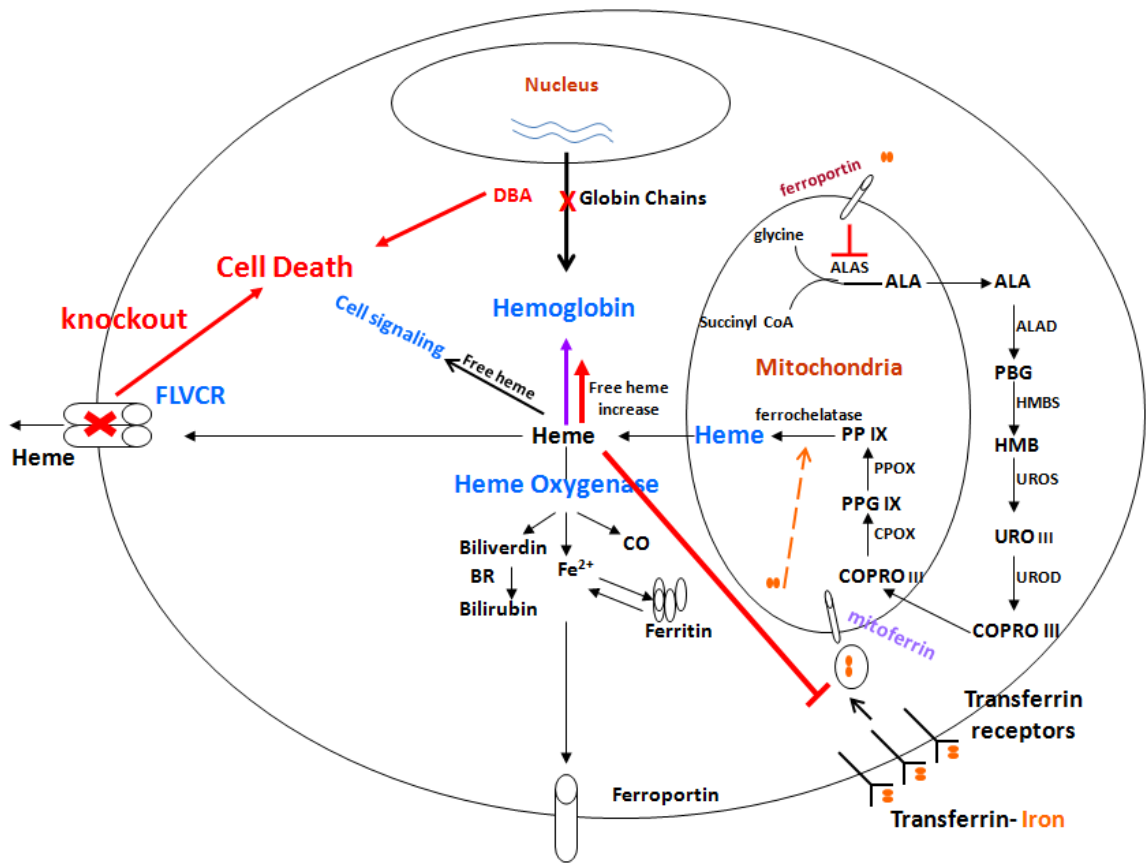
Figure 2. Intracellular free heme level control in erythroid cells. Free heme is synthesized and transported from mitochondria. In cytoplasm, free heme can be degraded by heme oxygenases[39], exported out of cells by FLVCR[40], or bind to globin chains to form hemoglobin. The rest intracellular free heme serves as a signal molecule regulating protein transcription and translation. Excess free heme is toxic to cells and can cause cell death[37]. Elevated free heme can inhibit iron absorption, and the iron limitation can further inhibit ALAS2 enzyme translation to decrease heme biosynthesis[38]. However, this negative feedback control may not be strong enough to reduce free heme to a normal level, since FLVCR knockout erythroid cells were blocked at proerythroblast stage by excess free heme[44]. The inhibition of globin synthesis in reticulocytes can result in free heme elevation[41,42]. It is proposed that in DBA disease, ribosome protein mutation cause the reduction of globin chain synthesis leading to intracellular free heme increase that kills erythroid cells at CFU-E/proerythroblast stage[44,48]. In this project, all adult hemoglobin genes were deleted and the role of free heme toxicity in erythroid development was examined.

CHAPTER 1

HB NULL EMBRYOS DIE IN MIDGESTION AND HAVE DEFECTIVE PRIMITIVE

ERYTHROPOIESIS

Because definitive erythroid cells solely express adult globin chains, one would expect that the deletion of adult mouse α and β globin genes would have a major effect on definitive erythropoiesis. However, what is the effect of the absence of the adult globin genes on primitive erythropoiesis? Primitive erythroid cells predominantly express embryonic β-like globin chains, but also express small amounts of the adult β globin gene[57]. More importantly, primitive erythroid cells express high levels of the adult α globin genes as the switch from embryonic ζ globin to the adult α globin genes occurs very early in development during primitive erythropoiesis. Also, definitive erythroid cells begin entering the peripheral blood from the fetal liver around E12.5 and function as the predominant cell for O_2 delivery from E14.5 onward[5]. Thus, the absence of adult hemoglobin may not only influence definitive erythropoiesis, but also affect primitive erythroid cells and early embryo development. To address these issues, I generated Hb Null mouse embryos that have all their adult globin genes deleted, and examined primitive erythropoiesis *in vivo* in the developing fetuses.

In order to generate Hb Null embryos and fetuses I interbred knockout-transgenic mice having doubly heterozygous or homozygous adult α and β globin gene knockouts with or

without human globin transgenes[54,56,58] together to generate Hb Null embryos (Table 1 and Figure 3,4). The gestational age of each embryo was determined from visualization of a vaginal plug with the morning after breeding designated E0.5. The genotype of each embryo was determined by PCR of embryo DNA using primers that differentiate wild type and knockout mouse α and β globin alleles and human globin transgenes (see Methods). Hb Null embryos were examined from E11.5 to E13.5 (Table 1). At E13.5, I did not find any viable Hb Null embryos, and at E12.5, only one third of Hb Null embryos were still alive as determined by the visualization of a beating heart. Although these Hb Null embryos appeared grossly normal in form and only slightly reduced in size, they were extremely pale and had a much smaller fetal liver, indicating that they had extreme anemia and their definitive erythropoiesis is severely impaired (Figure 4). At E11.5, Hb Null embryos were identified close to their expected Mendelian ratio, and their survival rate went up to 50% (3 out of 6 embryos), suggesting that most Hb Null embryos died between day 10.5 and day 12.5 (Table 1). This range in the age of death could be caused by genetic variations among the embryos.

Table 1 Hb Null Embryos Die in Midgestation

Hb Genotype of Breeding mice α/α β/β	Embryo Age (day)	Litter Number	Embryo Number[a]	Expected Hb Null Embryos	Hb Nul Embryos Alive/Total
Hb Null: 1/8 of embryos					
S3[b] 0/+ 0/0[c]					
X	11.5	1	11	1	0/1
S3 0/0 0/0					
Hb Null: 1/16 of embryos					
0/+ 0/+	11.5	7	52	3	1/3
X	12.5	21	147	9	2/4
0/+ 0/+ or S3 0/+ 0/0 or S3 0/0 0/+	13.5	9	37	2	0/3
Hb Null: 1/32 of embryos					
0/+ 0/+ or S3 0/+ 0/0 or S3 0/0 0/+	11.5	7	51	1~2	2/2
X	12.5	3	22	0~1	0/2
S3 0/+ 0/+	13.5	3	17	0~1	0

a: Number includes both living and dead embryos, but not reabsorbed embryos, which cannot be genotyped due to the contamination by maternal tissues.

b: "S3" means hemizygous human sickle globin transgene line 3[58].

c: "+" means wild type allele, and "0" means knockout allele.
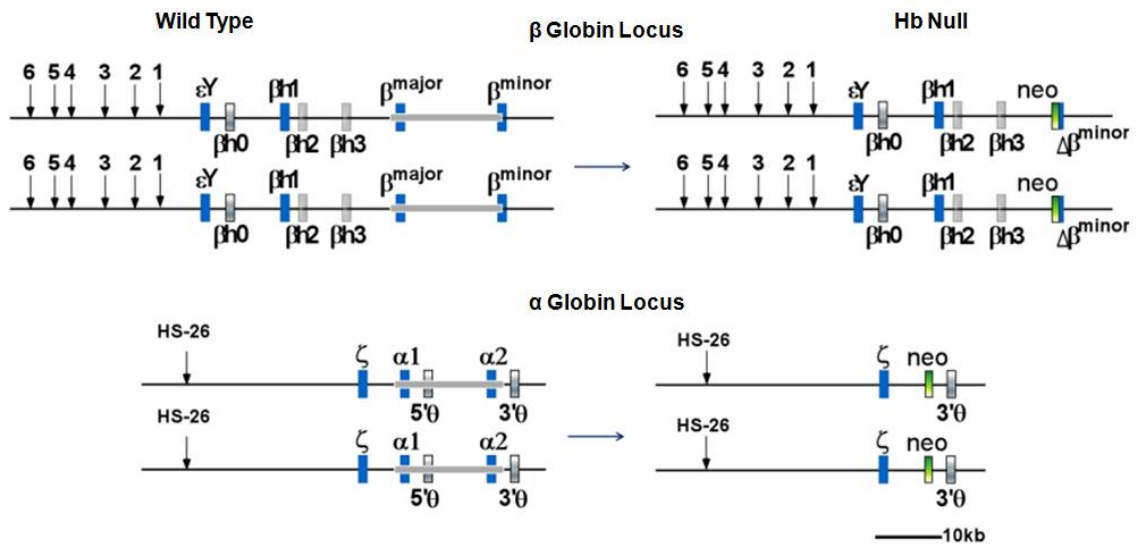
Figure 3. Schematic representation of the mouse α and β globin gene loci of Hb Null embryos and ES cells[54,56,58]. Deleted sequences are highlighted by thick gray lines. Arrows indicate DNase I hypersensitive sites in the locus control region. Δβ^{minor} represents the 3' part of the β^{minor} globing gene sequence that remains after knockout. Neo is neomycin resistance gene.
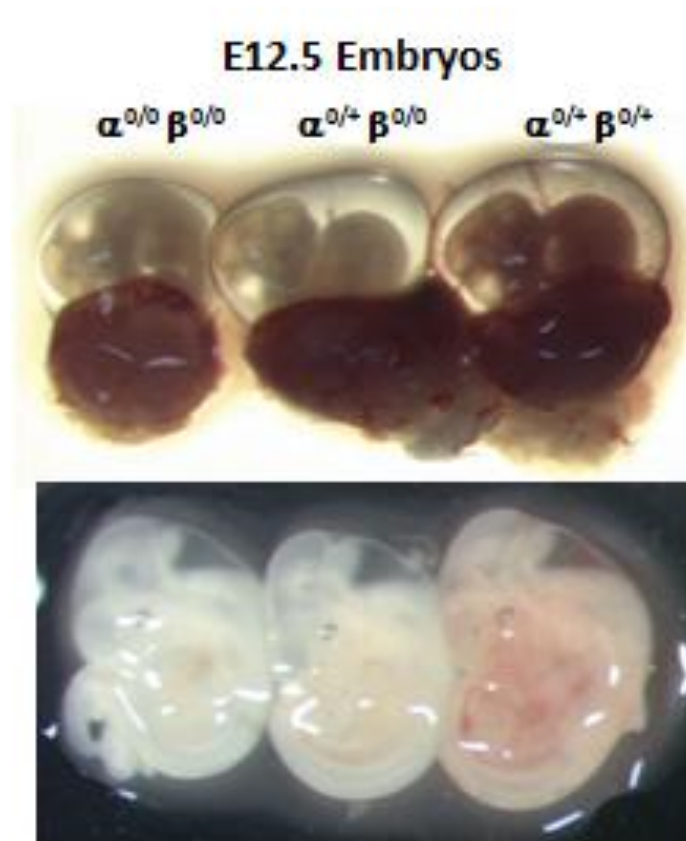
Figure 4. Viable E12.5 mouse embryos from one litter.

Studies have shown that primitive erythroid cells predominate in circulation until E12.5[5]. Hb Null embryos dying before this time point led us to suspect their primitive erythropoiesis may be influenced by deletion of the adult globin genes. I examined Hb Null primitive erythroid cells at E11.5 collected from cord blood, and found that the ratio of cytoplasm to nucleus in these cells is greatly reduced compared to that of wild type primitive erythroid cells (Figure 5). The cytoplasm of Hb Null primitive erythroid cells is less dense and more basophilic, and their nuclei appear less condensed and less granular than those of wild type (Figure 5). These results suggest that on average the Hb Null primitive erythroid cells remain in a less differentiated state and that their terminal maturation is evidently arrested, which is not surprising given that significant amounts of adult α globin chains need to be expressed in wild type primitive erythroid cells[57].
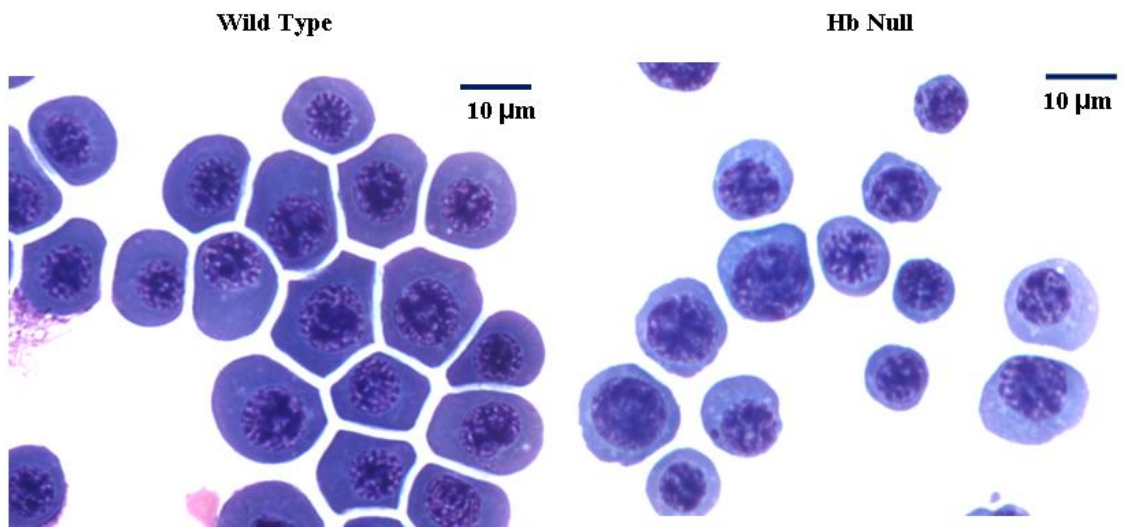
Figure 5. Cytospin and DipQuick staining of primitive erythroid cells from cord blood of

E11.5 wild type and Hb Null embryos.

In summary, by generating and studying Hb Null mouse embryos, I found that in deletion of the adult globin genes, mouse embryos died in midgestation between E10.5 and E12.5 due to extreme anemia, and that primitive erythropoiesis is compromised, exemplified by primitive erythroid cells showing less mature morphology. The effect of the absence of adult hemoglobin for definitive erythroid cells is discussed in the following chapters.

CHAPTER 2

ADULT HEMOGLOBIN IS NOT REQUIRED FOR ERYTHROID COMMITMENT

AND EARLY ERYTHROID PRECURSOR DEVELOPMENT

Globin and other lineage specific genes have been reported to be promiscuously expressed in hematopoietic stem cells and multipotent progenitors[59,60], and lineage commitment involves selectively consolidating the expression of lineage-relevant genes and abrogating the others[61]. During definitive erythropoiesis, hemoglobin content increases with erythroid terminal differentiation. Although hemoglobin is well known for its O_2 delivery function, its importance in erythroid lineage commitment, differentiation, and maturation is not clear. To address these issues, I examined definitive erythroid cells produced *in vivo* in developing embryos and also *in vitro* after the directed differentiation of Hb Null ES cells to the erythroid lineage.

In vivo definitive erythropoiesis was examined in the same Hb Null embryos that were studied in Chapter 1. Even though the majority of Hb Null embryos were dead by E11.5 due to defective primitive erythropoiesis, there were some viable E11.5 to E12.5 Hb Null embryos that could be studied. In E11.5 Hb Null embryos, the fetal liver was greatly reduced in size and cell number, but typical erythroid lineage precursor cells could be readily identified by their morphology on fetal liver cytospin slides (Figure 6), indicating that the adult globin genes are not required for definitive erythroid lineage commitment. However, the increased appearance of vacuoles in the Hb Null erythroid cell cytoplasm

implies more cells are dying at this stage compared to age-matched wild type fetal liver
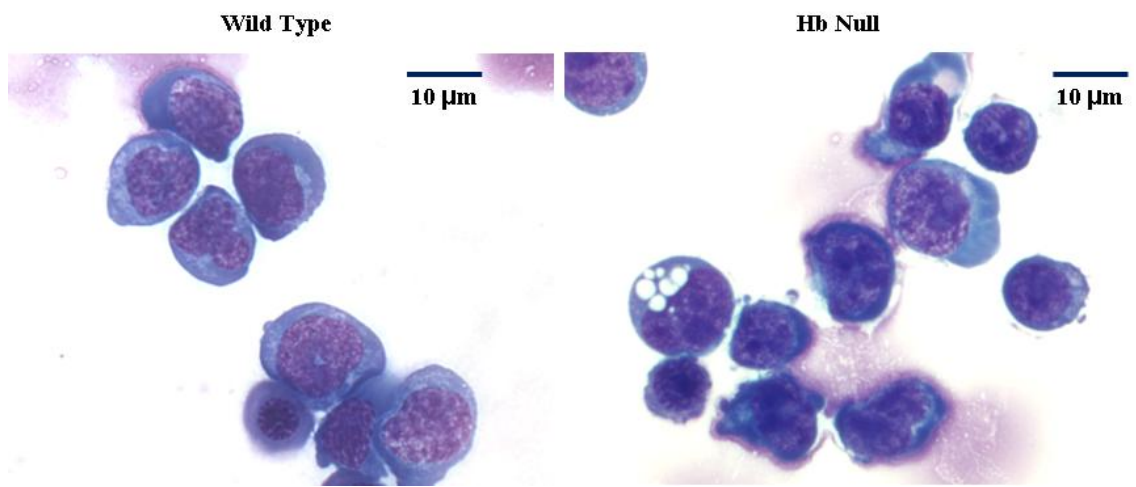
cells.

Figure 6. Cyospin and DipQuick staining of E11.5 dissociated fetal liver cells from wild type and Hb Null embryos.

I further analyzed fetal liver erythroid cells by Fluorescence Activated Cell Sorting (FACS) by staining dissociated cells with fluorescently labeled antibodies to the transferrin receptor CD71, and the erythroid specific antigen Ter119 (Figure 7). The staining pattern of these two antigens has been generally used to discriminate different developmental stages of erythroid cells[62,63]. The majority of E12.5 wild type fetal liver cells (82%) are Ter119+ and CD71^{hi}, which corresponds to proerythroblasts and basophilic erythroblasts. Doubly heterozygous mouse α and β globin knockout ($α^{+/0} β^{+/0}$) E12.5 fetal liver cells have a similar FACS profile, indicating that a balanced deficit in hemoglobin chain synthesis is not harmful for erythroid development. However, in the complete absence of adult hemoglobin, the number of Ter119+ and CD71^{hi} erythroid cells is markedly decreased (31%) with most cells (56%) accumulated at the Ter119 negative stage (Figure 7). Thus while Hb Null embryos can commit to the definitive erythroid lineage (Ter119+), there is a block in differentiation at the pro-/basophilic erythroblast stage in fetal liver erythropoiesis. Unexpectedly, fetal liver erythroid cells isolated from E12.5 embryos with a single α globin allele ($mα^{+/0} mβ^{0/0}$) exhibit an even worse impairment than Hb Null erythroid cells, with only 17% cells at Ter119+ and CD71^{hi} stage, which is likely caused by the toxicity of excess α globin chain precipitates[52]. I also observed a small population of Ter119+CD71^{low} cells (5~8%) in both Hb Null fetal liver and single α globin allele fetal liver which are not present in the wild type fetal liver FACS plot. I speculate that these cells are primitive erythroid cells that become enriched in the fetal liver due to the relatively low numbers of definitive erythroid cells. Interestingly, erythroid cells with a single β globin allele ($mα^{0/0} mβ^{+/0}$) display very normal development with no obvious block at above mentioned stage. Excess β globin

chains can a form β4 tetramer, which is more stable and soluble than unpaired α globin chains[64]. My data suggest that these excess β globin chains are beneficial for erythroid cell development compared to cells without any globin chains or cells with an excess of α globin chains.
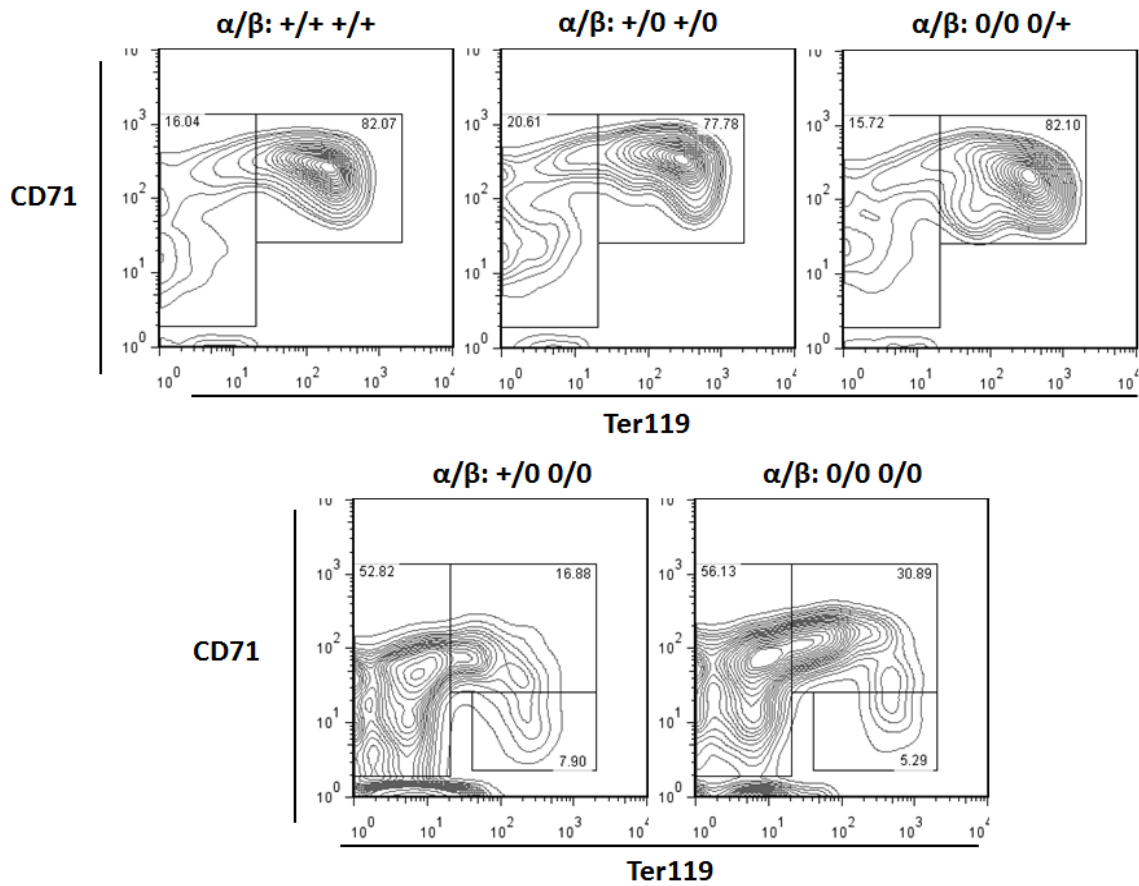
Figure 7. FACS analysis of fetal liver cells from viable E12.5 mouse embryos stained by CD71 and Ter119. Dead cells were gated out by 7AAD.

Although the above data suggest that Hb Null definitive erythroid cells were blocked at early precursor stage, we could not rule out the possibility that this block was the indirect result of severe anemia that might impair the fetal liver microenvironment. To further explore this issue, Hb Null ES cell lines ($m\alpha^{0/0} m\beta^{0/0}$) (Figure 3) were established from embryos made by breeding knockout-transgenic human adult hemoglobin A mice (HbA $m\alpha^{0/0} m\beta^{0/0}$) with knockout-transgenic human sickle hemoglobin S mice (HbS $m\alpha^{0/0} m\beta^{0/0}$) (Figure 8). One Hb Null ES cell line was confirmed to have a normal karyotype (Figure 9) and possessed the ability to generate 100% ES cell derived embryos (Figure 10) by tetraploid embryo complementation[65] or eight-cell stage embryo microinjection[66] though these embryos also died around E11.5 similar to the natural mating results described in Chapter 1. This Hb Null ES cell line was used for the *in vitro* and *in vivo* experiments described below and in later Chapters.

mα$^{+/+}$ mβ$^{+/+}$

Inject DNA containing human
adult α1 and Sickle β or wt β

mα$^{+/+}$ mβ$^{+/+}$ mα$^{+/+}$ mβ$^{+/+}$ HbS mα$^{+/+}$ mβ$^{+/+}$

mα$^{+/0}$ mβ$^{+/+}$ mα$^{+/+}$ mβ$^{+/0}$

HbS mα$^{+/+}$ mβ$^{+/0}$

HbS mα$^{+/0}$ mβ$^{+/0}$ HbS mα$^{+/0}$ mβ$^{+/0}$

HbS mα$^{0/0}$ mβ$^{0/0}$ HbA mα$^{0/0}$ mβ$^{0/0}$

Genotypes of ES cell lines {
HbS HbA mα$^{0/0}$ mβ$^{0/0}$
HbS mα$^{0/0}$ mβ$^{0/0}$
HbA mα$^{0/0}$ mβ$^{0/0}$
mα$^{0/0}$ mβ$^{0/0}$ (Null Hb)
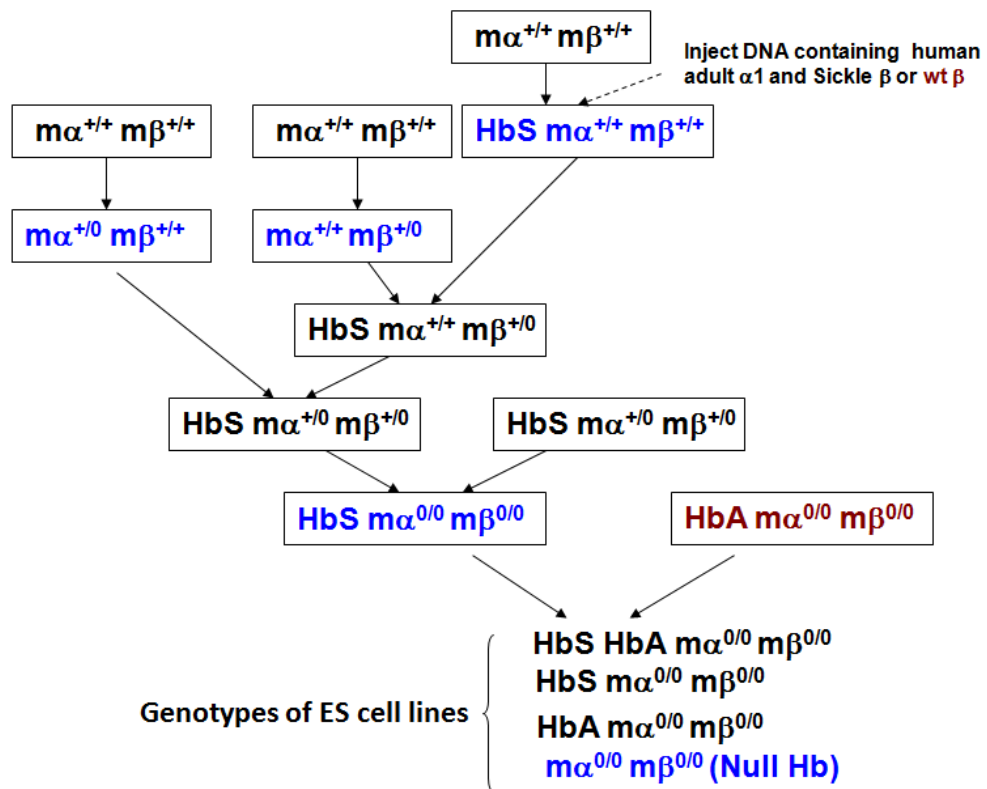
Figure 8. Breeding strategy used to generate Hb Null ES cell lines[54,56,58].
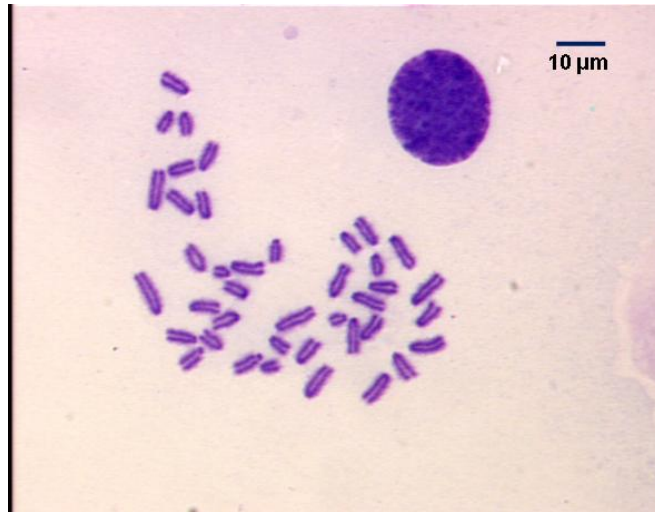
Figure 9. Hb Null ES cells have normal chromosome number.
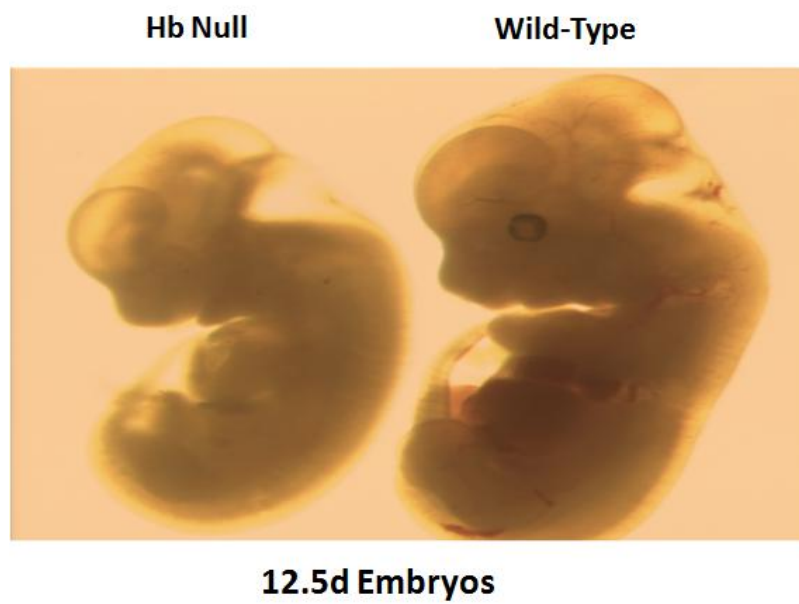
Figure 10. Hb Null embryos cloned from Hb Null ES cells by tetraploid complementation.

Hb Null ES cells were *in vitro* differentiated into definitive erythroid progenitor (ES-EP) cells as described previously[67] with some modification (see methods). Realtime PCR analysis of ES-EP cultures revealed that only erythroid lineage-affiliated genes were expressed, such as glycophorin A (GypA), erythropoietin receptor (EpoR), and Erythroid Krüppel-like Factor (EKLF), while genetic markers of other hematopoietic lineages were not expressed, such as c-mpl, CEBPα, GATA3, and PAX5, indicating this culture was purely erythroid (Table 2). Adult α and β globin genes were expressed in ES-EPs derived from wild type CCE ES cells[68] but not in Hb Null ES-EPs. Based upon their morphology and antigen staining, the majority of cells in the wild type CCE ES-EP cultures were at the proerythroblast stage of development along with a few basophilic erythroblasts (Figures 11, 12). I found Hb Null ES-EPs also exhibited normal proerythroblast morphology (Figure 11) and exhibited a similar Ter119 and CD71 FACS profile as the wild type CCE ES-EPs (Figure 12), suggesting Hb Null erythroid cells can develop normally at least to the proerythroblast stage.

Table 2: Realtime PCR Analysis of ES-EP Cells

Gene	Hb Null ES-EP	Wild Type CCE ES-EP	C57BL/6 Mouse Bone Marrow	Wild Type CCE ES	Specificity
beta-actin	100.0	100.0	100.0	100.0	Normalizer
β globin	0.0	7167.0	3279.3	0.0	definitive
α globin	0.0	5354.1	1967.2	0.1	definitive
βh1 globin	2.7	0.7	0.0	0.0	primitive
εy globin	4.9	0.3	0.0	0.0	primitive
EKLF	44.3	37.6	2.5	0.0	erythoid
GypA	28.3	26.0	5.3	0.0	erythoid
EpoR	15.8	12.3	1.2	0.2	erythoid
Gata1	22.8	26.5	0.8	0.1	erythoid
Tal1	18.7	9.5	1.5	0.1	erythoid
Gata2	1.4	2.0	0.6	0.1	erythoid
NF-E2	3.0	4.3	0.6	0.3	megakaryocyte
c-mpl	0.0	0.0	0.1	0.0	megakaryocyte
CD41b	0.5	0.4	0.3	0.1	megakaryocyte
CEBPa	0.0	0.0	2.4	0.2	myeloid
IL3Ra	0.0	0.0	0.2	0.0	myeloid progenitor
GATA3	0.0	0.0	0.3	0.3	T cell
PAX5	0.0	0.0	2.8	0.0	B cell
IL7R	0.1	0.0	1.1	0.0	Lymphoid
VE-Cadherin	0.0	0.0	0.1	0.0	Endothelial
flk1	0.0	0.0	0.0	0.0	Endothelial
Brachyury	0.0	0.0	0.0	0.0	Mesoderm
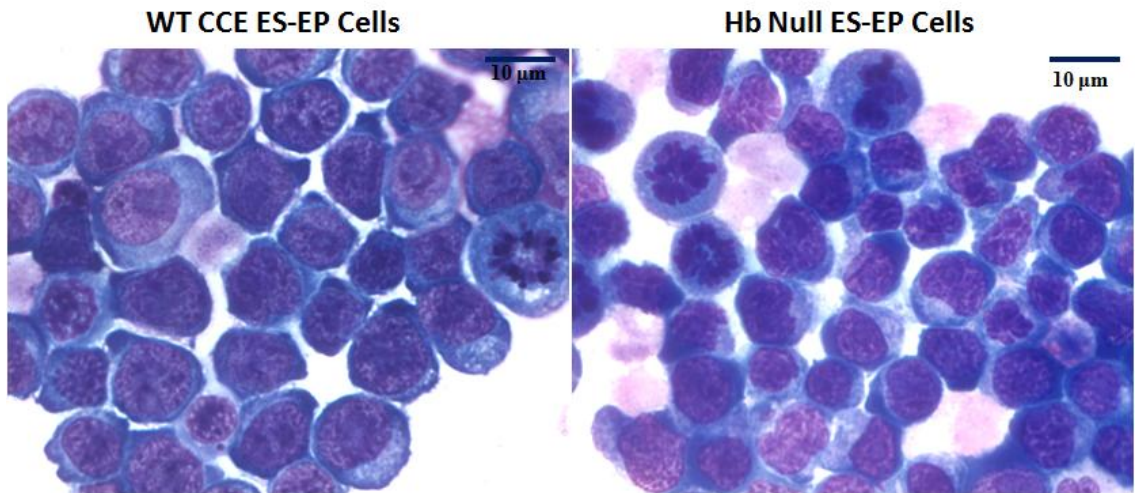
Figure 11. Cytospin and DipQuick staining of wild type CCE and Hb Null ES-EP cells.
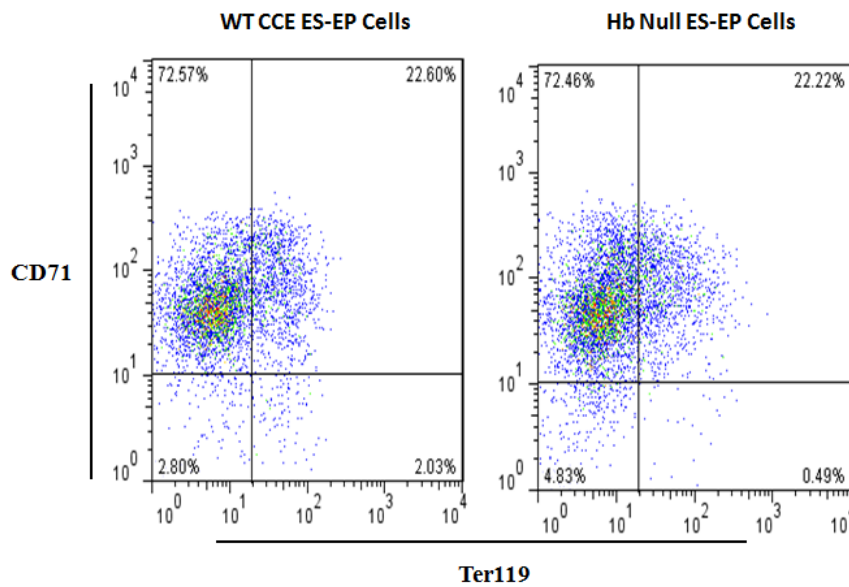
Figure 12. FACS analysis of wild type CCE and Hb Null ES-EP cells stained by CD71 and Ter119. Dead cells were gated out by 7AAD.

To investigate Hb Null erythroid cell development beyond the proerythroblast stage, I analyzed Hb Null ES-EP cultures after their terminal differentiation. Hb Null proerythroblasts were homogeneously purified from ES-EP cultures by removing the Ter119+ cells[69] and placing the remaining Ter119- erythroblasts into terminal differentiation media modified from a previous protocol[67](see methods). Upon terminal differentiation, the Hb Null proerythroblasts become Ter1119+; however the majority of the culture underwent apoptosis by 48 hours (7AAD-, Annexin V+) and were dead (7AAD+) by 72 hours (Figure 13). By contrast, the majority of wild type CCE proerythroblasts could survive the terminal differentiation process (7AAD-, Annexin V-, Figure 13).

The above *in vitro* differentiation experiments suggest that Hb Null derived erythroid cells die upon terminal differentiation beyond the proerythroblast stage. However, I found the terminal differentiation culture was not optimal for erythroid development, as CD71 expression did not decline on maturing cells and only a few cells could extrude their nuclei. Similar problems for *in vitro* culture have been described by other groups[63,70]. So at this point, we were unable to determine whether this developmental block accurately represents true Hb Null erythroid cells development. To clarify this issue, I sought to study Hb Null erythroid cells *in vivo* in adult chimeric mice.
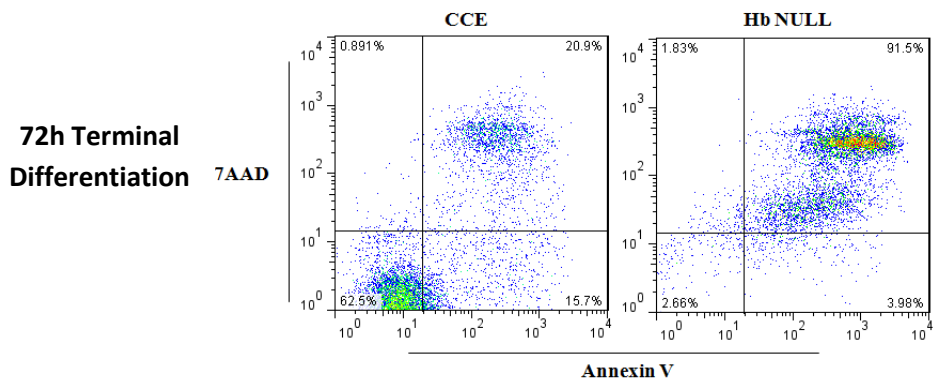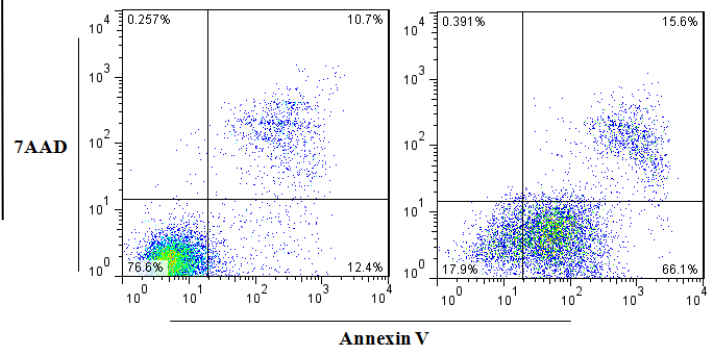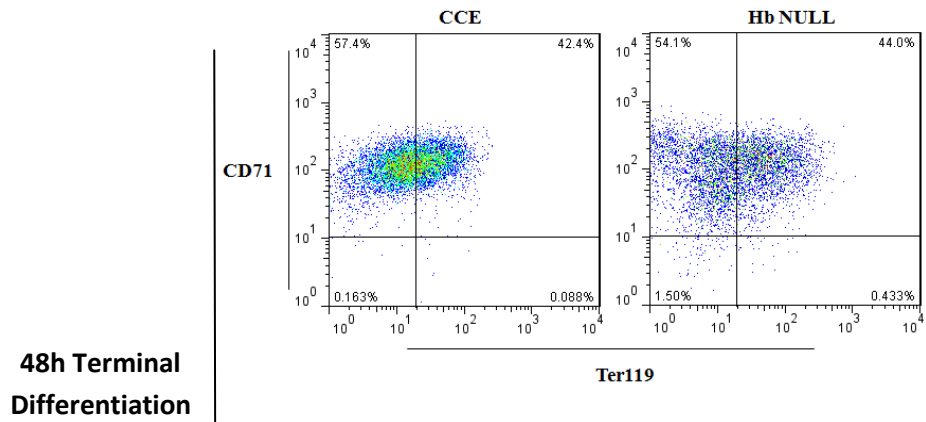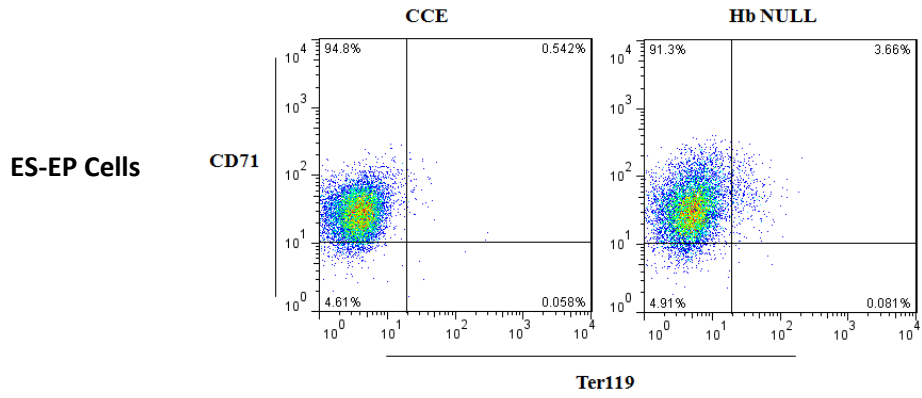
Figure 13. Upon terminal differentiation, Hb Null ES-EP cells die through apoptosis. Ter119 negative wild type CCE ES-EP and Hb Null ES-EP cells (top two plots) were cultured in erythroid terminal differentiation media. Most Hb Null ES-EP cells underwent apoptosis by 48 hours (7AAD-, Annexin V+) (middle four plots) and were dead (7AAD+) by 72 hours (bottom two plots).

In summary, the existence of definitive erythroid precursors in Hb Null fetal liver indicated that adult hemoglobin is not required for definitive erythroid lineage commitment. This was further confirmed by the ability of Hb Null ES cells to differentiate into erythroid progenitor cells *in vitro*. Analyses of definitive Hb Null erythroid development *in vivo* in the fetal liver and *in vitro* in ES-EP terminal differentiation cultures suggested that Hb Null erythroid cells were arrested beyond proerythroblast stage. However, this arrest could result from an indirect effect of severe anemia in the early embryos or due to non-optimal *in vitro* culture conditions instead of from a direct effect of the absence of hemoglobin. This issue will be clarified in the following chapters.

CHAPTER 3

ADULT HEMOGLOBIN IS NOT ESSENTIAL FOR DEFINITIVE NUCLEATED ERYTHROID DEVELOPMENT

The study of Hb Null definitive erythropoiesis in the early embryo or after *in vitro* differentiation of ES cells demonstrated clear defects in their development, but would adult bone marrow Hb Null definitive erythropoiesis also be affected? In the absence of adult hemoglobin, Hb Null embryos die too early in development due to defective primitive erythropoiesis and anemia, making it impossible to fully analyze definitive erythropoiesis. Although Hb Null ES cells can be differentiated into definitive erythroid cells *in vitro*, the early differentiation block observed beyond the proerythroblast stage during terminal differentiation in culture may not accurately reflect what occurs *in vivo*. In order to generate viable adult mice for the study of Hb Null definitive erythropoiesis, I attempted to generate chimeric mice by the injection of Hb Null ES cells into wild type blastocysts. The RBCs produced from the wild type erythroid progenitors in the chimeric bone marrow would provide the necessary oxygen delivery function required for the animal's survival, while the Hb Null derived erythroid cells could simultaneously develop under optimal *in vivo* conditions in the bone marrow (Figure 14). Because chimeric bone marrow would consist of two distinct erythroid populations, wild type or Hb Null derived cells, it is necessary to label Hb Null erythroid cells in a manner that they can be distinguished from the wild type erythroid cells (Figure 14).

EKLF Tagged with EGFP Marks Nucleated Erythroid Cells in Mouse Bone Marrow

Although our Hb Null ES cells carry the panhematopoietic antigen CD45.1 allele (CD45.1/ CD45.2) and the injected wild type C57BL/6J blastocysts are homozygous for the CD45.2 allele (CD45.2/ CD45.2) (Figure 14), CD45 is only efficiently expressed on white blood cell lineages but not on differentiating erythroblasts[71,72]. In order to distinctly label the Hb Null derived erythroid cells in the bone marrow of chimeras I tagged the erythroid specific transcription factor EKLF[73] with EGFP in the Hb Null ES cells. To validate the feasibility of this strategy, I first generated wild type EGFP-EKLF mice and examined the expression of the EGFP-EKLF fusion protein during bone marrow erythropoiesis.

I targeted EGFP into the EKLF locus by homologous recombination in wild type V6.5 ES cells[74] to produce an EGFP-EKLF fusion protein that has an insertion of a three glycine linker between them (Figure 15, 16, 17). Then I micro-injected targeted V6.5 ES cells into 3.5-day wild type C57BL/6J blastocysts and produced chimeric mice.
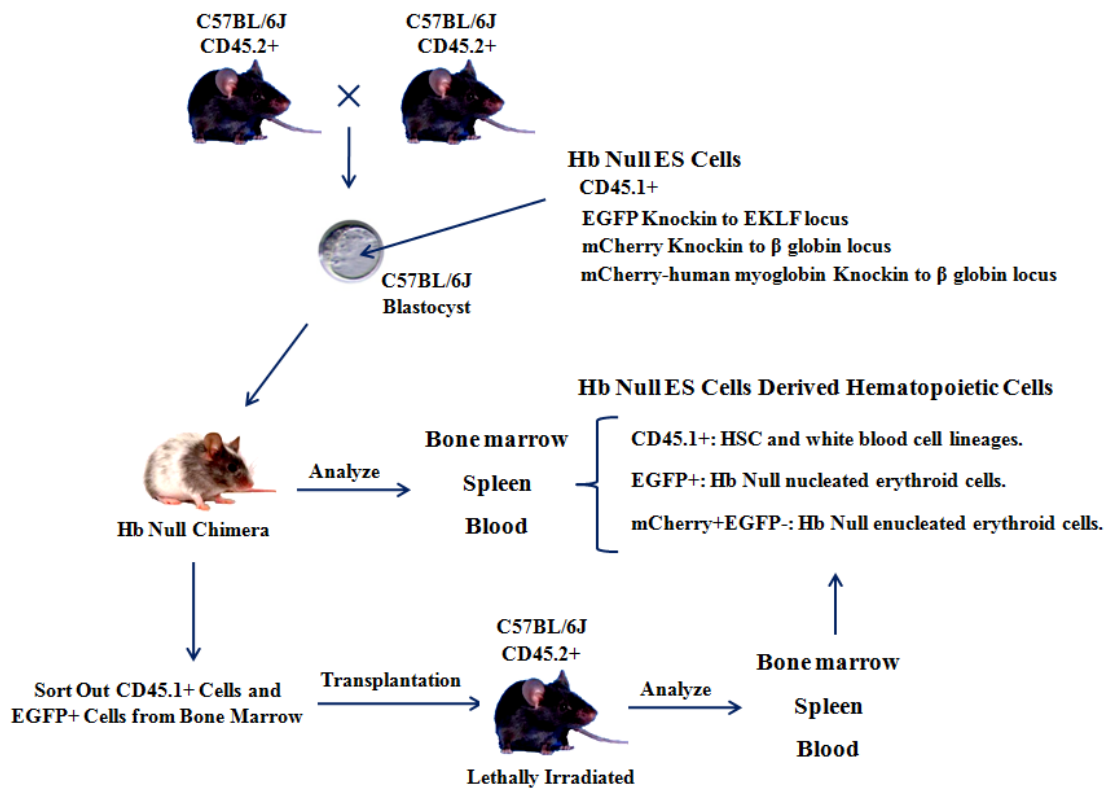
Figure 14. Strategy for studying Hb Null derived erythroid cells in chimeric and transplanted mice.
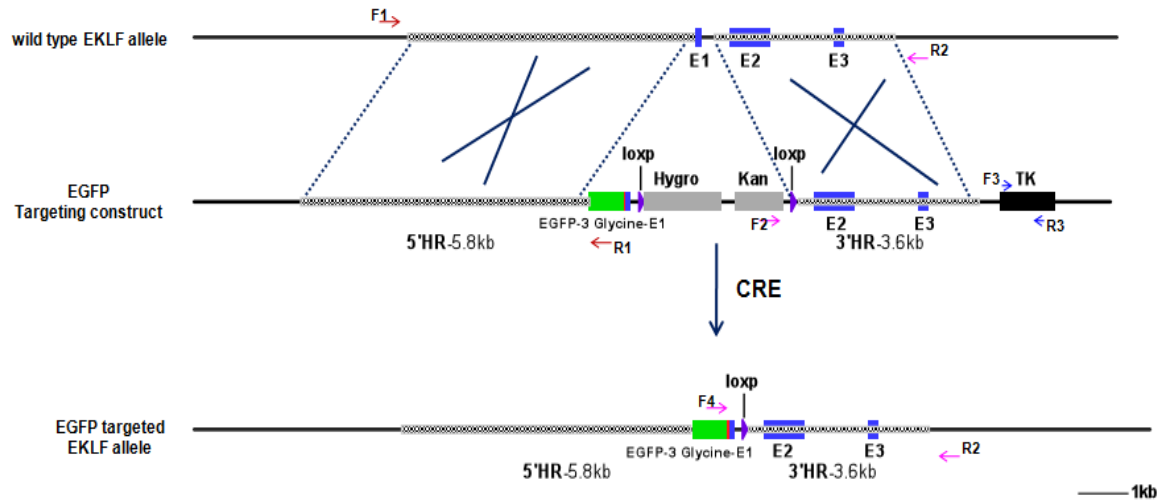
Figure 15. Schematic representation of EGFP targeting into the EKLF locus. EGFP coding sequence including an ATG start codon was inserted just before the EKLF ATG start codon. The sequence for a three amino acid glycine linker was inserted after the EGFP coding region and before the first amino acid codon in exon1 (E1) of EKLF. Homologous sequences (HR) are highlighted by thick grey dash lines. Arrows represent the primers used for colony screening. Hygro is hygromycin resistance gene. Kan is kanamycin resistance gene. TK is herpes simplex virus thymidine kinase gene. Loxp is the target sequence for Cre recombinase. After targeting, selection markers were deleted by transient transfection of Cre recombinase followed by subcloning.
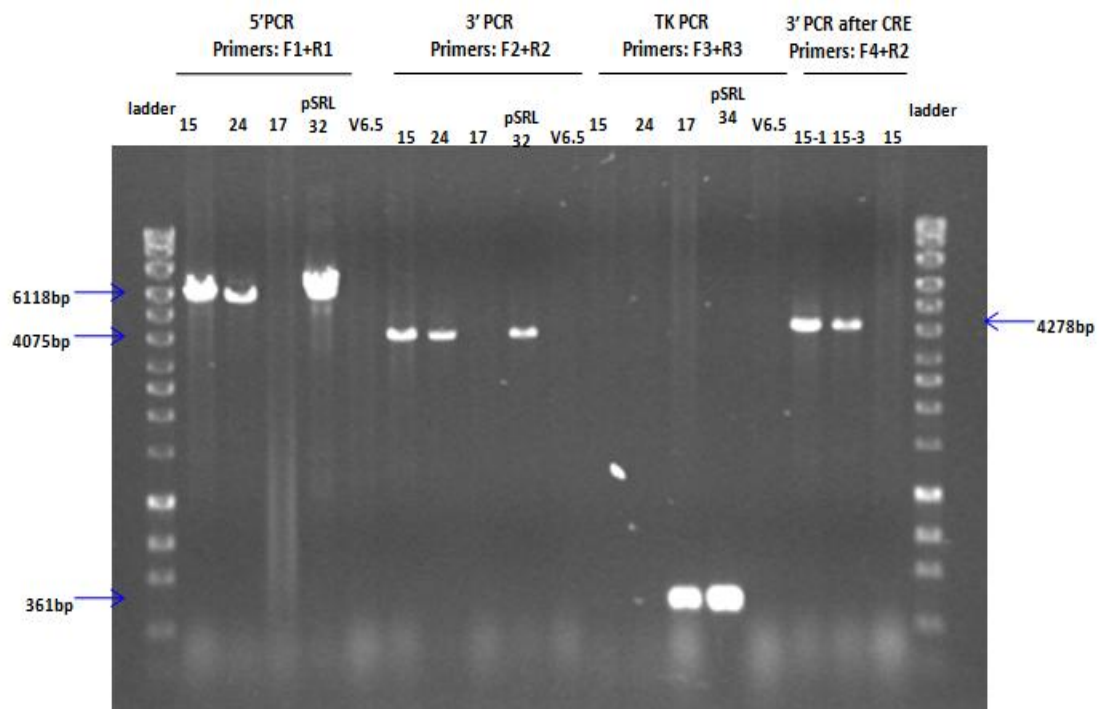
Figure 16. V6.5 ES cells were targeted by EGFP-EKLF construct (pSRL34). Clone #15 and 24 are positive for targeting (5' and 3' PCR +, and TK-). Clone #17 is negative for targeting (5' and 3' PCR -, and TK+). pSRL32 is EKLF BAC with EGFP targeted in EKLF locus that served as a positive control, and V6.5 ES cell DNA was used for negative control. The selection markers of V6.5 ES clone#15 subclone #1 (pSRL34-15-1) and #3 (pSRL34-15-3) were successfully deleted by Cre.
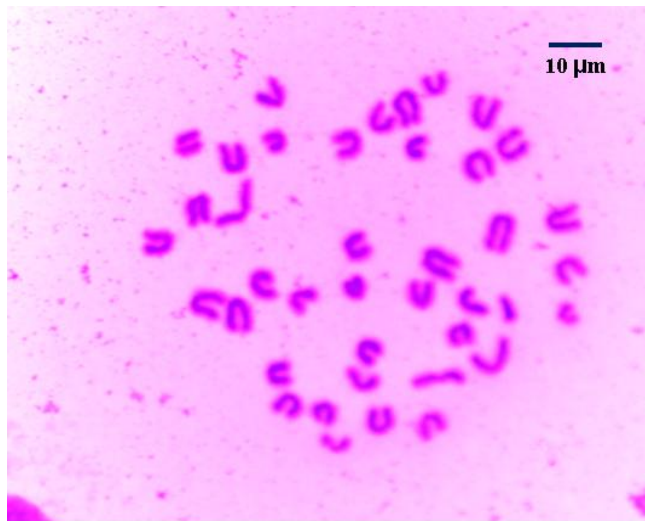
V6.5 clone pSRL34-15-1

Figure 17. V6.5 cells with EGFP-EKLF targeting have correct chromosome number.

The knockin EGFP-EKLF allele was bred into wild type mice by crossing EGFP-EKLF chimeric mice with C57BL/6J mice. Both heterozygous and homozygous knockin EGFP-EKLF wild type mice developed normally with no apparent hematological phenotype, indicating that the EGFP-EKLF fusion protein does not interfere with normal EKLF function. Examination of EGFP-EKLF wild type mouse bone morrow by flow cytometry illustrated that nearly all GFP+ cells (>95%) were Ter119+ albeit a minor population of cells were Ter119- (Figure 18). Our results were consistent with previously published data that showed the expression pattern of an EKLF promoter driven EGFP transgene in fetal liver cells[75]. The small amounts of Ter119- EGFP+ cells were mostly early proerythroblasts, but also included small numbers of enriched CFU-Es, BFU-Es, megakaryocytic-erythroid progenitors (MEPs), megakaryocytes, monocytes, and granulocytes (Figure 19 and reference[75]).
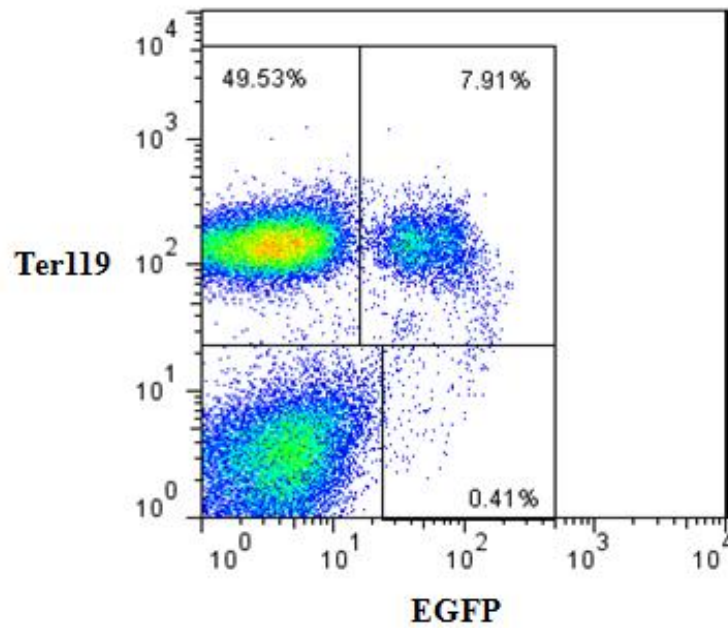
Figure 18. FACS analysis of wild type EGFP-EKLF/EKLF mouse bone marrow by Ter119 and EGFP. Nearly all EGFP+ cells are also Ter119+. Dead cells were gated out by 7AAD.
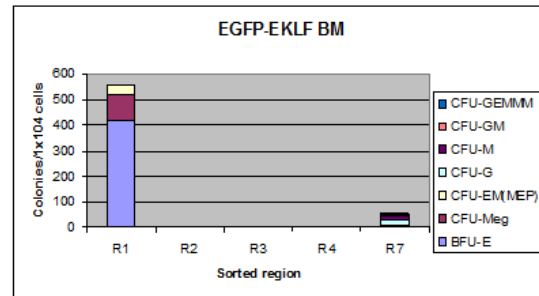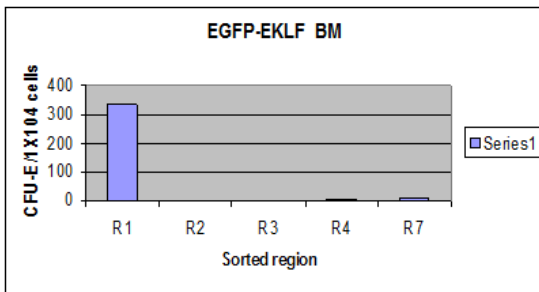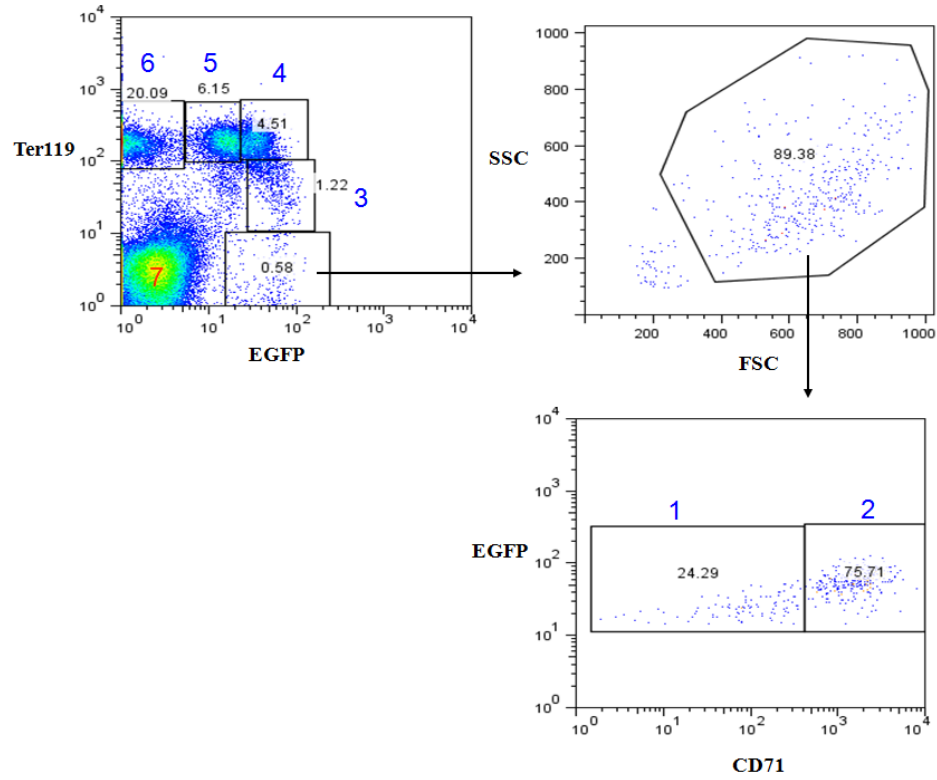
Figure 19. Colony assay of sorted cells from EGFP-EKLF/EKLF wild type mouse bone marrow.

It is noteworthy that not all Ter119+ erythroid cells in bone marrow are EGFP+. To further characterize EKLF expression, I stained bone marrow cells with the nuclear dye Hoechst 33342 and found about 93% of nucleated erythroid cells (Ter119+ Hoechst^{hi}) were GFP+, whereas less than 1% enucleated cells (Ter119+ Hoechst$^{low\ to\ negative}$) were EGFP+ (Figure 20). In fact, these few EGFP+ enucleated cells represented very early reticulocytes. Additionally, I didn't see any EGFP+ positive cells in peripheral blood (Figure 21).
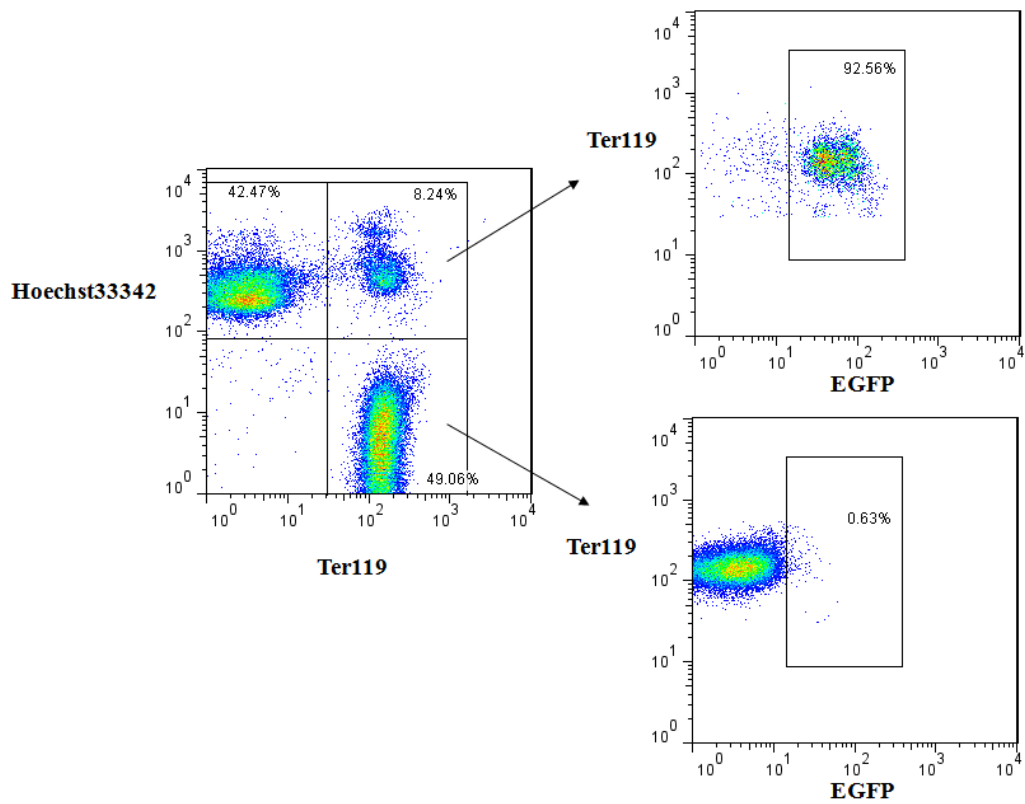
Figure 20. FACS analysis of wild type EGFP-EKLF/EKLF mouse bone marrow by Ter119, Hoechst 33342 and EGFP. Over 90% nucleated erythroid cells (Ter119+ Hoechst+) are EGFP+, and less than 1% enucleated erythroid cells (Ter119+ Hoechst-) are EGFP+. Dead cells were gated out by 7AAD.
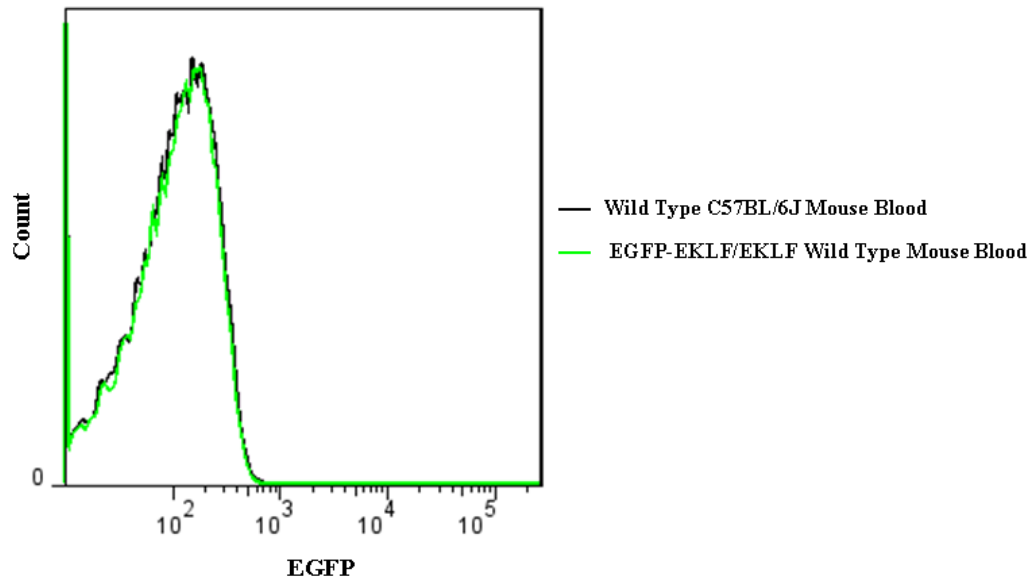
Figure 21. FACS analysis of wild type EGFP-EKLF/EKLF mouse peripheral blood.

EGFP is not expressed in mature red cells.

Taken together, these data demonstrated that EKLF tagged with EGFP could specifically mark nucleated erythroid cells in bone marrow. Furthermore, nucleated erythroid cells could also be separated from enucleated cells simply by their forward scatter (FSC) and side scatter (SSC) properties as shown in Figure 22. The combination of EGFP fluorescence with FSC and SSC enable me to strictly isolate Hb Null enucleated erythroid cells from nucleated erythroid cells as discussed below (Figure 38).
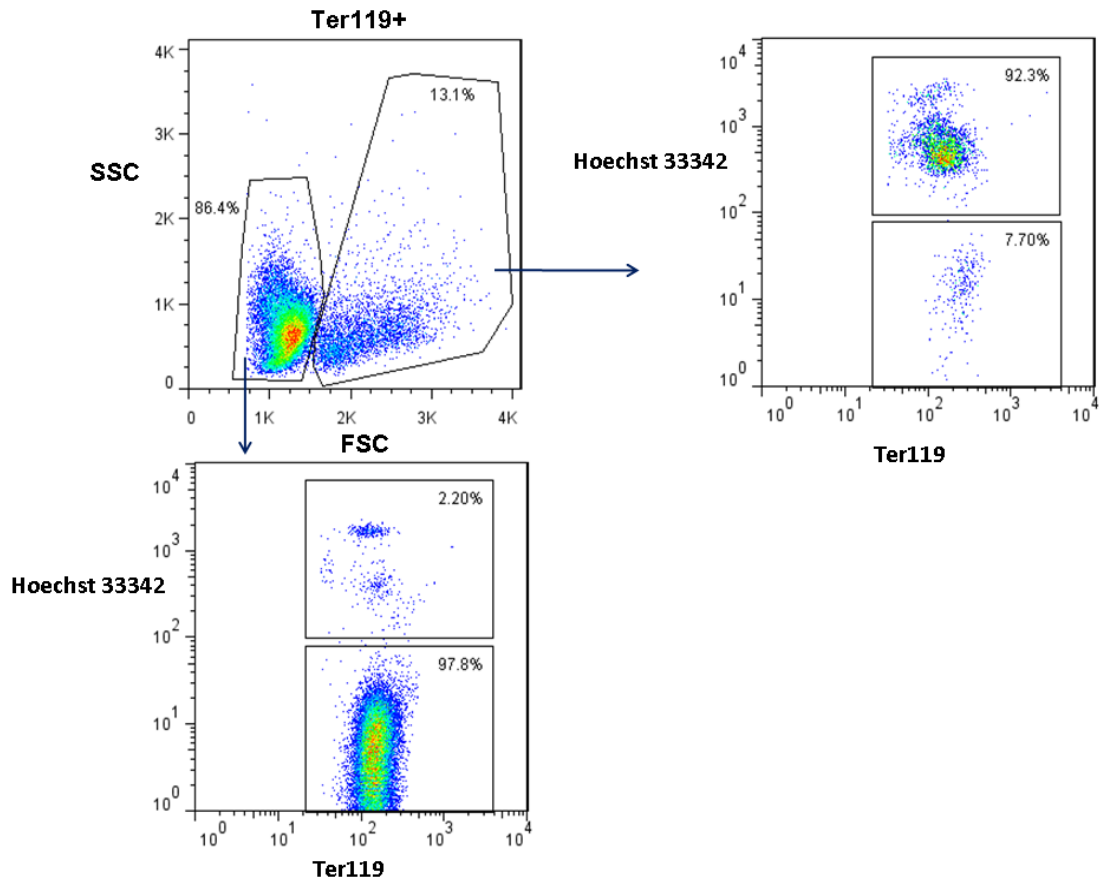
Figure 22. Separation of nucleated from enucleated erythroid cells by FSC-SSC FACS plot. More than 92% Ter119+ FSC^{hi} erythroid cells are nucleated (Hoechst+) cells. Over 97% Ter119+ FSC^{low} erythroid cells are enucleated (Hoechst $^{low\ to\ negative}$) cells. Dead cells were gated out by 7AAD.

Adult Hemoglobin Is Not Essential for Definitive Nucleated Erythroid Development

Hb Null derived definitive erythroblasts could easily be identified and studied in Hb Null chimeric mouse bone marrow by tagging the EKLF gene with EGFP. Therefore, I targeted EGFP into the EKLF locus in Hb Null ES cells as described above (Figures 15, 23, 24), micro-injected Hb Null EGFP-EKLF ES cells (CD45.1/CD45.2) into C57BL/6J blastocysts (CD45.2/CD45.2) (Figure 14), and obtained Hb Null chimeric mice.
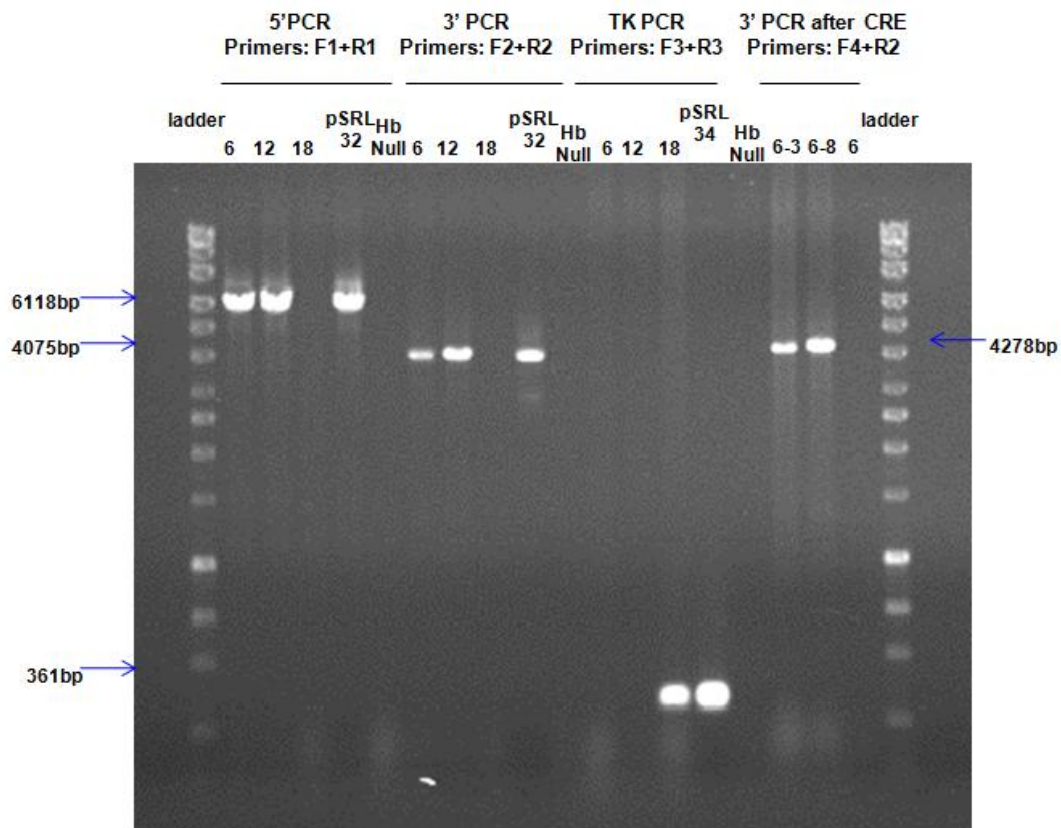
Figure 23. Hb Null ES cells were targeted by EGFP-EKLF construct (pSRL34). Clone #6 and 12 are positive for targeting (5' and 3' PCR +, and TK-). Clone #18 is negative for targeting (5' and 3' PCR -, and TK+). pSRL32 is EKLF BAC with EGFP targeted in EKLF locus that served as a positive control. Hb Null ES cell DNA was used for negative control. The selection markers of Hb Null ES clone#6 subclone #3 (pSRL34-6-3) and #8 (pSRL34-6-8) were successfully deleted by Cre.
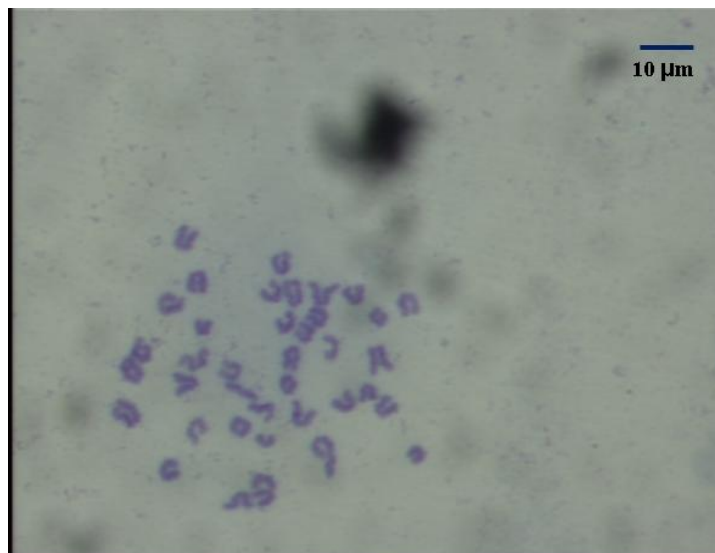
Hb Null clone pSRL34-6-3

Figure 24. Hb Null ES cells targeted with EGFP have correct chromosome number.

Through analysis of CD45.1+ (Hb Null derived) and CD45.2+ (wild type derived) cells in conjunction with various white blood cell lineage markers (T cell, B cell, granulocytes and monocytes), I verified Hb Null ES cells could contribute to all hematopoietic lineages normally present in peripheral blood and bone marrow (Figure 25). This result demonstrates that hemoglobin is not required for the *in vivo* differentiation of Hb Null derived hematopoietic stem cells to the various white blood cell lineages. Surprisingly, there were also abundant EGFP+ Hb Null derived erythroid cells present in each chimeric mouse bone marrow. The ratio of GFP+ to GFP- nucleated erythroid cells in the chimeric bone marrow roughly correlated with the degree of coat color chimerism in individual chimeras.
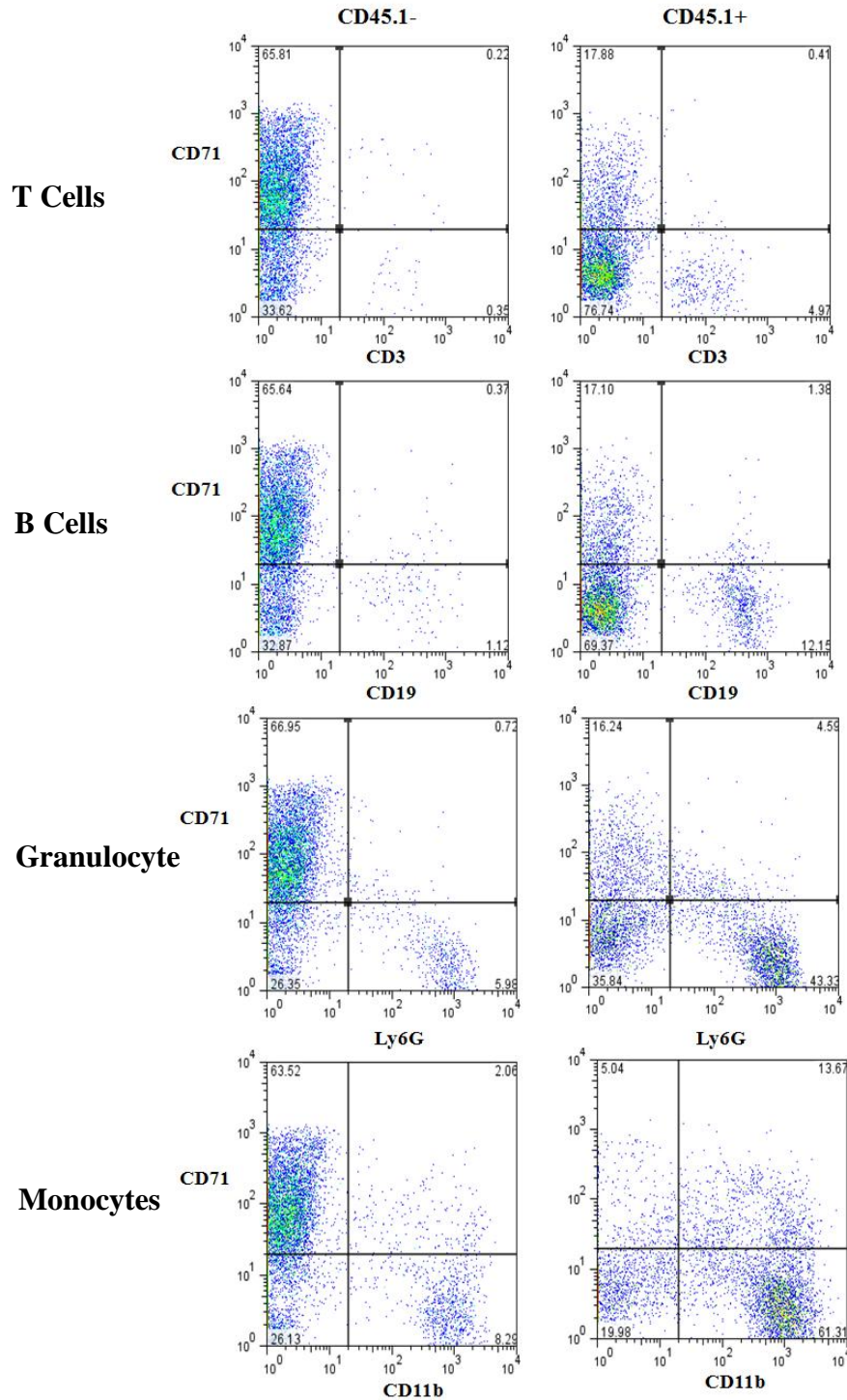
Figure 25. Hb Null ES cells contribute normally to non-erythroid lineages in chimera bone marrow. CD45.1- cells are wild type C57BL/6J blastocyst-derived, and CD45.1+ are Hb Null ES cell-derived. Dead cells were gated out by 7AAD.

An analysis of bone marrow cells from both wild type and Hb Null EGFP-EKLF chimeric mice by flow cytometry was done for the expression of Ter119 and CD71 (Figure 26). In this analysis EGFP+ Ter119+ erythroid cells were divided into three populations, CD71^{hi} (R1), CD71^{med} (R2), and CD71^{low} (R3), which represent proerythroblasts/basophilic erythroblasts (R1), late basophilic/polychromatophilic (R2), and orthochromatophilic erythroblasts (R3) respectively, based upon previous studies[62]. Unexpectedly, the relative ratios of each population (R1 to R3) to the entire population of GFP+ Ter119+ cells are very similar between Hb Null chimeras and wild type mice, suggesting that Hb Null nucleated erythroid cells developed relatively normally from the proerythroblast to the orthochromatic erythroblast. In addition, the wild type nucleated erythroid cells from the Hb Null chimeric bone marrow were assayed by gating EGFP-Ter119+ FSC^{hi} cells into three populations R1 to R3 (Figure 26). These cells served as a better control for the Hb Null nucleated erythroid cells since both of them developed in the exact same bone marrow environment. Compared to the wild type R3 erythroid cells in the same chimera, the Hb Null R3 cells were reduced (11% versus 22%); however, their overall FACS profiles were remarkably similar to each other and to the wild type EGFP-EKLF mouse control. The morphology of nucleated definitive Hb Null and wild type erythroid cells sorted from regions R1 to R3 were examined microscopically. As illustrated in Figure 27, compared to wild type cells, the cytoplasm of Hb Null nucleated erythroid cells appeared less dense, especially in cells from R3 population, which is consistent with the fact that the synthesis of major protein, hemoglobin, is missing in these cells. However, they can still progressively decrease in cell size and condense their

nuclei from R1 to R3, closely resembling their wild type counterparts. There were no other obvious aberrations observed in these Hb Null nucleated erythroid cells.

Wild Type EGFP-EKLF/EKLF Mouse Bone Marrow

Hb Null ES Cells-Derived Nucleated Erythroid Cells in Chimera

Hb Null EGFP-EKLF Chimeric Mouse Bone Marrow

Wild Type Blastocyst-Derived Nucleated Erythroid Cells in Chimera
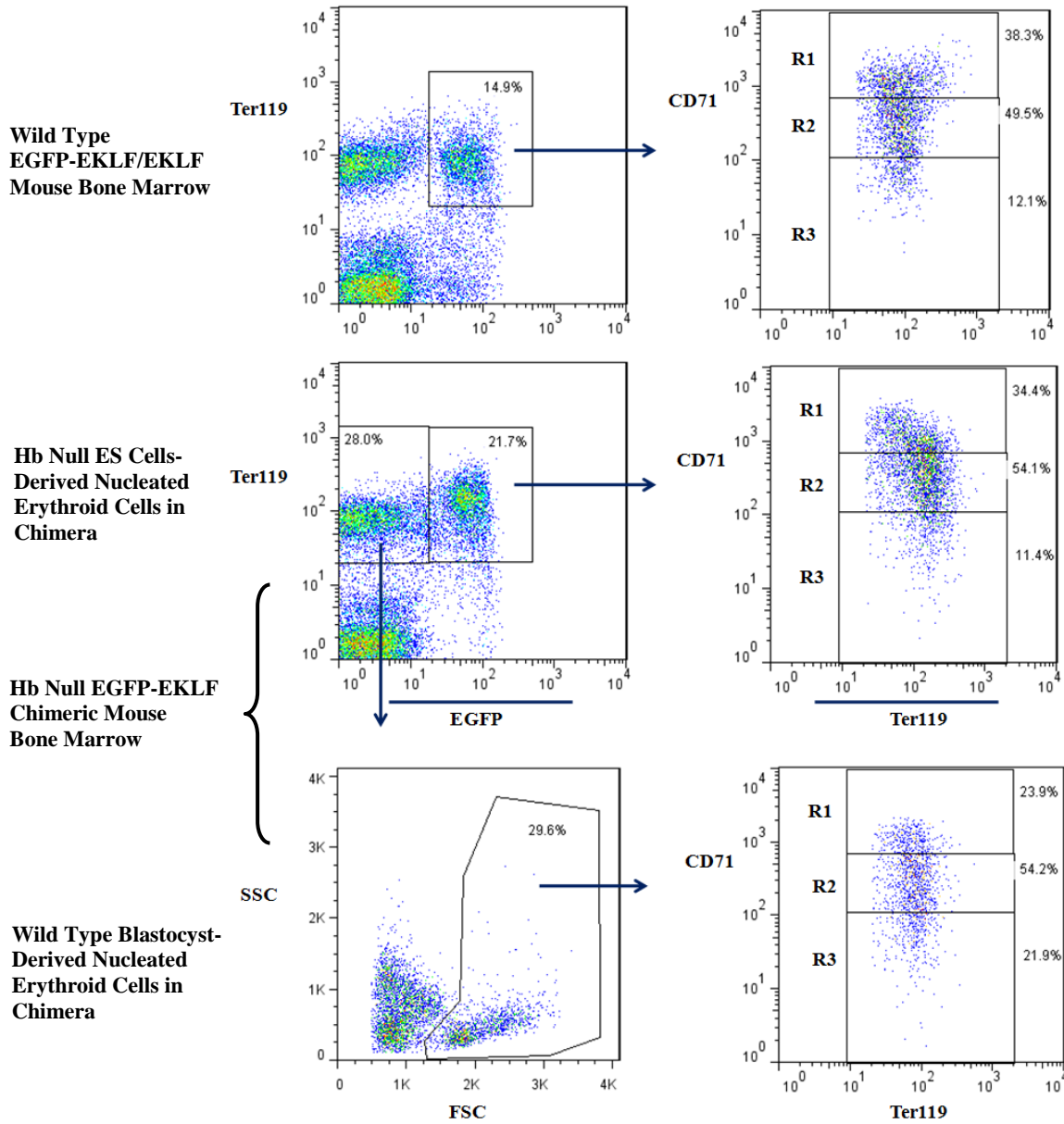
Figure 26. CD71 and Ter119 FACS analysis of bone marrow EGFP+ Ter119+ nucleated erythroid cells. EGFP+ Ter119+ cells from Hb Null EGFP-EKLF chimeric mouse bone marrow (middle two plots) and from wild type EGFP-EKLF/EKLF mouse bone marrow (top two plots), and also EGFP- Ter119+ FSC^{hi} wild type nucleated erythroid cells from the same chimeric bone marrow (bottom two plots) were gated into three regions (R1-R3) (right three plots).   Hb Null cells (middle right plot) exhibit a similar profile as wild type cells (top and bottom right plots). Dead cells were gated out by 7AAD.
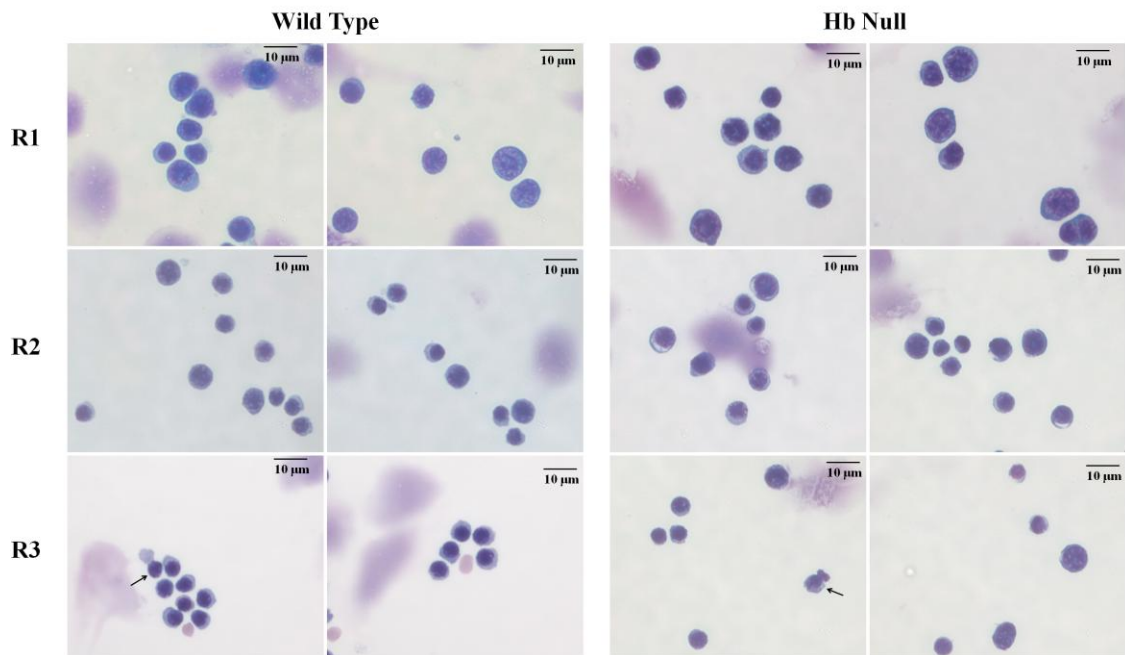
Figure 27. Morphologies of different stages of nucleated Hb Null and wild type erythroid cells. R1 to R3 regions of erythroid cells from wild type EGFP-EKLF/EKLF mouse (Figure 26, top right) and Hb Null EGFP-EKLF chimeric mouse bone marrow (Figure 26, middle right) were sorted by FACS. Cytospins of the sorted cell populations were stained by DipQuick solutions. The morphology of Hb Null nucleated erythroid cells is similar to their wild type counterparts. Dead cells were gated out by 7AAD. Arrows: enucleating erythroid cells.

An improved method for separation of erythroid cells from different developmental stages has recently been published[27]. In this method, CD44 and FSC, instead of Ter119 and CD71, were used for FACS analysis. I applied this method to our study. Namely, EGFP+ TER119+ nucleated erythroid cells from wild type and chimeric mouse bone marrow, as well as the EGFP- TER119+ FSC[hi] wild type nucleated erythroid cells from the same chimeric bone marrow, were gated into three populations (R1 to R3) based upon their CD44 and FSC FACS profile as has been described (Figure 28)[27]. The relative ratios of each nucleated Hb Null erythroid cell population to the total number of nucleated Hb Null erythroid cells were very similar to both wild type controls from R1 to R3. Gating erythroid populations based upon their CD44 and FSC properties showed that wild type and Hb Null erythroid cell populations within the same chimeric bone marrow were more similar than their Ter119 and CD71 results.

Wild Type EGFP-EKLF/EKLF Mouse Bone Marrow

Hb Null ES Cells-Derived Nucleated Erythroid Cells in Chimera

Hb Null EGFP-EKLF Chimeric Mouse Bone Marrow

Wild Type Blastocyst-Derived Nucleated Erythroid Cells in Chimera
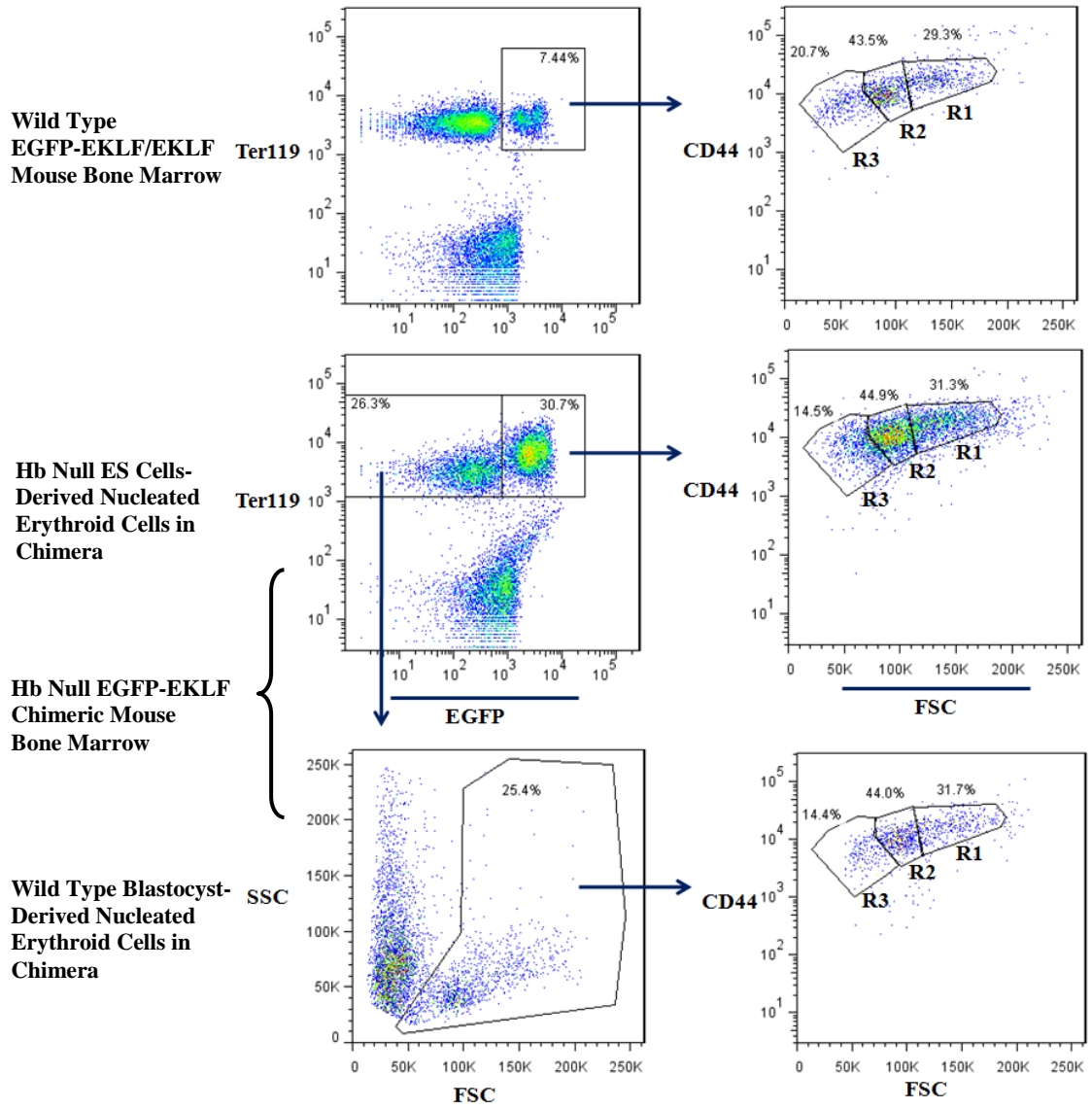
Figure 28. CD44 and FSC^{hi} FACS analysis of bone marrow EGFP+ Ter119+ nucleated erythroid cells. EGFP+ Ter119+ cells from Hb Null chimeric mouse bone marrow (middle two plots), from wild type EGFP-EKLF/EKLF mouse bone marrow (top two plots), and also EGFP- Ter119+ FSC^{hi} wild type nucleated erythroid cells from the same chimeric bone marrow (bottom two plots) were gated into three regions (R1-R3) (right three plots).   Hb Null erythroid cells (middle right plot) exhibit a similar profile as wild type cells (top and bottom right plots). Dead cells were gated out by 7AAD.

In summary, knockin of an EGFP gene into the erythroid specific transcription factor EKLF generates an EGFP-EKLF fusion protein that labels virtually all nucleated erythroid cells in mouse bone marrow without effecting erythropoiesis. Knockin of EGFP to the EKLF allele in Hb Null ES cells allows all Hb Null derived nucleated erythroid cells to be identified in chimeric bone marrow. Hb Null derived cells can contribute to all hematopoietic lineages in chimeric mice. Compared to wild type nucleated erythroid cells, Hb Null nucleated erythroid cells develop in relatively normal ratios from the proerythroblast to the orthochromatic erythroblast. Although Hb Null nucleated erythroid cells have less cytoplasm content due to the loss of their major cytoplasmic protein hemoglobin, they otherwise display similar morphology to their wild type counterparts. These results indicate that adult hemoglobin is not essential for definitive nucleated erythroid development. The importance of adult hemoglobin for enucleated RBC development will be discussed in the next chapter.

CHAPTER 4

HB NULL ERYTHROID CELLS CAN ENUCLEATE TO FORM RETICULOCYTES

Although EGFP-EKLF targeting can track nucleated Hb Null erythroid cells in chimeras, we are not able to follow enucleated Hb Null erythroid cells in chimeras since the nuclear transcription factor EKLF is no longer present after enucleation (Figure 20, 21). Previous results showed that Hb Null nucleated erythroid cells develop relatively normally. It is thus possible that they can further mature to the enucleated reticulocyte stage. Some Hb Null EGFP-EKLF erythroid cells were observed in the process of expelling their nuclei as shown in Figure 27. In order to track Hb Null erythroid development/maturation beyond the nucleated bone marrow stage in chimeric mice, I would need to tag a cytosolic protein in the Hb Null derived erythroid cells.

In mature red cells, the nuclei are disgorged, all cytosolic organelles are degraded, and nearly all the cytosolic protein is hemoglobin. Therefore, the best method to label enucleated erythroid cells should be to drive marker gene expression from an endogenous globin gene promoter. Thus, I replaced the original neomycin resistance gene in the knockout β globin locus with the red fluorescent protein (RFP) gene, mCherry, driven by the endogenous mouse β^{major} globin gene promoter via homologous recombination in Hb Null EGFP-EKLF ES cells (Figures 29, 30, 31). mCherry is a monomeric RFP and is generally non-toxic[76,77]. Hb Null EGFP-EKLF mouse β globin promoter-mCherry ES cell derived erythroid cells in the bone marrow of chimeric mice should display both GFP

and RFP fluorescence in the nucleated erythroblasts and only RFP fluorescence in enucleated erythroid cells. The Hb Null EGFP-EKLF mouse β globin promoter-mCherry cells will be labeled as Hb Null mCherry-EGFP in the remainder of this dissertation.

In my preliminary experiments, a recombinant lentivirus, which contained the human β globin locus control region (LCR) DNase I hypersensitive sites (HS) 4, 3, and 2 with the human adult β globin gene promoter driving mCherry expression, was used to infect mouse bone marrow and murine erythroleukemia (MEL) cells, and it confirmed that mCherry can be strongly expressed in enucleated red cells (see Future Directions, Figures 63, 64, 65, 66). By directly targeting the mCherry gene into the endogenous β globin locus, the unpredictable effects of random lentivirus insertions were avoided (Figure 29). I injected Hb Null mCherry-EGFP ES cells into C57BL/6J blastocysts and generated chimeric mice (Figure 14).
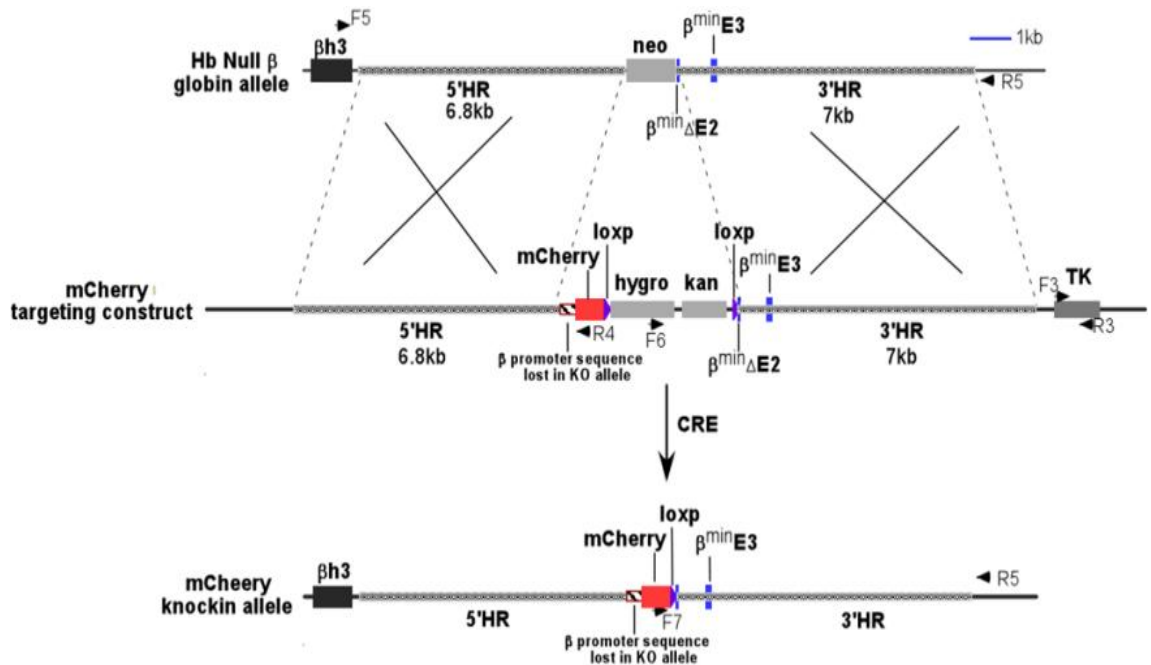
Figure 29. Schematic representation of mCherry targeting to β globin locus. mCherry coding sequence (red box) was targeted to the β globin locus downstream of the $β^{major}$ globin gene promoter. Hatched box represents the mouse $β^{major}$ globin gene promoter sequence that was deleted in the original β globin knockout allele, but was reintroduced into the locus with the insertion of the mCherry gene sequence. Homologous sequences (HR) are highlighted by thick grey dash lines. Arrow heads represent the primers used for colony screening. Neo is neomycin resistance gene. Hygro is hygromycin resistance gene. Kan is kanamycin resistance gene. TK is herpes simplex virus thymidine kinase gene. After targeting, selection markers were deleted by electroporation of plasmids expressing Cre into ES cells.
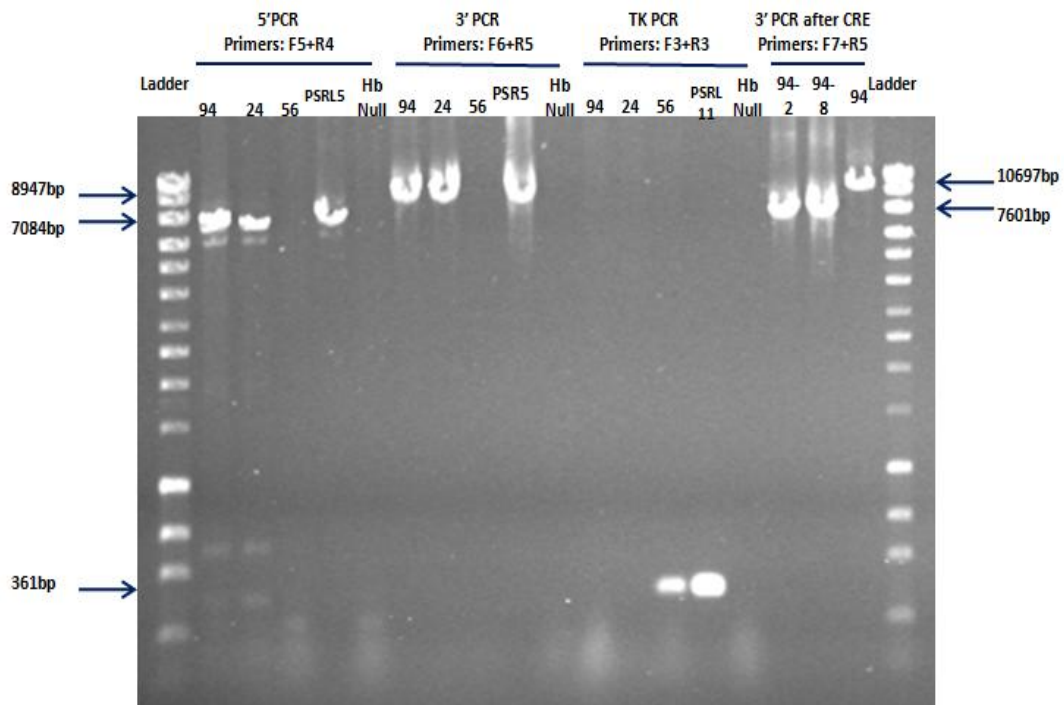
Figure 30. Hb Null EGFP-EKLF ES cells (Hb Null clone pSRL34-6-3) were targeted with the mCherry construct (pSRL11). Clone #94 and 24 are positive for targeting (5' and 3' PCR +, and TK-). Clone #56 is negative for targeting (5' and 3' PCR -, and TK+). pSRL5 is mouse β globin BAC with β^{major} and β^{minor} globin genes replaced by mCherry that served as a positive control, and Hb Null clone pSRL34-6-3 ES cell DNA was used for negative control (Hb Null lane). The selection markers of Hb Null ES Null clone pSRL34-6-3-pSRL11-94 subclone #2 and #8 were successfully deleted by Cre.
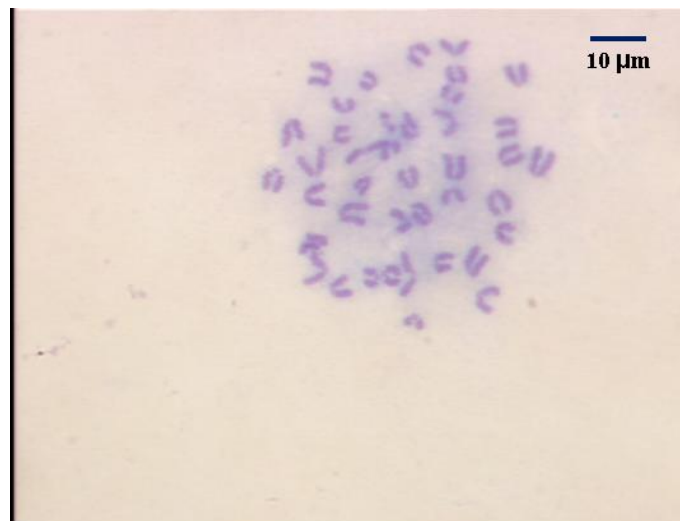
Hb Null clone pSRL34-6-3-pSRL11-94-8

Figure 31. Hb Null ES cells targeted with mCherry have correct chromosome number.

Analysis of Hb Null mCherry-EGFP chimeric bone marrow revealed that mCherry was highly expressed in many cells, and nearly all mCherry positive cells were also Ter119 positive (Figure 32). Thus, mCherry could specifically monitor Hb Null mCherry-EGFP derived erythroid cells in chimeras. When mCherry and EGFP expression were analyzed together (Figure 32), I found a small fraction of cells that were mCherry positive but EGFP low to negative and also a few cells that were EGFP positive but mCherry negative. The majority of cells were either mCherry and EGFP double positive or double negative. The mCherry and EGFP double negative cells were wild type hematopoietic cells and Hb Null mCherry-EGFP ES cell derived non-erythroid cells. Most of the EGFP single positive cells should represent Hb Null mCherry-EGFP ES cell derived myeloid cells expressing EKLF as discussed above, which is beyond the scope of this study. mCherry and EGFP double positive cells were nucleated erythroid cells which were studied earlier in the Hb Null EKLF-EGFP chimeric mice. The mCherry positive and EGFP low to negative cells should label the enucleated Hb Null derived erythroid cell population.
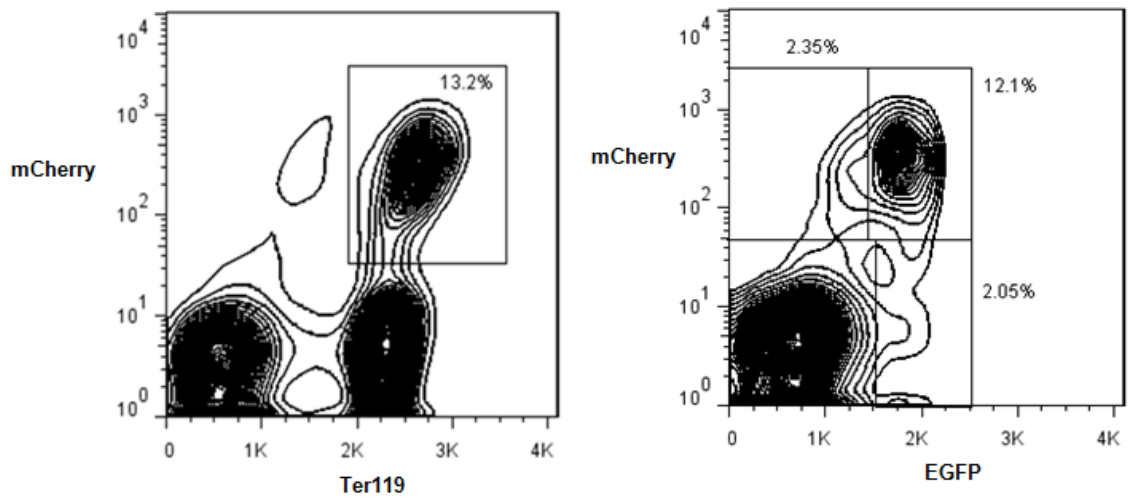
Figure 32. mCherry expression in Hb Null mCherry-EGFP erythroid cells. Nearly all mCherry+ cells are Ter119+ (left plot). Most mCherry+ cells are also EGFP+, and a few cells are mCherry or EGFP single positive (right plot).

To confirm the identity of these single mCherry positive cells in the Hb Null mCherry-EGFP chimeric mice, the bone marrow cells were fluorescently stained with a nuclear dye, Dyecycle Violet, and a RNA dye, Thiazole Orange (TO), along with Ter119 and CD71 antibodies. As illustrated in Figure 33, there are a number of cells (1.3% of total bone marrow cells for this chimera) that are Dyecycle Violet-, Ter119+, and mCherry+, which represent Hb Null derived enucleated erythroid cells. Additionally, I found about 97% of these enucleated cells were Thiazole Orange and CD71 double positive, and only a tiny percent of cells were double negative, indicating that nearly all enucleated Hb Null derived erythroid cells were still at the reticulocyte stage with very few of them developing to TO negative mature RBCs.
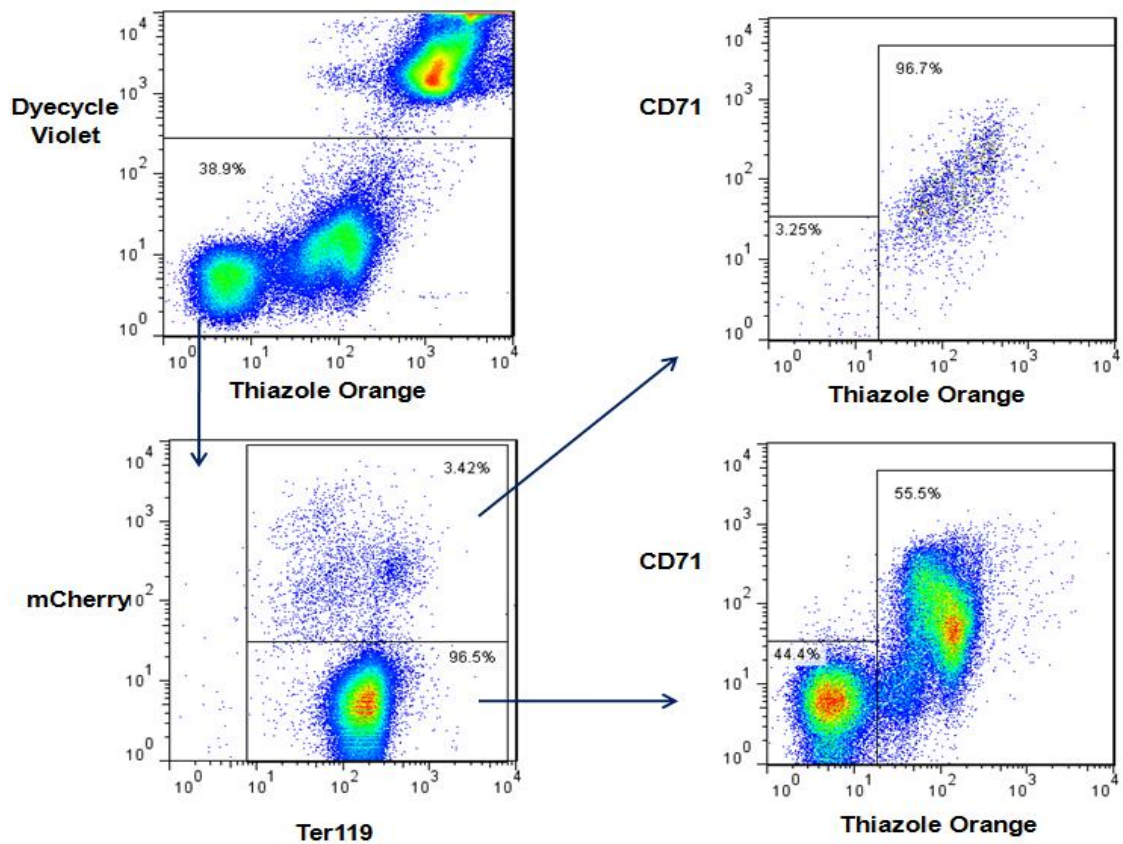
Figure 33. FACS analysis of Hb Null mCherry-EGFP chimeric mouse bone marrow stained with Ter119, CD71, RNA dye Thiazole Orange and DNA dye Dyecycle Violet. Hb Null erythroid cells can enucleate (mCherry+, Ter119+, Dyecycle Violet-), and nearly all these enucleated cells are CD71+ and Thiazole Orange+ reticulocytes.

Enucleated Hb Null derived erythroid cells were sorted from chimeric bone marrow by flow cytometry (Dyecycle Violet-, Ter119+, mCherry+) and their morphology was examined microscopically (Figure 34). These cells exhibit marked variations in size and shape, with most diameters ranging from 3 to 8 μm, and their cytoplasm is heterogeneous, grainy, and still very basophilic. Conspicuously, most of these cells contain a large vacuole, which is often slightly tinted, and is likely the empty space left by nuclear extrusion rather than the autophagic vacuoles described in wild type reticulocytes by many groups[78,79]. These characteristics suggest that these cells are very nascent reticulocytes that have just finished disgorging their nuclei. Notably, there were very few mCherry+ cells in the peripheral blood of Hb Null chimeras. Even in the highest chimera (>80% chimerism based on coat color) the percentage of mCherry+ cells in the peripheral blood was only around 0.02%. I sorted out these cells and found they shared a similar morphology to the enucleated mCherry+ cells isolated from the bone marrow (Figure 35).
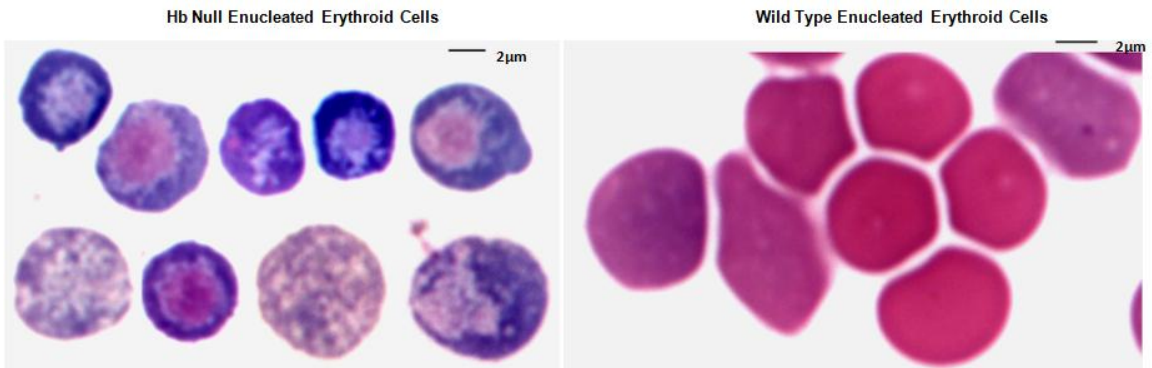
Figure 34. Morphology of enucleated Hb Null derived erythroid cells from chimeric bone marrow. Enucleated Hb Null erythroid cells (Dyecycle Violet-, Ter119+, mCherry+) (left panel) and wild type reticulocytes (Dyecycle Violet-, Ter119+, mCherry-, Thiazole Orange+) (right panel) were FACS sorted from Hb Null mCherry-EGFP chimeric bone marrow. Cytospins of sorted cells were stained with DipQuick solutions. Hb Null sorted cells from eight individual fields were combined together (left panel).
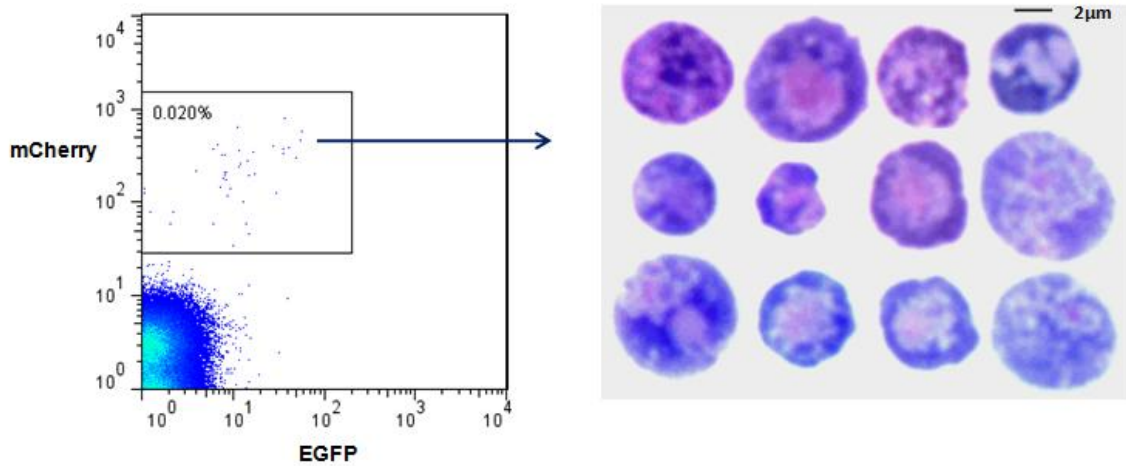
Figure 35. Morphology of enucleated Hb Null erythroid cells from peripheral blood. mCherry+ peripheral blood cells from Hb Null mCherry-EGFP chimeric mice were FACS sorted, cytospun onto glass slides, and stained with DipQuick solutions. Hb Null cells from twelve individual fields were combined together (right panel).

The ratio of Hb Null nucleated erythroid cells to Hb Null enucleated cells did not match the ratio observed in wild type mice. In chimeric bone marrow, 12% of Hb Null nucleated erythroid cells (EGFP+) in Figure 32 only generated 1.3% enucleated cells in the same mouse in Figure 33; whereas, in a wild type C57BL/6J mouse bone marrow, 12% nucleated erythroid cells could produce 17% reticulocytes (Figure 36), which means Hb Null nucleated erythroid cells only generated about 8% (1.3/17) of the reticulocytes that the same amount of wild type nucleated erythroid cells could produce.

To more accurately determine this reticulocyte reduction, Hb Null mCherry-EGFP chimeric bone marrow cells were fluorescently stained with a nuclear dye, Hoechst33342, and Ter119. Figure 37 shows that, of total bone marrow erythroid cells (Ter119+), 30% wild type nucleated erythroid cells (Ter119+, Hoechst^{hi}, mCherry-) generated 12% reticulocytes (Ter119+, Hoechst^{low}, mCherry-), while 50% Hb Null nucleated erythroid cells (Ter119+, Hoechst^{hi}, mCherry+) only produced 1.4% reticulocytes (Ter119+, Hoechst^{low}, mCherry+). These numbers demonstrate that Hb Null reticulocytes were only present at 7% of the level of wild type reticulocytes relative to the same number of nucleated erythroid cells. However, due to the limitation of available channels in the flow cytometer, I was unable to remove all dead cells by adding an additional marker, such as 7AAD, in this method. Alternatively, we could count Hb Null nucleated erythroid cells in chimeric bone marrow as mCherry and EGFP double positive and enucleated erythroid cells as mCherry+EGFP-CD71+FSC^{low}. Similarly in wild type EGFP-EKLF bone marrow, nucleated erythroid cells are Ter119 and EGFP double positive and enucleated erythroid cells are Ter119+EGFP-CD71+FSC^{low}, as shown in Figure 38. This more strict

calculation renders Hb Null reticulocytes generated at only 2.6% of their wild type counterparts.
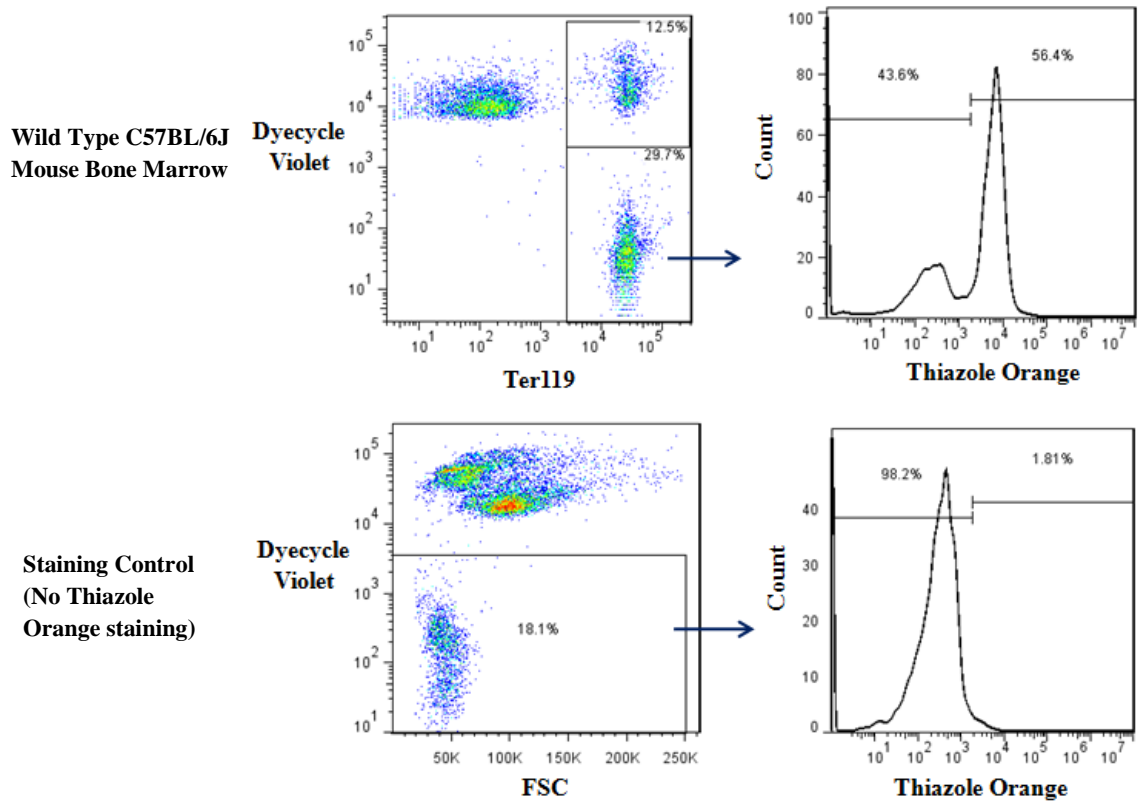
Figure 36. The ratio of reticulocytes in wild type C57BL/6J mouse bone marrow. 12.5% nucleated erythroid cells produce 17% reticulocytes (29.7% × 56.4% = 17%) (top two plots). Dead cells were gated out by 7AAD.
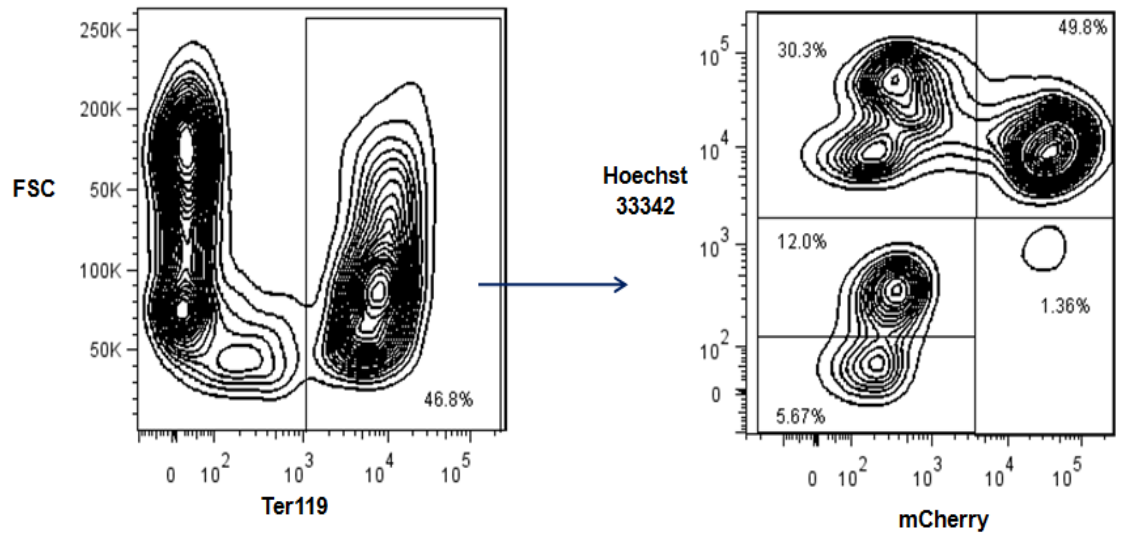
Figure 37. Total erythroid cells from mCherry-EGFP Hb Null chimera bone marrow (Ter119+) (left plot) were analyzed by mCherry and Hoechst 33342 (right plot). The ratio of nucleated erythroid cells (Ter119+ Hoechst^{hi}) to reticulocytes (Ter119+ Hoechst^{low}) in wild type part (mCherry-) is 2.5:1 (30.3%: 12%), whereas it in Hb Null part (mCherry+) is 36.7:1 (49.9%: 1.36%). Dead cells marker could not be used in this assay.
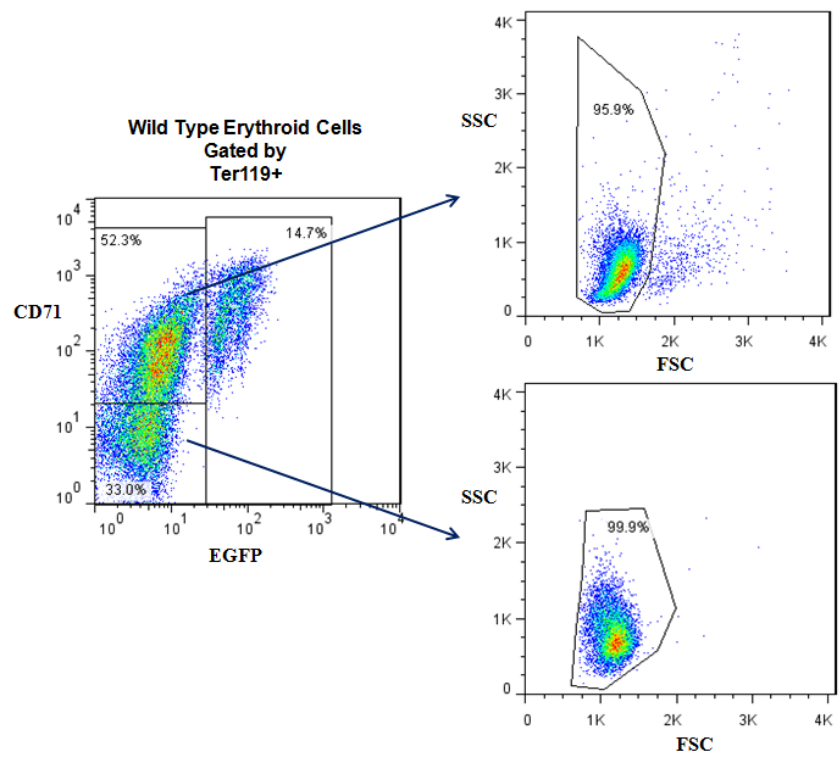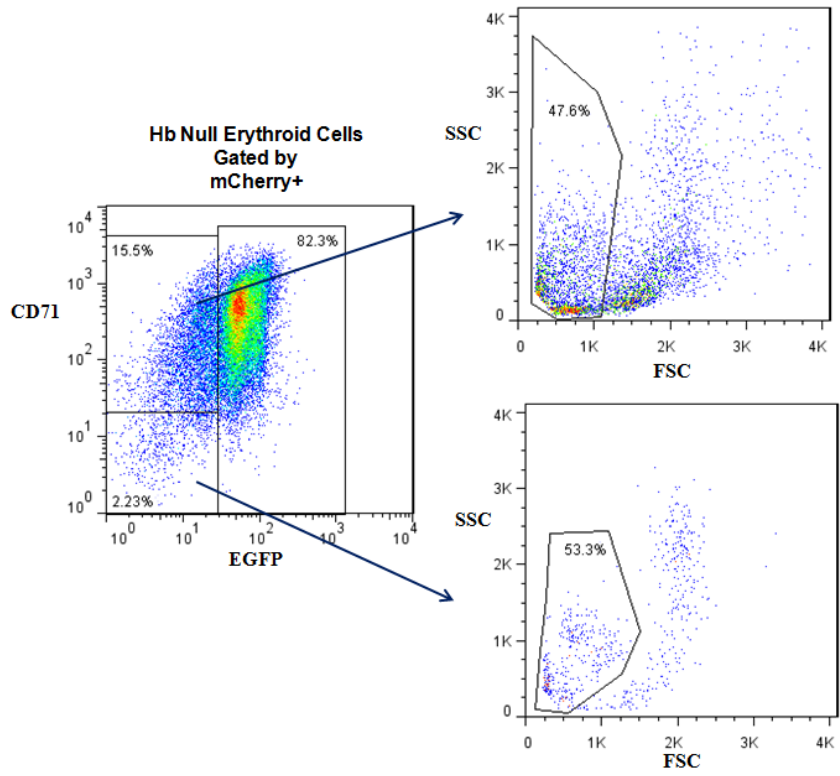
Figure 38. Erythroid cells from Hb Null mCherry-EGFP chimeric bone marrow and wild type EGFP-EKLF/EKLF mouse bone marrow were analyzed by plots of CD71 versus EGFP in combination with FSC versus SSC. Hb Null nucleated erythroid cells (mCherry+ EGFP+): 82.3%; Hb Null reticulocytes (mCherry+EGFP-CD71+FSC^{low}): 15.5% x 47.6% = 7.4%; wild type nucleated erythroid cells (Ter119+ EGFP+): 14.7%; wild type reticulocytes (Ter119+ EGFP- CD71+ FSC^{low}): 52.3% x 95.9%= 50.2%. Dead cells were removed by SYTOX Blue.

In summary, by targeting mCherry into the β globin locus downstream of the endogenous β^{major} globin gene promoter, I could successfully track Hb Null derived enucleated erythroid cells in chimeras. I discovered that in the absence of adult hemoglobin, definitive erythroid cells can enucleate and form reticulocytes in the bone marrow. A small number of Hb Null reticulocytes were even found in the peripheral blood. However, compared to wild type reticulocyte levels, the numbers of enucleated Hb Null erythroid cells were reduced by more than 90%. This result suggests that Hb Null reticulocytes are very short lived and seldom fully develop to mature Thiazole Orange negative RBCs. To further confirm this conclusion, I sought to study Hb Null erythroid development in a relative pure Hb Null adult mouse without mixing with many wild type erythroid cells, and this will be addressed in the next chapter.

CHAPTER 5

HB NULL ERYTHROID CELL DEVELOPMENT IN TRANSPLANTED MICE

The combination of EGFP and mCherry fluorescence allowed us to identify the production of both nucleated and enucleated Hb Null derived erythroid cells in chimeric mice. However, I was not able to easily examine Hb Null derived erythroid cells in situ in the bone marrow or spleen as the fluorescence was destroyed during the sample processing, making it difficult to separate the Hb Null from wild type erythroid cells in situ. The ability to examine pure Hb Null erythropoietic tissue in the absence of wild type erythroid cells would enable the visualization of developing Hb Null cells directly in their bone marrow microenvironment.

As discussed previously, our Hb Null ES cells are heterozygous for the CD45.1 allele, while wild type C57BL/6J mice are homozygous for the CD45.2 allele (Figure 14). It is known that CD45 is expressed on hematopoietic stem cells (HSCs)[80]. Therefore, Hb Null HSCs can be isolated from Hb Null chimeric bone marrow by sorting for CD45.1 positive marrow cells by FACS. After depletion of the endogenous hematopoietic cells of recipient wild type mice by lethal irradiation, CD45.1 positive Hb Null marrow cells could be transplanted into the irradiated recipients to reconstitute their hematopoietic system. The transplanted Hb Null HSCs will proliferate in the recipient mouse bone marrow replacing all red and white blood cell lineages. As the Hb Null erythroid cells are devoid of adult hemoglobin and cannot deliver oxygen, the irradiated recipient mice

must survive post-transplantation solely on the wild type RBCs that were present in their circulation at the time of irradiation. As these wild type RBCs senesce the recipient mice will become progressively anemic resulting in an expansion of the donor Hb Null HSC derived erythroid progenitors in their bone marrow and spleen until they succumb to a lethal anemia. Theoretically, after several weeks all nucleated erythroid cells in this transplanted mouse should be derived from the donor Hb Null HSCs. These Hb Null transplanted mice can be euthanized prior to death and their pure Hb Null HSC derived erythroid tissues can be studied.

To test this strategy, I FACS sorted CD45.1+ cells and also EGFP+ cells from Hb Null mCherry-EGFP chimeric bone marrow and transplanted them into lethally irradiated C57BL/6J wild type mice (Figure 14). Engrafted mice survived from 4 to 12 weeks, longer than controls without transplantation (less than 3 weeks). I analyzed one mouse at 12 weeks post-transplantation prior to death, and found all nucleated erythroid cells (Hoechst^{hi} Ter119+) in its bone marrow and spleen were mCherry+ EGFP+ (Figures 39 and 40), and Hb Null enucleated erythroid cells (Hoechst$^{low\ to\ negative}$, Ter119+, mCherry+) were increased almost to the level of the wild type enucleated erythroid cells still circulating in these tissues (Hoechst$^{low\ to\ negative}$ Ter119+ mCherry-) (Figures 39 and 40). This mouse with pure Hb Null nucleated erythroid cells is abbreviated as PHNNEC mouse. Its ratio of spleen to body weight was ten times that of wild type mice, while the hematocrit level was only 10% (Figure 41), and its liver had marked iron-overload (Figure 42). These data indicate that there was severe ineffective erythropoiesis in this mouse.
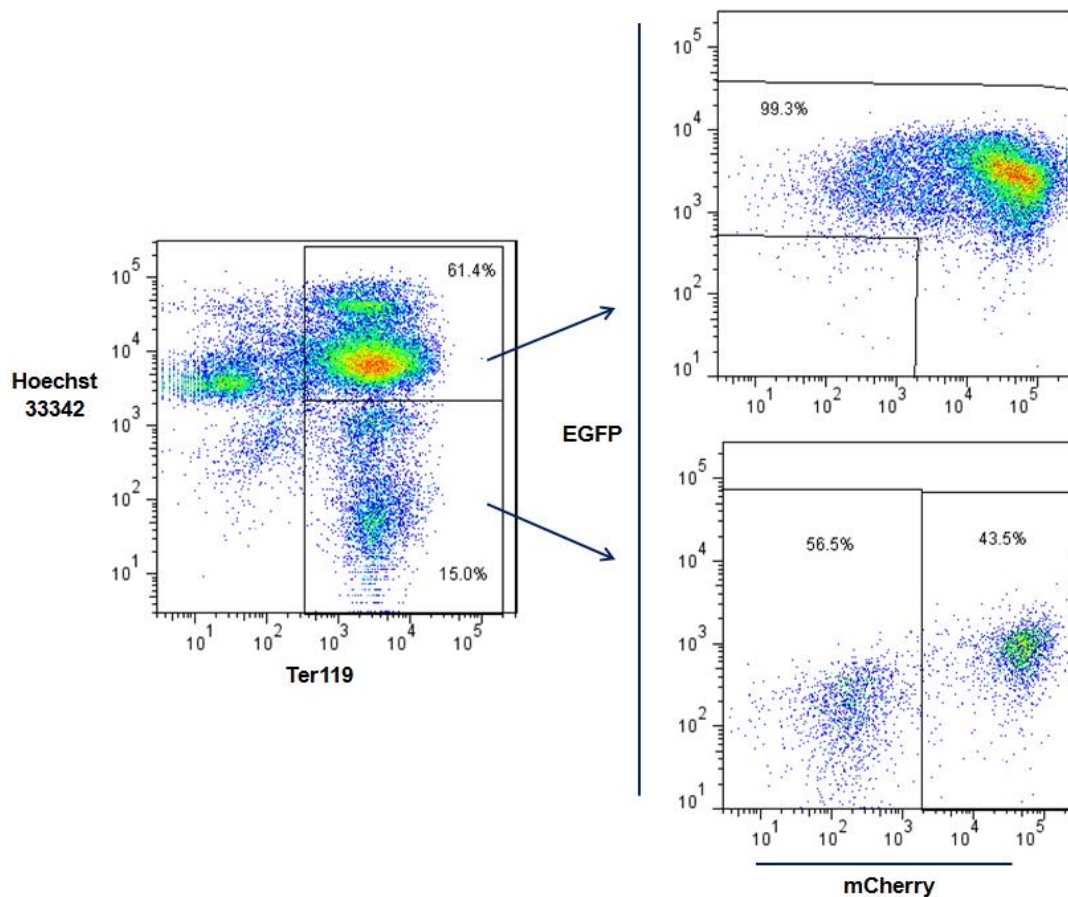
Figure 39. FACS analysis of PHNNEC mouse bone marrow. All nucleated erythroid cells (Hoechst+ Ter119+) are Hb Null ES cells-derived (mCherry+ EGFP+). Enucleated erythroid cells include endogenous wild type cells (mCherry-) and Hb Null cells (mCherry+). The ratio of Hb Null nucleated erythroid cells to Hb Null enucleated is 9.4:1 [61.4 % : (15.0% × 43.5%)].
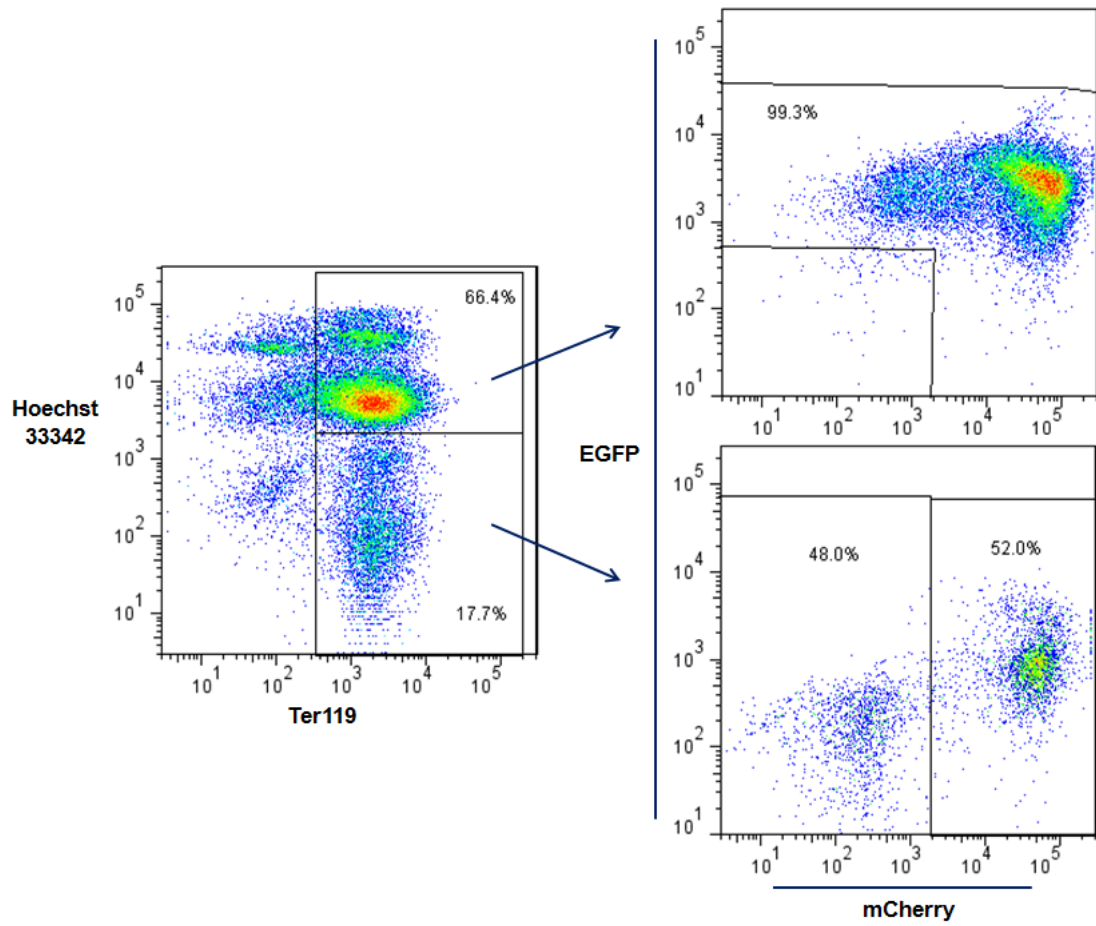
Figure 40. FACS analysis of PHNNEC mouse spleen. All nucleated erythroid cells (Hoechst+ Ter119+) are Hb Null ES cells-derived (mCherry+ EGFP+). Enucleated erythroid cells include endogenous wild type cells (mCherry-) and Hb Null cells (mCherry+).
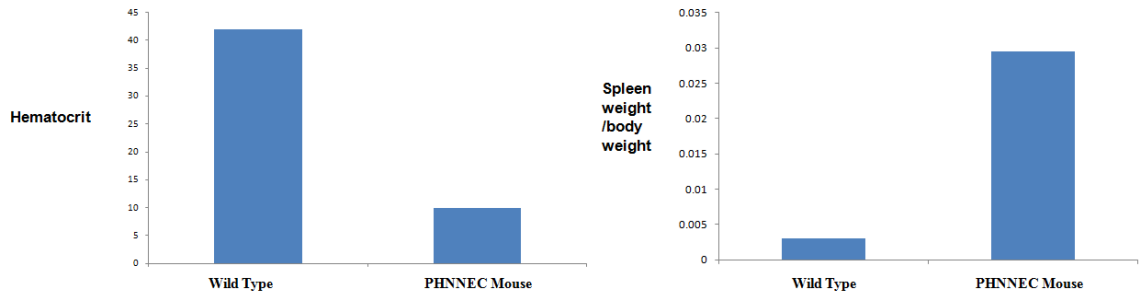
Figure 41. Hematocrit and spleen size of PHNNEC mouse
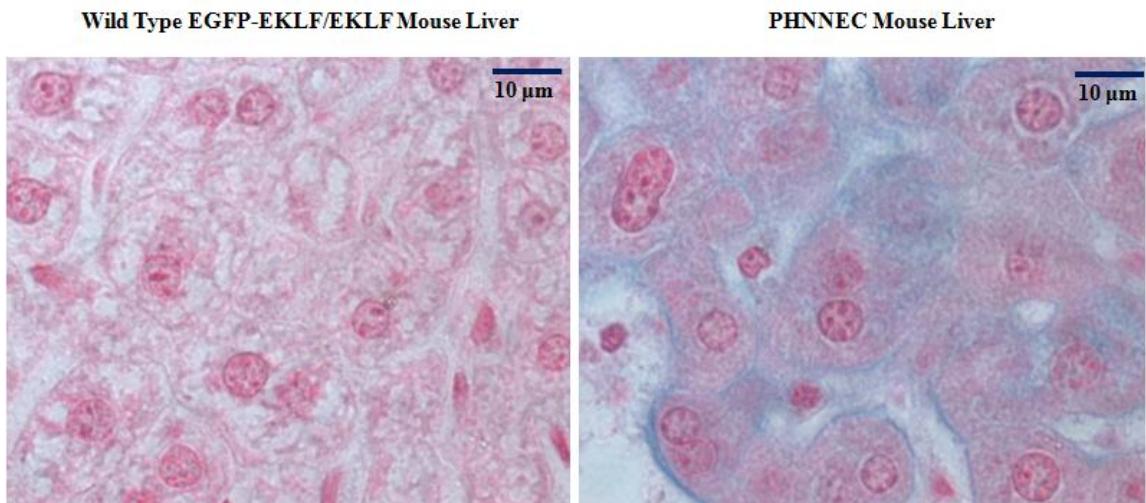
Figure 42. Iron staining by Prussian Blue of liver tissue sections of PHNNEC mouse. PHNNEC mouse liver (right) is markedly increased for iron.

Ter119 and CD71 analysis of PHNNEC mouse bone marrow cells shows that Hb Null nucleated erythroid cells (Ter119+ EGFP+) developed grossly normally (Figure 43) compared with those from EGFP-EKLF/EKLF wild type mouse. Calculation of the ratio of nucleated erythroid cells to reticulocytes in PHNNEC mouse and wild type mouse bone marrow indicates that equivalent numbers of Hb Null nucleated erythroid precursors could only produce about 5% of the reticulocytes produced in the wild type mouse (Figures 39 and 44). mCherry+ cells in PHNNEC mouse peripheral blood increased to 1%, and nearly all of them were reticulocytes (Hoechst[low] Thiazole Orange+) (Figure 45), and these enucleated Hb Null cells could be readily identified on blood smears (Figure 46). Different stages of Hb Null erythroblasts, enucleating and enucleated cells can be easily found on the cytospin slides of dissociated cells from PHNNEC mouse bone marrow and spleen (Figures 47, 48, and 49).
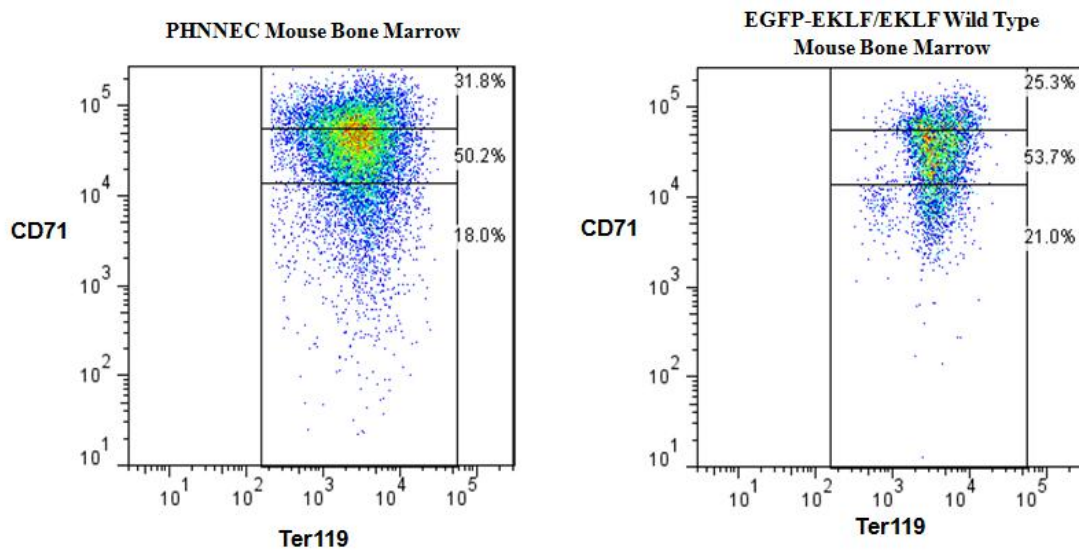
Figure 43. FACS analysis of nucleated Hb Null erythroid development in PHNNEC mouse bone marrow by CD71 and Ter119 staining. Ter119+ EGFP+ nucleated Hb Null and wild type erythroid cells respectively from PHNNEC mouse bone marrow (left) and EGFP-EKLF/EKLF wild type mouse bone marrow (right) are divided into three populations, R1 to R3, according to their CD71 expression. The ratio of each population of Hb Null cells is similar to that of the wild type cells. Dead cells were removed by SYTOX Blue.
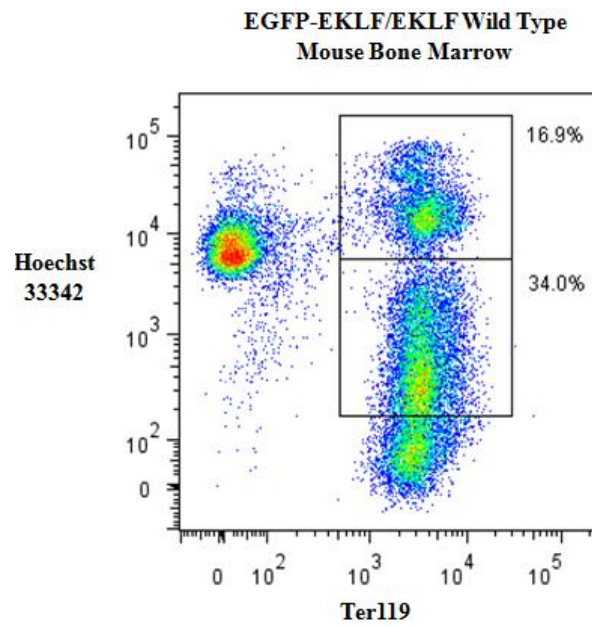
Figure 44. FACS analysis of reticulocyte production in EGFP-EKLF/EKLF wild type mouse bone marrow. The ratio of wild type nucleated erythroid cells to reticulocytes is 1:2 (16.9% : 34%).
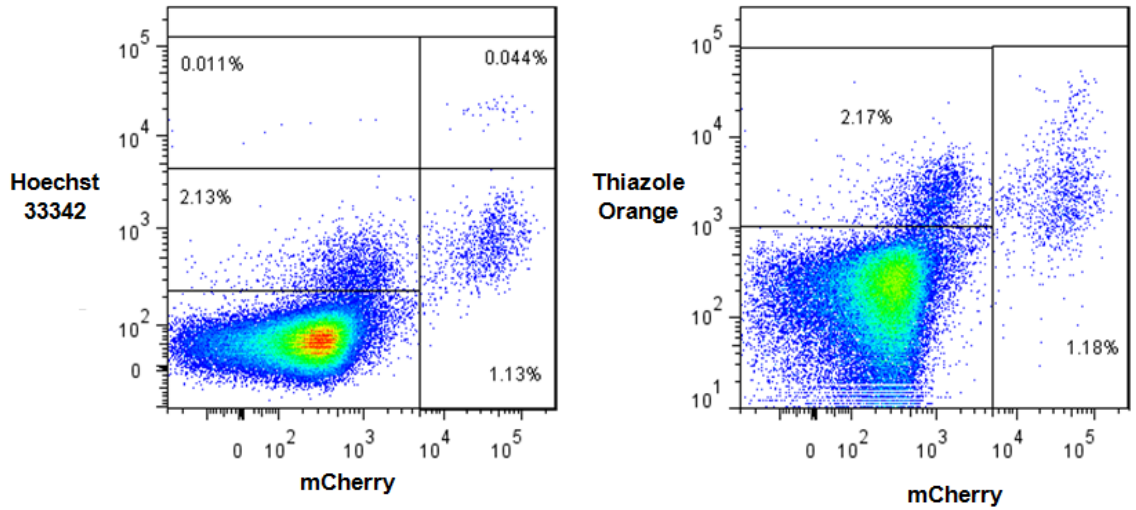
Figure 45. FACS analysis of PHNNEC mouse peripheral blood. Nearly all Hb Null erythroid cells (mCherry+) in blood are enucleated (Hoechst [low to negative]) (left plot) but still contained RNA (Thiazole Orange+) (right plot).
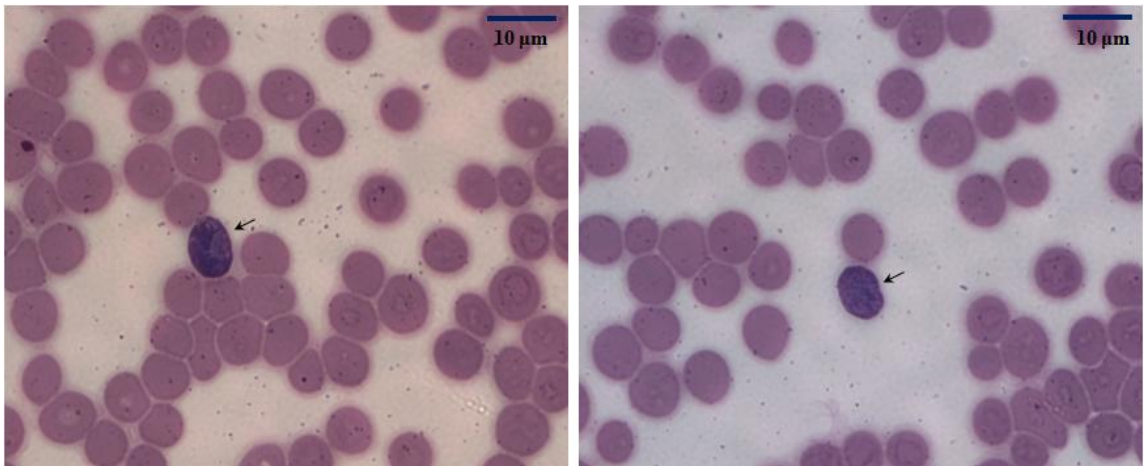
Figure 46. PHNNEC mouse peripheral blood smear stained by DipQuick solutions. Arrows: Hb Null enucleated erythroid cells.
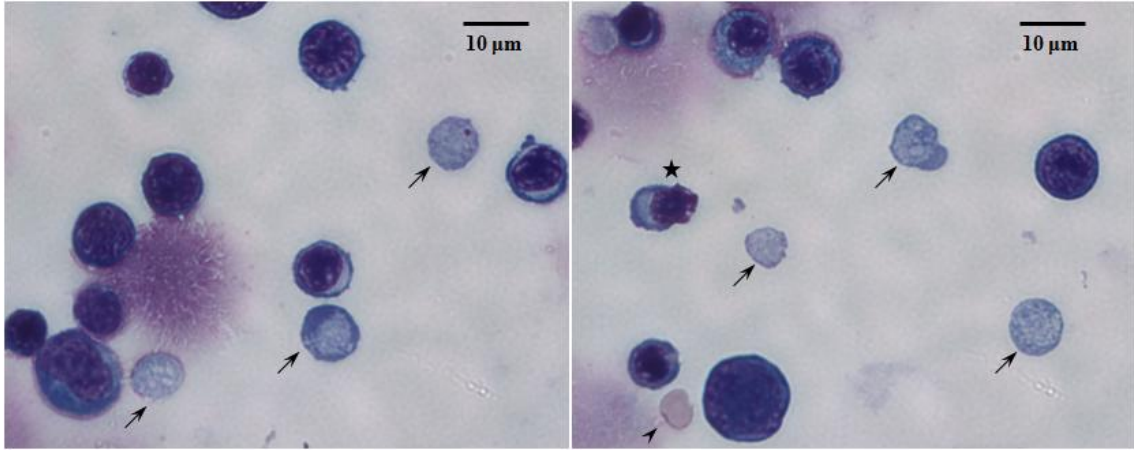
Figure 47. Cytospin and DipQuick staining of PHNNEC mouse bone marrow cells. Different stages of Hb Null nucleated erythroid cells and also enucleated cells (arrows) can be readily identified. Star: enucleating cell. Arrow heads: wild type enucleated erythroid cell.
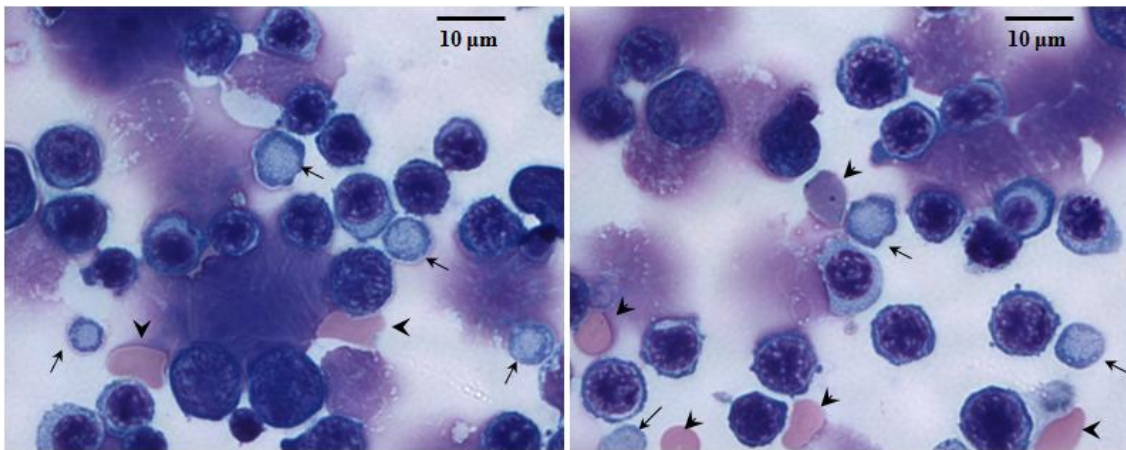
Figure 48. Cytospin and DipQuick staining of dissociated PHNNEC mouse spleen cells. Arrows: Hb Null enucleated erythroid cells. Arrow heads: wild type enucleated erythroid cells.
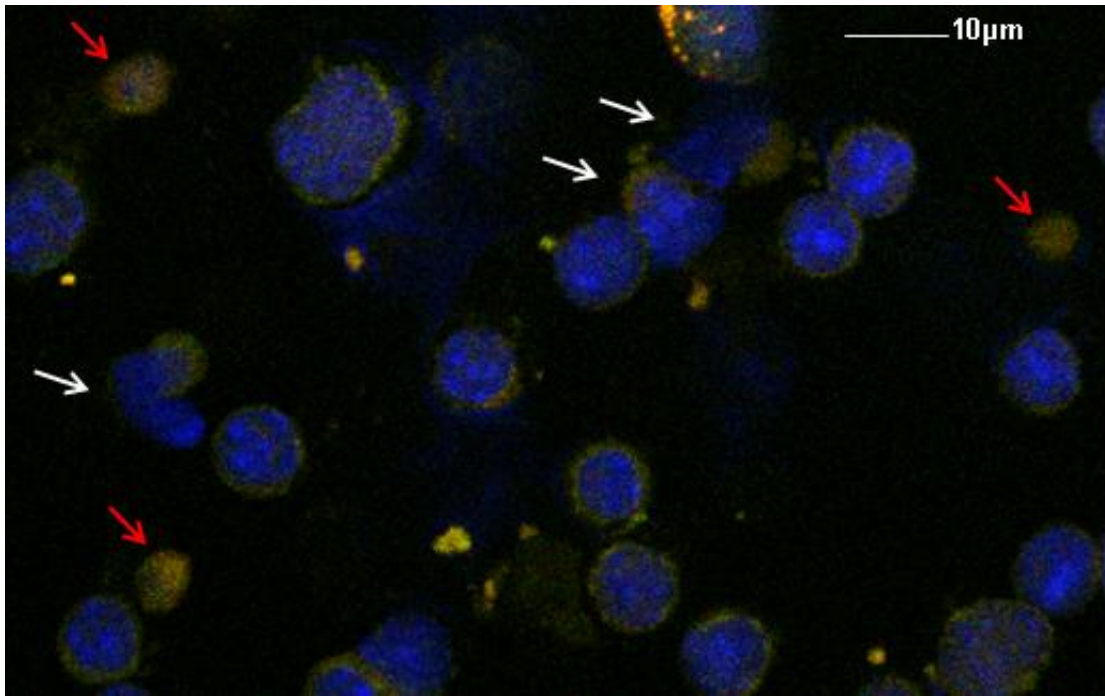
Figure 49. A representative fluorescence image of cytospin of dissociated cells from PHNNEC mouse spleen stained with Hoechst 33342. Red: mCherry. Green: EGFP. Blue: Hoechst 33342. White arrows: enucleating Hb Null erythroid cells. Red arrows: enucleated Hb Null erythroid cells.

Most importantly, this method enables us to observe Hb Null erythroid cells in situ. PHNNEC mouse bone marrow and spleen tissue sections clearly exhibit different stages of Hb Null erythroid cells, including numerous enucleating cells (Figure 50). I also examined PHNNEC mouse bone marrow and spleen tissues by electron microscopy (EM), and typical erythroblastic islands were identified, which are exemplified in Figure 51 that demonstrates an erythropoietic island containing a central macrophage surrounded by different stages of erythroblasts. Typical Hb Null enucleating erythroid cells were also observed by EM as displayed in Figure 52. Additionally, I did not observe obvious abnormalities in Hb Null nucleated cells in any of these morphological examinations.

Taken together, donor Hb Null HSCs transplanted into lethally irradiated wild type recipient mice, can successfully generate mice with pure Hb Null nucleated erythroid cells, and these Hb Null nucleated erythroid cells can be examined in situ by EM or tissue section staining. Hb Null enucleated cells were also greatly enriched in this mouse and can be easily observed from hematopoietic tissues (bone marrow, spleen and blood) without sorting. The results from this Hb Null transplant model fully confirm my previous observations in Hb Null chimeric mice. Namely, Hb Null erythroid cells can proliferate and differentiate all the way to reticulocytes. However, most Hb Null reticulocytes died in the bone marrow and were unable to enter the peripheral blood. The mechanism of reticulocyte death will be explored in the next chapter.
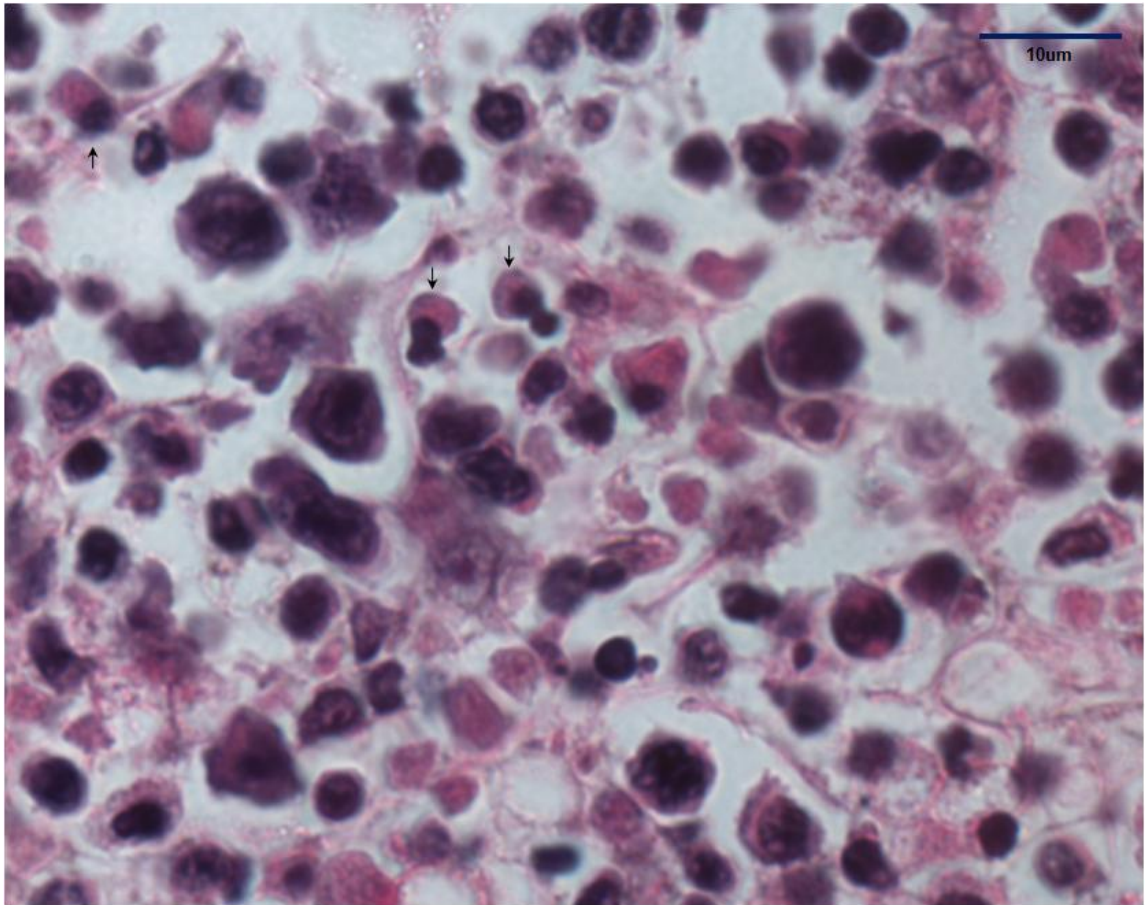
Figure 50. Hematoxylin and Eosin Staining of PHNNEC mouse bone marrow tissue section. Hb Null enucleating erythroid cells can be easily identified (arrows).
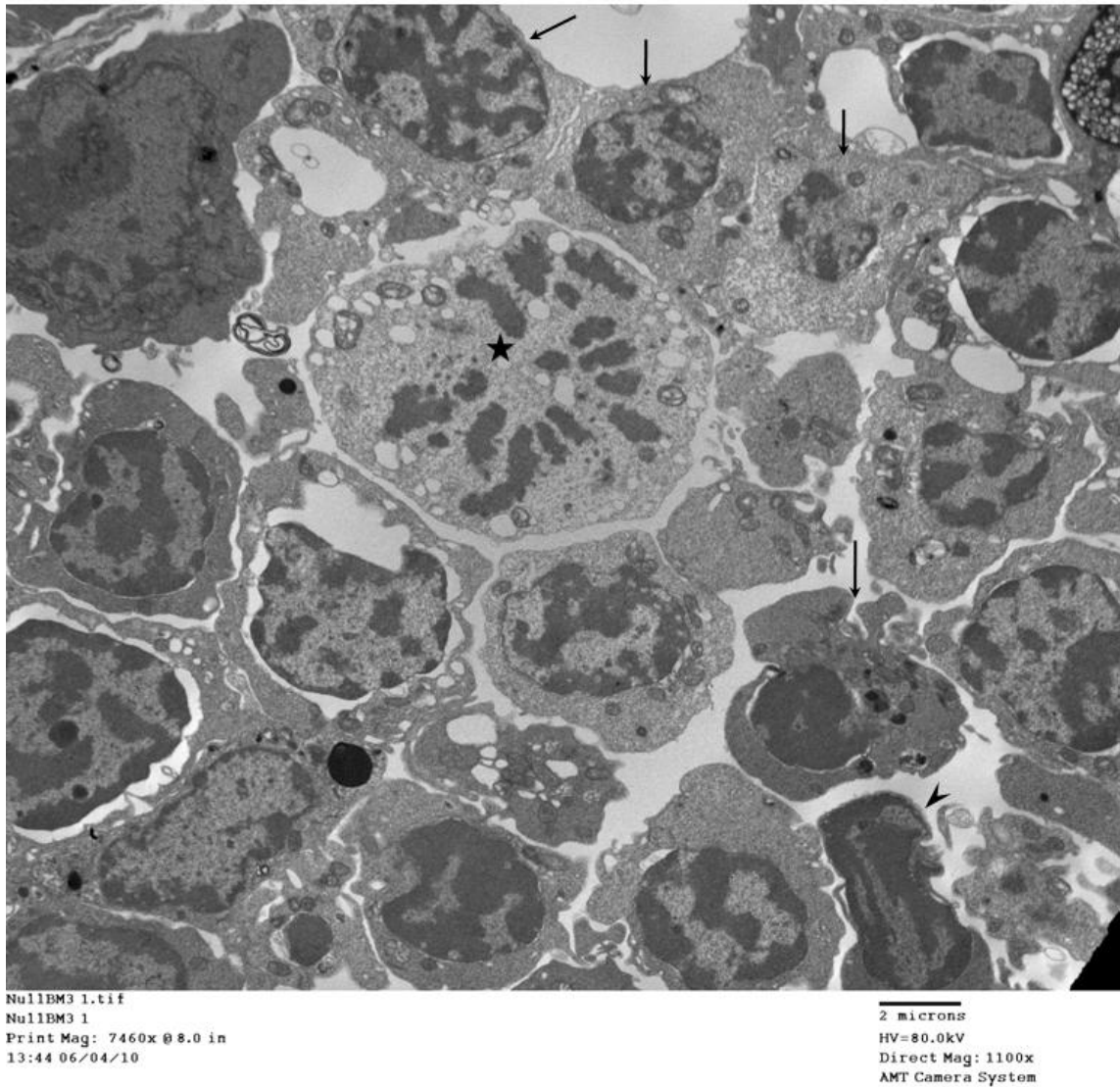
Figure 51. An EM picture of PHNNEC mouse bone marrow. A typical erythroblastic island is shown, including a presumable macrophage (star) surrounded by different stages of erythroblasts (arrows). An enucleating cell is also shown (arrow head).
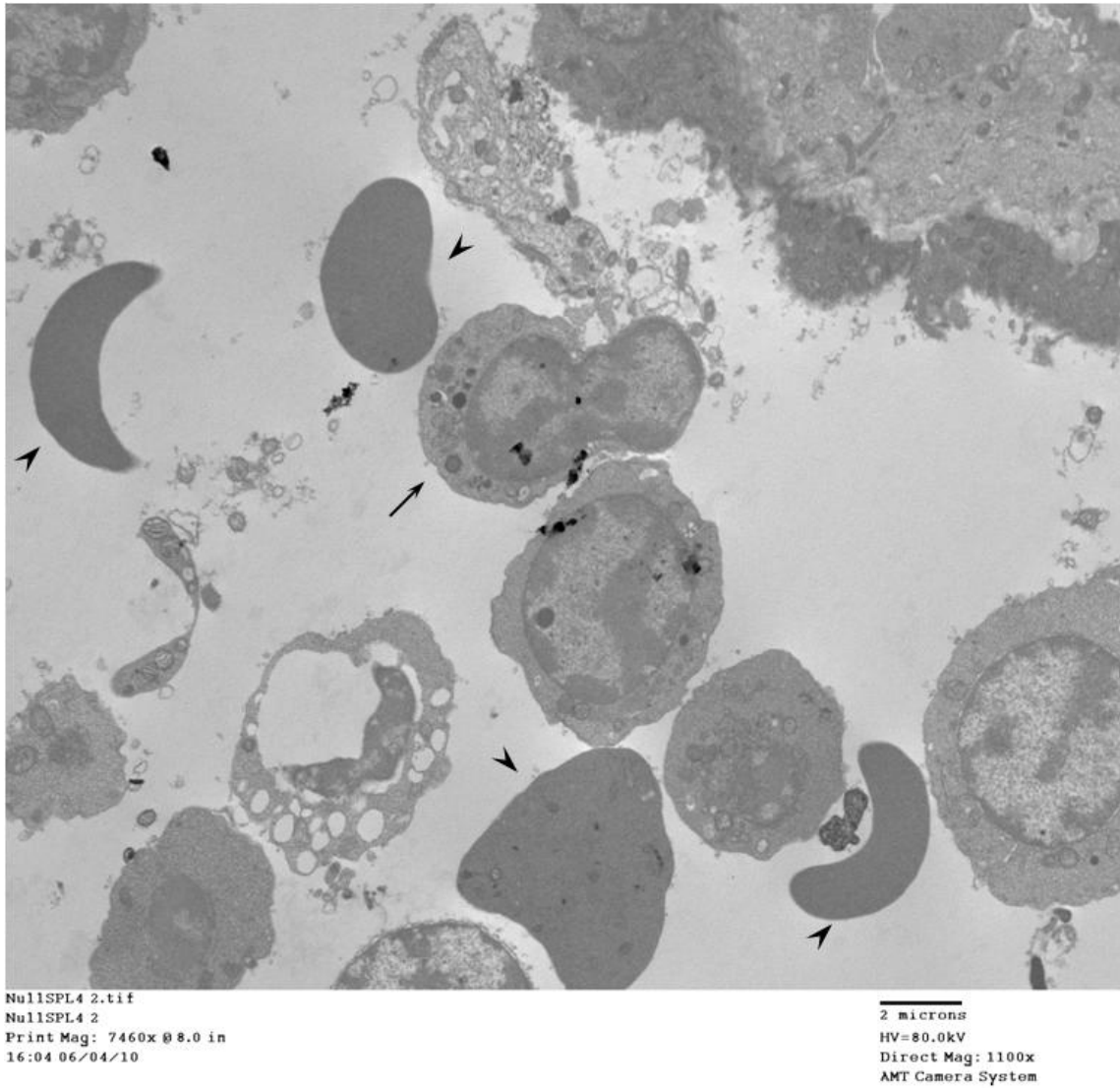
Figure 52. An EM picture of PHNNEC mouse spleen. A typical enucleating Hb Null erythroid cells (arrow) is found in spleen sinus. Arrow heads: wild type enucleated erythroid cells.

CHAPTER 6

HEME REGULATION IN HB NULL ERYTHROID CELLS

Through analysis of Hb Null chimeric and transplanted mice, I clearly show that Hb Null erythroid cells are underrepresented at the reticulocyte stage. What is the mechanism of Hb Null reticulocyte death? I propose that elevated free heme resulting from the absence of globin chains could play a critical role in Hb Null reticulocyte death. Studies have shown that elevated free heme level resulting from a defect in the heme exporter, FLVCR, can cause erythroid development to arrest at the proerythroblast stage[44]. In light of the fact that hemoglobin is the main force to eliminate free heme in erythroid cells, it was further proposed that the decrease in hemoglobin synthesis can also elevate free heme level, which could in turn impair erythroid development[44,48]. Evidence does exist showing that inhibition of protein synthesis in reticulocytes can increase intracellular free heme level[41,42]. Based on these earlier experiments, it is tempting to speculate that free heme can be incrementally built up in differentiating Hb Null erythroblasts as a consequence of the absence of globin chains until the free heme concentration reaches a toxic threshold that eventually kills the maturing cells at the reticulocyte stage.

Free Heme Detoxification by Human Myoglobin Could Not Rescue Hb Null Erythroid Cell Development

To test the hypothesis that the increasing free heme level in the absence of hemoglobin causes reticulocyte death, I attempted to express human myoglobin, a heme binding protein, specifically in Hb Null erythroid cells to detoxify the free heme to see whether Hb Null reticulocytes can be rescued. Myoglobin is a monomeric water soluble globular hemoprotein that is little affected by environmental conditions [81].

I tagged human myoglobin with mCherry at its 5' end to make a fusion protein and targeted this mCherry-myoglobin coding sequence to the mouse β globin locus downstream of the β^{major} globin gene promoter by homologous recombination in Hb Null EGFP-EKLF ES cells (Figures 53, 54, and 55). Correctly targeted mCherry-myoglobin knockin Hb Null EGFP-EKLF ES cells were micro-injected into 3.5-day C57BL/6J blastocysts to produce chimeric mice (Figure 14).
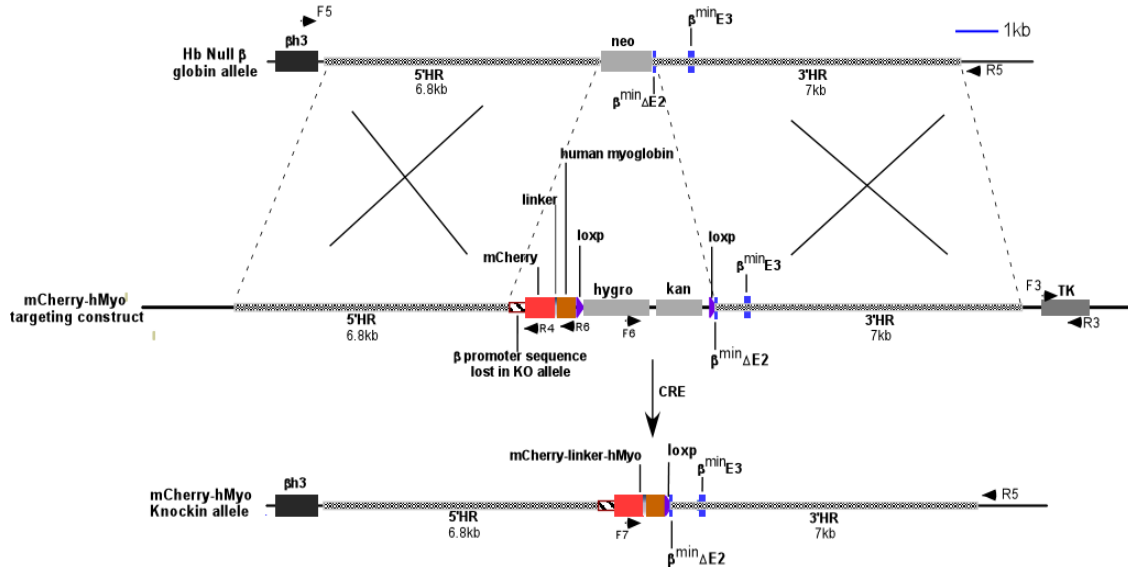
Figure 53. Schematic representation of human myoglobin targeting to mouse β globin locus. Human myoglobin (brown box) was tagged with mCherry (red box) at its 5' end, and a five-amino acid linker (Ser-Gly-Leu-Arg-Ser) was inserted between mCherry and human myoglobin. mCherry-linker-myoglobin coding cassette was targeted to β globin locus driven by the β^{major} globin gene promoter. Hatched box represents the β^{major} globin gene promoter sequence that was reinserted into the Hb Null β globin knockout allele upon myoglobin targeting. Homologous sequences (HR) are highlighted by thick grey dash lines. Arrow heads represent the primers used for colony screening. Neo is neomycin resistance gene. Hygro is hygromycin resistance gene. Kan is kanamycin resistance gene. TK is herpes simplex virus thymidine kinase gene. After targeting, selection markers were deleted by electroporation of plasmids expressing Cre into ES cells.

99
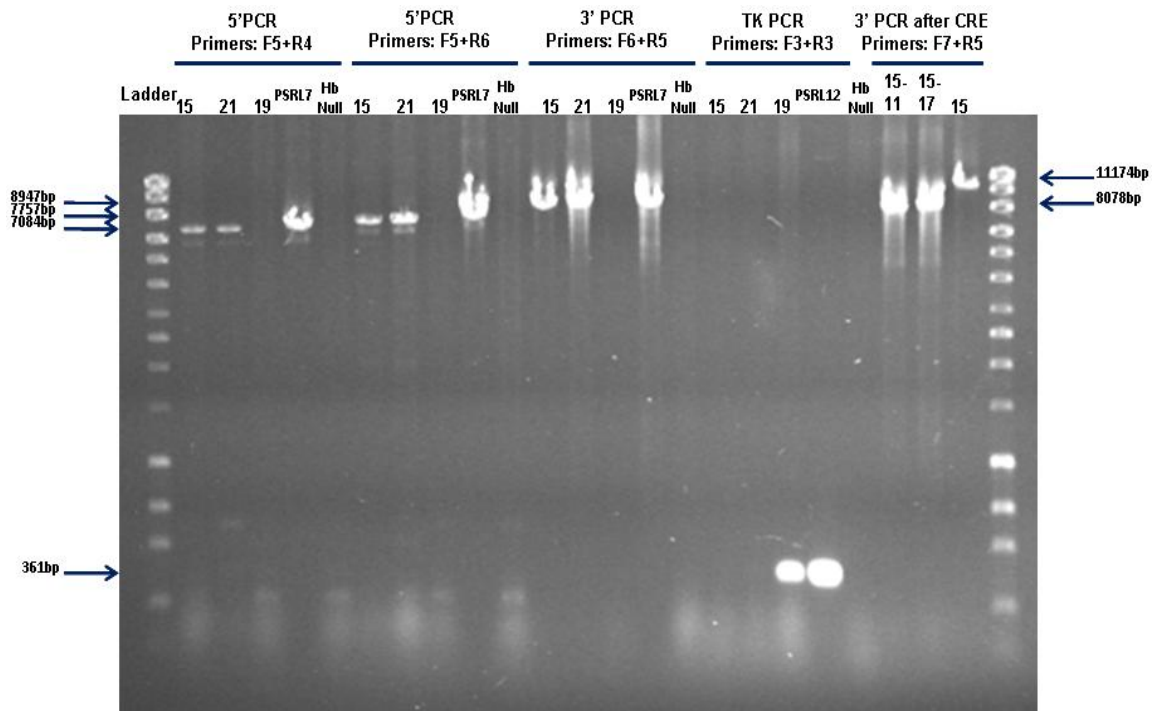
Figure 54. Hb Null ES cells (without EGFP targeting) and Hb Null EGFP-EKLF ES cells (Hb Null clone pSRL34-6-3) were targeted with a mCherry-human myoglobin construct (pSRL12). Clone #15 and 21 are positive for pSRL12 targeting (5' and 3' PCR +, and TK-) (Clone #15 has EGFP targeting, but Clone #21 has no EGFP-EKLF targeting). Clone #19 is negative for targeting (5' and 3' PCR -, and TK+). pSRL7 is the mouse β globin BAC with β^{major} and β^{minor} globin genes replaced by mCherry-human myoglobin used for positive control, and Hb Null clone pSRL34-6-3 ES cell DNA was used for negative control (Hb Null lane). The selection markers of Hb Null ES clone pSRL34-6-3-pSRL12-15 subclone #11 and #17 were successfully deleted by Cre.
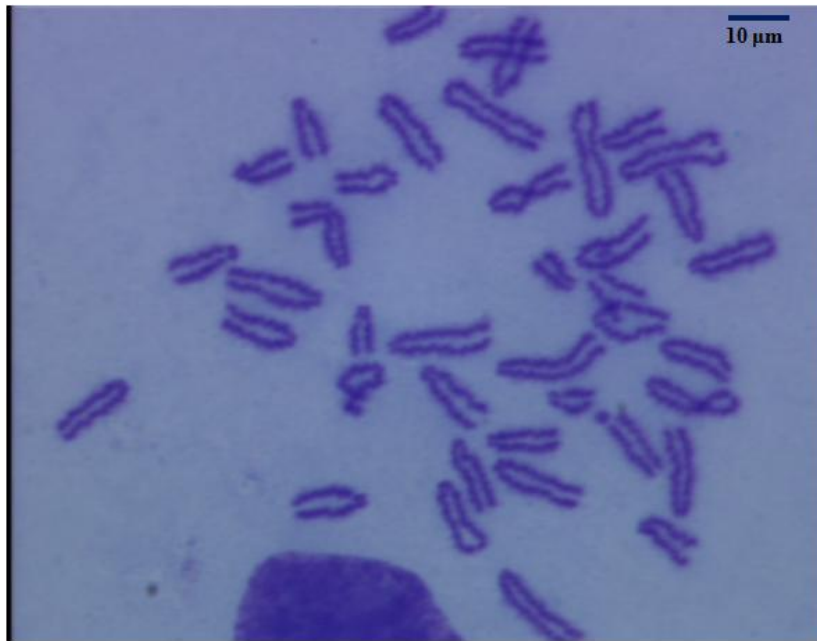
Hb Null clone pSRL34-6-3-pSRL12-15-17

Figure 55. Hb Null ES cells targeted with mCherry-human myoglobin have correct chromosome number.

I analyzed these chimeric mouse bone marrows, and found Hb Null erythroid cells expressing myoglobin developed similarly to those Hb Null erythroid cells without myoglobin. Namely, they could contribute to all stages of nucleated erythroid cells (EGFP+ Ter119+) at relative normal ratios (Figure 56), but were apparently still reduced in number at the reticulocyte stage. Calculation of the ratio of nucleated erythroid cells (Ter119+, Hoechst^{hi}, mCherry+) to reticulocytes (Ter119+, Hoechst^{low}, mCherry+) revealed that myoglobin-expressing Hb Null nucleated erythroid cells could only generate 4.8% of the reticulocytes that the same number of wild type nucleated erythroid cells could produce (Figure 57), implying that human myoglobin expression did not improve Hb Null reticulocyte survival, and that elevated free heme is unlikely the reason for Hb Null reticulocyte death.

**Wild Type
EGFP-EKLF/EKLF
Mouse Bone Marrow**

**mCherry-human myoglobin
EGFP-EKLF Hb Null ES
Cells-Derived Nucleated
Erythroid Cells in Chimera**

**mCherry-human myoglobin
EGFP-EKLF Hb Null
Chimeric Mouse Bone
Marrow**

**Wild Type Blastocyst-
Derived Nucleated
Erythroid Cells in Chimera**
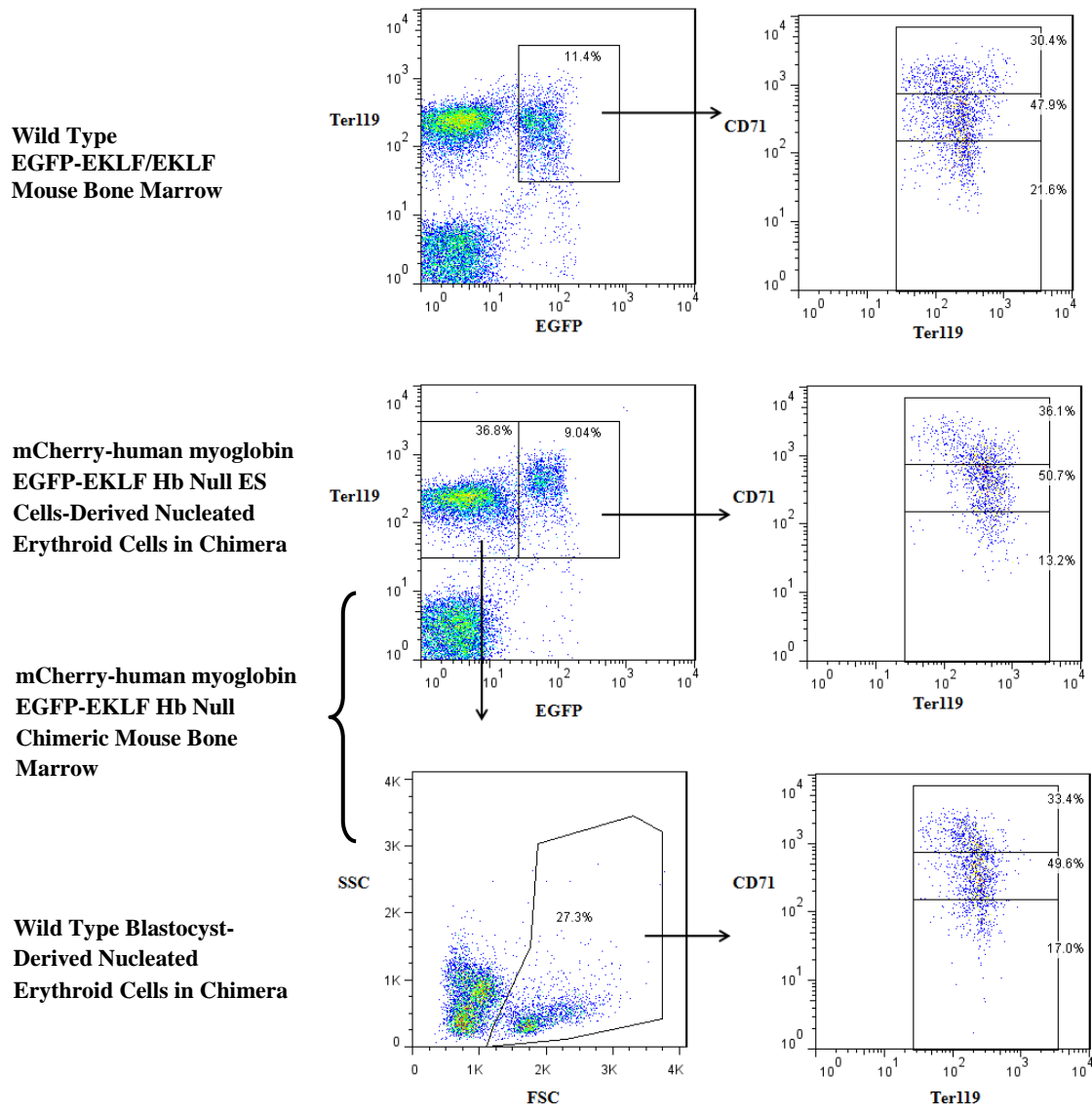
Figure 56.   CD71-Ter119 FACS analysis of human myoglobin-expressing Hb Null EGFP-EKLF nucleated erythroid cells in chimeric bone marrow. Dead cells were gated out by SYTOX Blue.
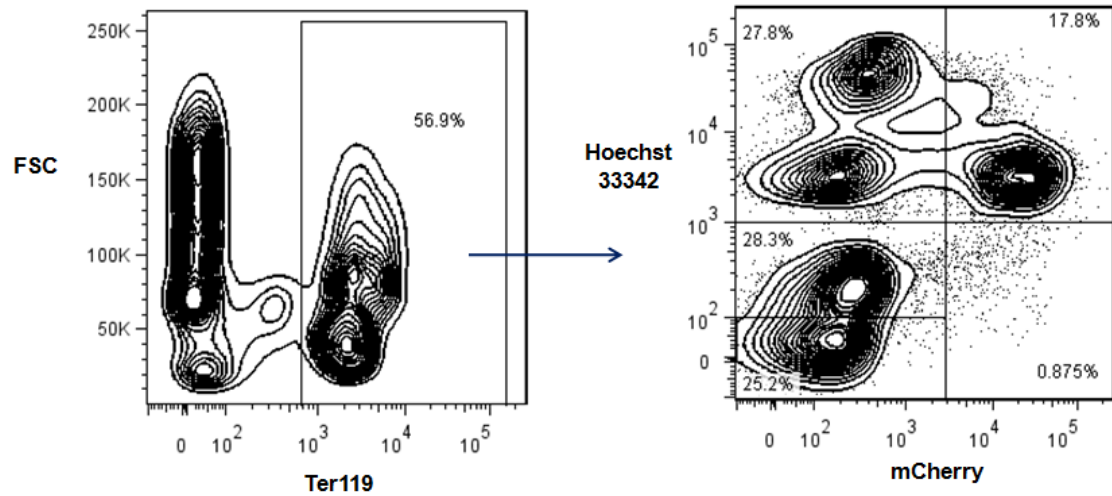
Figure 57. Human myoglobin expression did not improve Hb Null reticulocyte survival.
Total erythroid cells from mCherry-human myoglobin Hb Null EGFP-EKLF chimeric
bone marrow (Ter119+) (left plot) were analyzed by FACS for mCherry and Hoechst
33342 fluorescence (right plot). The ratio of nucleated erythroid cells (Ter119+ Hoechst[hi])
to reticulocytes (Ter119+ Hoechst[low]) in wild type cells (mCherry-) is 1:1 (27.8%: 28.3%),
whereas in Hb Null erythroid cells (mCherry+) the ratio is 20.3:1 (17.8%: 0.875%).

Gene Expression Analysis of Heme Pathway in Hb Null Erythroid Cells

I next asked the question of how the heme level is regulated in the absence of adult hemoglobin in definitive erythroid cells. Understanding heme regulation in erythroid cells is important because free heme can regulate gene expression. Since each globin chain of hemoglobin is destined to bind a heme moiety, the initial anomaly that arises in Hb Null erythroid cells must be some extra free heme. Heme is biosynthesized by a series of eight enzymes in the cytoplasm and mitochondria. 5-aminolevulinate synthase (ALAS), the first enzyme in heme production, exists in two isoforms-ubiquitously expressed ALAS1 and erythroid specific ALAS2[82]. Realtime PCR analysis of RNA isolated from sorted EGFP+ Ter119+ bone marrow cells demonstrated that neither isoform of ALAS was affected in Hb Null nucleated erythroid cells (Figure 58), which is in agreement with the notion that ALAS is not the rate-limiting enzyme for heme biosynthesis in erythroid cells and ALAS2 activity depends on the availability of iron for translation via the iron-responsive elements (IREs)/iron-regulatory proteins (IRPs) system[38] (Figure 2). I measured total heme content for Hb Null erythroid cells, and found that their total heme level (protein-bound and unbound) was greatly reduced compared with that in wild type cells (Figure 59). Protoporphyrinogen oxidase (PPOX) is the seventh enzyme that produces protoporphyrin IX, and ferrochelatase is the last enzyme with the function of inserting ferrous iron into protoporphyrin IX to form heme. Both of them have been previously reported by *in vitro* assays that their activities could be affected by free heme[83-85]. In this study, I found ferrochelatase transcripts were not altered in Hb Null nucleated erythroid cells, whereas PPOX was reduced about 50% compared with that in wild type cells (P=0.01) (Figure 58). Excess free heme could be degraded by heme

oxygenase, or exported by the heme exporter FLVCR. There are two isozymes for heme

oxygenase, heme inducible HO-1 and constitutive expressed HO-2[82]. However, neither of

them was changed in Hb Null erythroid cells (Figure 58). In addition, FLVCR was barely

detectable in EGFP+ Ter119+ nucleated erythroid cells (Figure 58), implying it may not

play an important role in maintaining the free heme level in the erythroid precursor stages,

which include cells at least from late proerythroblasts to orthochromatic erythroblasts.

Studies have shown that erythroid specific HRI mRNA levels can be increased by heme

in erythroid cell lines[86]. In our study, although HRI mRNA in Hb Null erythroid cells is

increased about 25% when normalized by actin and compared with that in wild type cells

(P=0.009), the statistical significance of this increase disappeared if the normalizer was

changed to EF1α (P= 0.58) (Figure 58), indicating the free heme level may be only

marginally, if any, elevated.

Erythroid cells acquire iron from the plasma via the transferrin receptor CD71. Given that

the CD71 expression profile of Hb Null nucleated erythroid cells is similar to that of wild

type cells (Figure 26) an initial excess of free heme must restrict iron absorption on

and/or after transferrin endocytosis steps as has been proposed by others[38]. Cytoplasm

iron is transported into mitochondria by mitoferrin[87]. Ubiquitous mitoferrin2 mRNA is

expressed at low levels and shows no difference between Hb Null and wild type

nucleated erythroid cells. Erythroid specific mitoferrin1 mRNA is decreased albeit not

significantly (P=0.17) in Hb Null erythroid cells (Figure 58), suggesting Hb Null

erythroid cells might also restrict iron entering mitochondria for producing otherwise

even more free heme. Excessive iron can be sequestered in ferritin or exported out of

cells by ferroportin (FPN1)[88]. Ferroportin has two transcripts, FPN1A and FPN1B, and

FPN1B is the major source of encoded FPN1 and correlates with protein expression in erythroid precursors[89]. None of these three mRNA (ferritin, FPN1A and FPN1B) expression levels was significantly different between Hb Null and wild type nucleated erythroid cells (Figure 58).
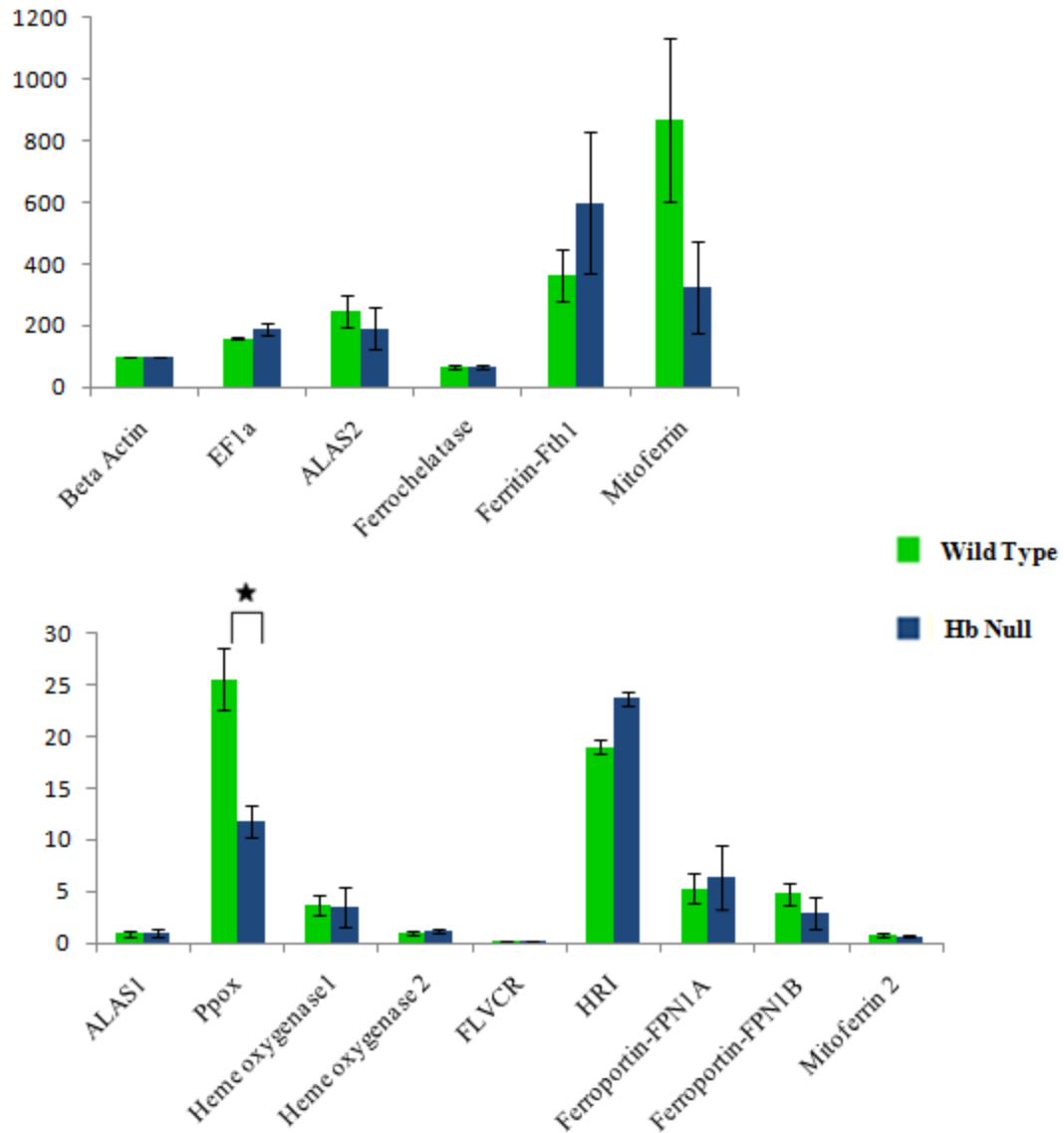
Figure 58. Realtime PCR analysis of genes regulating heme and iron. EGFP and Ter119 double positive cells were sorted from three Hb Null chimera and three EGFP-EKLF/EKLF wild type mouse bone marrows. Beta actin is used as the normalizer. Error bar: S.E.M. Star: $P=0.01$ (N=3, two-tailed Student's t- test).
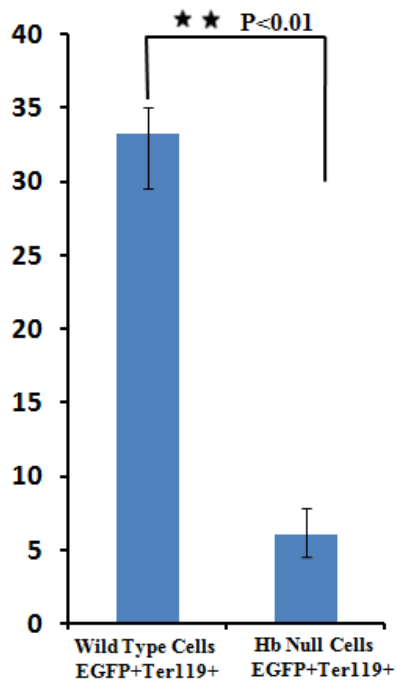
Figure 59. Total heme content in Hb Null and wild type erythroid cells. EGFP+Ter119+ cells sorted from three Hb Null chimeric mouse bone marrows and also from three wild type C57BL/6J mouse bone marrows were measured for total intracellular heme content. The average heme level in sorted wild type erythroid cells is 33.3 pmol/10^6 cells, and in sorted Hb Null erythroid cells is 6.1 pmol/10^6 cells. Star: P=0.0098 (N=3, two-tailed Student's t- test).

Excess free heme would generate more ROS which can further elicit cell death through apoptosis[37,90]. Apoptosis caused by heme and/or ROS has been implicated in several red cell diseases[91-93]. A variety of ROS were evaluated by fluorescent probes RedoxSensor Red CC-1[94,95] and dihydroethidium[96,97] via flow cytometry, and I found Hb Null nucleated erythroid cells (EGFP+) exhibited ROS at a similar level to wild type cells (Figure 60). Apoptosis was assessed by labeling nucleated erythroid cells (EGFP+ Ter119+) with Annexin V, and the expression profiles of Annexin V (SYTOX blue-Annexin V+) were also very similar between Hb Null and wild type erythroid cells (Figure 61).
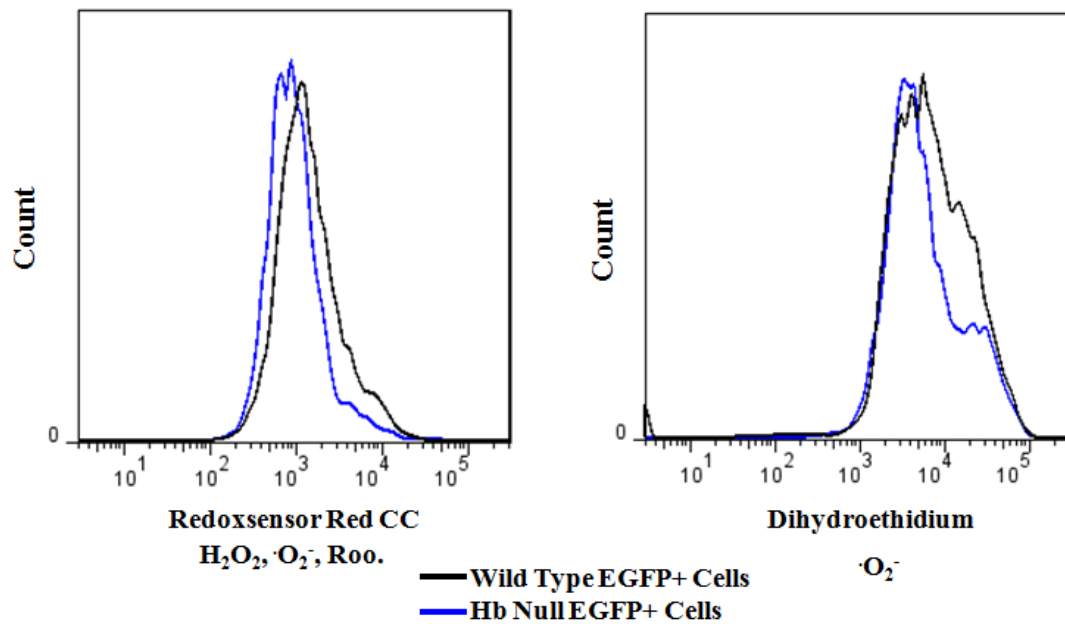
Figure 60. A representative ROS measurement of Hb Null nucleated erythroid cells by fluorescent probes RedoxSensor Red CC (left) and Dihydroethidium (right). EGFP+ cells were gated from Hb Null chimera (blue) and EGFP-EKLF/EKLF wild type (black) mouse bone marrow. Dead cells were removed by SYTOX Blue. RedoxSensor Red CC can detect H_2O_2, .O2-, ROO. and Dihydroethidium can detect .O2-.
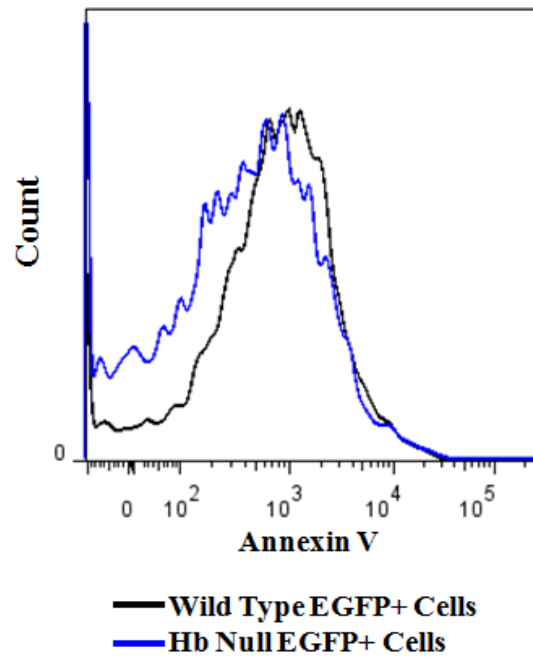
Figure 61. Apoptotic assay of Hb Null nucleated erythroid cells by Annexin V staining.

EGFP+ cells were gated from Hb Null chimera (blue) and EGFP-EKLF/EKLF wild type

(black) mouse bone marrow. Dead cells were removed by SYTOX Blue.

Collectively, the above data strongly argue that the free heme in Hb Null erythroid cells is maintained at a relatively normal level similar to that in wild type erythroid cells. Maintaining a normal free heme level in the absence of hemoglobin could be achieved by a free heme-initiated negative feedback control of iron absorption and its mitochondrial transport, and this iron limitation can subsequently inhibit the heme biosynthetic enzyme ALAS2 activity by binding of activated IRPs to the IRE of its mRNA 5'UTR[38,88]. The initial extra uncommitted free heme in Hb Null erythroid cells could be the trigger for this auto-regulation. Additionally, I found free heme can also directly inhibit PPOX expression. Reduced ALAS2 and PPOX activities not only suppress further elevation of free heme, but also protect Hb Null erythroid cells from generating toxic heme biosynthetic intermediate products as illustrated in porphyria diseases.

DISCUSSION

Hemoglobin was described more than 160 years ago[98]. Hemoglobin is well known for its function as the oxygen carrier in erythrocytes. However, its importance in erythroid cell development has never been well studied. In this dissertation, definitive erythroid cells without any adult hemoglobin were successfully generated, and I found hemoglobin is not essential for nucleated erythroid cell commitment, differentiation, and maturation. However, hemoglobin does play an important role in reticulocyte survival and its terminal maturation to RBCs.

In the absence of adult hemoglobin, mouse embryos died between E10.5 and E12.5 (Table 1). Primitive erythroid cells are predominant in the circulation until E12.5 to E13.5[5]. Absence of primitive RBCs leads to fetal death between E9.5 and E10.5 as exemplified by SCL and GATA1 knockout mice[99-101]. Lack of c-myb results in complete elimination of definitive red cells and mice die between E15.5 and E16.5[102]. In light of these reports, our results indicate that Hb Null primitive erythroid cells were compromised. Additionally, it has been reported that homozygous α globin knockout mice ($m\alpha^{0/0} m\beta^{+/+}$) die between E14.5 and E16.5[56]. In this study, about 80% embryos with a single adult β globin allele ($m\alpha^{0/0} m\beta^{0/+}$) were still alive at E12.5. The longer survival time of these embryos with only β globin gene expression than those embryos without any hemoglobin (Hb Null) suggests that, comparing with the complete absence of hemoglobin ($m\alpha^{0/0} m\beta^{0/0}$), solely β globin gene expression ($m\alpha^{0/0} m\beta^{+/+}$ or $m\alpha^{0/0} m\beta^{0/+}$)

could confer some survival or functional advantage for the primitive erythroid cells, which is surprising since they are thalassemic[5]. In fact, many lines of evidence suggest excess β globin chains are not as toxic as excess α globin chains. Excess β globin can form β4 tetramers which are more soluble and stable than unpaired α globin chains[64]; β globin precipitates exist in late instead of early erythroid precursors[103]; the stability of α thalassemic RBC membranes are normal or only marginally affected[104]; relative to β thalassemia, α thalassemia phenotype is mild[105,106]; unlike α globin precipitates, excess β globin precipitates don't influence erythroid proliferation[103]; in α thalassemia, the apoptosis of erythroid progenitors is normal or only moderately increased[106,107]. In this study, the advantage of β globin expression in primitive cells is further documented by the examination of erythroid development in mouse fetal livers with a single β allele ($m\alpha^{0/0}$ $m\beta^{0/+}$). At E12.5, their FACS profiles are very similar to those of wild type embryos (Figure 7), implying that in these embryos ($m\alpha^{0/0}$ $m\beta^{0/+}$), primitive cells can still function and support fetal liver development which could in turn support definitive erythropoiesis. The developmental block for the fetal liver with a single α allele (Figure 7) could be due to the toxic effect from excess α globin chains. Another alternative explanation is definitive erythroid cells with a single β allele expression are more resistant to anemic stress, but this wouldn't explain why homozygous α knockout embryos could survive longer than Hb Null embryos, because at E12.5, the prevalent cells are primitive cells. Also, definitive erythroid cells with only β globin gene expression wouldn't be functional for oxygen delivery due to the high oxygen affinity of the β4 tetramer[108,109].

Although FACS data of fetal liver cells from Hb Null embryos show that definitive erythroid cells were blocked at the pro-/basophilic erythroblast stage (Figure 7), the presence of relatively normal Hb Null derived nucleated erythroid cells in chimeric mice suggest that the early block in Hb Null embryos was actually an indirect effect of profound anemia that results in severe impairment of the fetal liver microenvironment. Early embryonic death from severe anemia also make it difficult to exhaustively study many other genes' function in the homozygous knockout mice, such as gene knockouts of ALAS2[35], GATA1[110,111] and transferrin receptor[112]. In this study, I took advantage of chimeric mice, in which the wild type erythroid cells could support the developing embryos into adulthood.

By tagging EKLF with EGFP, I was able to track the nucleated Hb Null derived erythroid cells in chimeras (Figures 14, 20, 21), and surprisingly, no major aberrations were observed during nucleated definitive erythroid development (Figures 26, 27, 28). Nucleated Hb Null erythroid cells can progressively decrease cell size and condense their nuclei (Figure 27).

The FACS plot of CD71 versus Ter119 has been widely utilized to segregate different stages of erythroid cells[62,63]. An improvement of this method based on the expression of CD44 versus FSC claims a better resolution of developing stages of erythroblasts[27]. In practice, however, there is significant overlap of these different stages of erythroid cells using either method. Especially for reticulocytes, which express high levels of both CD71 (Figure 38) and CD44, can greatly skew the interpretation of the results. To avoid this issue, reticulocytes in the bone marrow can be gated out by their lack of EGFP-EKLF expression (Figure 20), lack of nuclear dye staining by Hoechst or Dyecycle Violet

(Figure 33), or simply by their FSC and SSC properties (Figure 22). An additional staining with Thiazole Orange or CD71 can further separate reticulocytes from mature erythrocytes (Figure 33). In this regard, I found CD71 staining provides a better isolation of reticulocytes than CD44. Nevertheless, nucleated Hb Null erythroid cells displayed normal FACS profiles for both CD71 versus Ter119 and CD44 versus FSC (Figures 26, 28), suggesting they develop *in vivo* similar to wild type erythroid cells.

However, under nonphysiological conditions, as exemplified by *in vitro* terminal differentiation of ES-EP cells, all Hb Null nucleated erythroid cells died through apoptosis (Figure 13), suggesting that Hb Null erythroid cells have a reduced capability to resist micro-environmental stress. I also found that Hb Null nucleated erythroid cells are more fragile than their wild type counterparts. So there must still be some defects that exist in nucleated Hb Null erythroid cells, but are not manifested under optimal *in vivo* conditions and remain to be further investigated.

To further trace Hb Null enucleated erythroid cells, mCherry was targeted into the β globin locus driven by the endogenous mouse β^{major} globin gene promoter (Figure 29). I discovered that Hb Null erythroid cells can enucleate and form reticulocytes (Figures 33, 34, 35). However, those Hb Null reticulocytes were produced at less than 10% of the wild type levels (Figures 37, 38), and very few of them could be detected in the peripheral blood (Figures 35, 45). Thus, although all Hb Null erythroid cells in chimeras could be tracked by mCherry expression, the high level expression of mCherry inside the RBC did not rescue the terminal maturation of Hb Null erythroid cells.

In an effort to examine Hb Null erythroid cells in situ, I transplanted CD45.1+ and EGFP+ Hb Null hematopoietic cells into lethally irradiated wild type C57BL/6J mice (Figure 14). Engrafted mice survived between 4 to 12 weeks post-transplantation with progressive decrease of body weight and hematocrit. In the PHNNEC mouse that was examined at 12 weeks post-transplantation, all nucleated erythroid cells were derived from the transplanted donor Hb Null HSCs (Figures 39, 40). This PHNNEC mouse developed splenomegaly (Figure 41), osteopenia, and liver iron overload (Figure 42), indicating the presence of massive ineffective erythropoiesis. Different stages of nucleated erythroid cells, including numerous enucleating erythroid cells were observed in situ by EM and in histological tissue sections (Figures 50, 51, 52). Many enucleated Hb Null reticulocytes were readily found in bone marrow and spleen cytospin slides (Figures 47, 48, 49). This PHNNEC data confirmed the results found in the Hb Null chimeras that under optimal physiological conditions, Hb Null nucleated erythroid cells develop relatively normally. This transplant model system differs from the report by Rivella et al.[113] in which E14.5 fetal liver cells from homozygous β globin knockout mice (Hbb$^{th3/th3}$) were transplanted into lethally irradiated C57BL/6J mice. Those engrafted mice survived between 7 to 9 weeks after transplantation and served as a Cooley's anemia mouse model.

Studies have shown that common myeloid progenitors (CMPs) and MEPs but not granulocyte/monocyte-restricted progenitors (GMPs) can protect lethally irradiated mice from death within 12-18 days caused by bone marrow failure, suggesting that erythrocytes, platelets, or both are the critical effectors of radioprotection[114]. Since Hb Null erythroid cells do not enter the peripheral blood in large numbers and do not have

118

the capacity to functionally deliver oxygen due to the absence of hemoglobin, the radioprotective activity of transplanted Hb Null CD45.1+ and EGFP+ cells strongly supports the notion that it is the platelets that actually provide the protection against bone marrow failure.

Diamond-Blackfan anemia (DBA) is a pure red blood cell aplasia of childhood that can be caused by ribosomal protein mutations. It's still an unanswered question why the dysfunction of ubiquitously expressed ribosome proteins can render an erythroid specific phenotype[115]. It's been recently proposed that the reduction of hemoglobin synthesis resulting from impaired ribosome biogenesis can lead to a relative excess of intracellular free heme that then kills erythroid cells at the CFU-E to proerythroblast stage of development[44,48]. This proposition is based on the fact that mice with knockout of heme exporter FLVCR have a similar phenotype as DBA and their erythroid development was blocked at the proerythroblast stage[44]. However, in this study, in the complete absence of adult hemoglobin, definitive erythroid cells can develop well beyond the proerythroblast stage, and no arrest is seen at any nucleated erythroblast stage (Figures 26, 27, 28, 43), indicating that free heme toxicity is unlikely the cause for the anemia in DBA disease. Additionally, so far there have been no reports for FLVCR mutations in DBA patients. Since hemoglobin is the major force to detoxify free heme in erythroid cells, there is an apparent discrepancy between our study and the FLVCR knockout report[44]. One possible explanation is that at the CFU-E and proerythroblast stages, the majority of heme is utilized by non-hemoglobin proteins[116], and FLVCR may play a more critical role than hemoglobin in maintaining free heme level at these early stages. However, this explanation cannot answer why FLVCR defect can result in an erythroid specific

phenotype. An alternative possibility is that the anemia caused by FLVCR deletion might be an indirect effect of macrophage malfunction. This assumption is based on the evidence that (1) FLVCR is highly expressed on macrophages and FLVCR knockout impairs CFU-GM colony growth[44]; (2) the macrophages in erythroblastic islands function as a "nurse" cell providing interactions that support erythroid proliferation and differentiation[117]; (3) heme oxygenase 1 knockout can cause macrophage cell death from elevated heme leading to anemia[118]; (4) a considerable number of CFU-Es adhering to macrophages were found in erythroblastic islands[119], and the abrogation of stromal macrophages of splenic red pulp of phlebotomized mice suppressed erythropoiesis at the CFU-E level[120]. FLVCR knockout chimeric mice will be informative in discriminating this indirect effect of macrophages from intrinsic erythroid defects caused by FLVCR deletion.

In this study, I found the total heme level is decreased in Hb Null nucleated erythroid cells (Figure 59), indicating that in the absence of hemoglobin, erythroid cells can effectively limit their heme biosynthesis and maintain a relative balance between heme and globin chains. It is known that free heme can inhibit iron absorption in erythroid cells, but it is unclear at which step this inhibition occurs[38]. This inhibition is certainly not through reducing transferrin receptor expression since CD71 expression profiles are similar between Hb Null and wild type nucleated erythroid cells (Figures 26, 43). Free heme might also influence iron access into mitochondria, since mitoferrin1 transcripts show tendency of decrease in Hb Null erythroid cells (Figure 58, P=0.17). It has been well accepted that iron reduction can inhibit heme biosynthesis by suppressing ALAS2 translation via activation of IRPs[38,88]. Here, I show that free heme might also exert

negative feedback directly by inhibition of PPOX expression (Figure 58), but the mechanism needs to be further explored. HO-1 can be induced at the transcriptional level by free heme and ROS[82,121], but its role in erythroid cells is not fully understood. It's been shown that in ALAS2^{-/-} erythroblasts HO-1 transcripts are decreased[122], and in murine erythroleukemia (MEL) β thalassemic model HO-1 expression is increased[123]. However, in our Hb Null erythroblasts HO-1 mRNA level is not altered compared with wild type cells (Figure 58), implicating that HO-1 might not play a critical role in erythroid cells, or the uncommitted free heme and ROS levels are not significantly elevated to induce HO-1 expression. Indeed, by using different ROS probes, I found the ROS level of Hb Null nucleated erythroid cells is not altered (Figure 61). Taken together, these data suggest that erythroid cells have a strong ability to auto-regulate the heme biosynthetic pathway, and in the absence of hemoglobin, the initial generated uncommitted heme can elicit a negative feedback control for heme biosynthesis to prevent further free heme elevation and maintain free heme at a relative normal range. This notion is consistent with the observation that in β thalassemic erythroid cells, HRI is activated by denatured globins[124] instead of inactivation by free heme which presumably can result from the β globin reduction. It also reconciles with the finding that inhibition of protein synthesis by cycloheximide or puromycin in reticulocytes resulted in the reduction of heme synthesis[125], and favors the view that the synthesis of globin plays a role in regulating the synthesis of heme[125].

It is an intriguing question why in the absence of hemoglobin, there are only a few Hb Null reticulocytes develop in the chimeric bone marrow (Figures 37, 38). The facts that Hb Null nucleated erythroid cells are not accumulated at the orthochromatic erythroblasts

(Figures 26, 27, 28, 43), and that there are plenty of enucleating erythroid cells seen on PHNNEC mouse bone marrow (Figure 50) and spleen tissue sections, imply that all Hb Null erythroid cells have the ability to enucleate and they die after the enucleation. It is unlikely that these reticulocytes die through apoptosis *in vivo* since no sign of increased apoptosis was detected for Hb Null erythroid cells in chimeric bone marrows (Figure 61). Additionally, less than 1% Mac-1+ monocytes were found in PHNNEC mouse spleen (Figure 62) and they are simply not numerous enough to phagocytose all the potential apoptotic reticulocytes. Expression of human myoglobin cannot rescue these reticulocytes (Figure 57), lending support for the notion that excess free heme, if any, is unlikely the reason for their death.

It's been generally accepted that reticulocytes need to traverse pores in the sinus walls, which separate the marrow hematopoietic cords from sinus compartments, to gain access to the circulation[126-128]. The driving force for this migration may come from a hydrostatic pressure difference across the pore[129]. The average diameter of those pores was estimated to be around 3 μm[128,130]. To squeeze through these small openings, reticulocytes have to show remarkable flexibility and deformability. One determinant of RBC deformability is the homogeneous fluid hemoglobin contents[131-133]. Erythrocytes with hypoosmolality (214 mosmol/kg H_2O) and decreased mean corpuscular hemoglobin concentration (MCHC) have greatly reduced deformability, and most of them were lysed when passing through 2.6 μm pores[133]. I predict that in the absence of hemoglobin, reticulocytes would lose most of their deformability and flexibility, and could be easily lysed by the mechanical stress encountered in the process of egress to the bone marrow sinuses. In fact, I do find Hb Null nucleated erythroid cells are more fragile and susceptible to lysis

during handling than wild type cells. This hypothesis does not exclude other possibilities that may contribute to Hb Null reticulocyte death. It is noteworthy that the expression of mCherry or human myoglobin from one β globin locus driven by the $β^{major}$ globin gene promoter could not rescue Hb Null reticulocyte survival. This could be due to the amount of protein synthesized is not as high as the globin chains expressed in wild type reticulocytes, or this could suggest that reticulocytes specifically need hemoglobin, especially β globin chains, to survive and fully mature. The broad inactions between hemoglobin and the cytoskeleton[17,20,21,26] could play roles in the latter possibility.
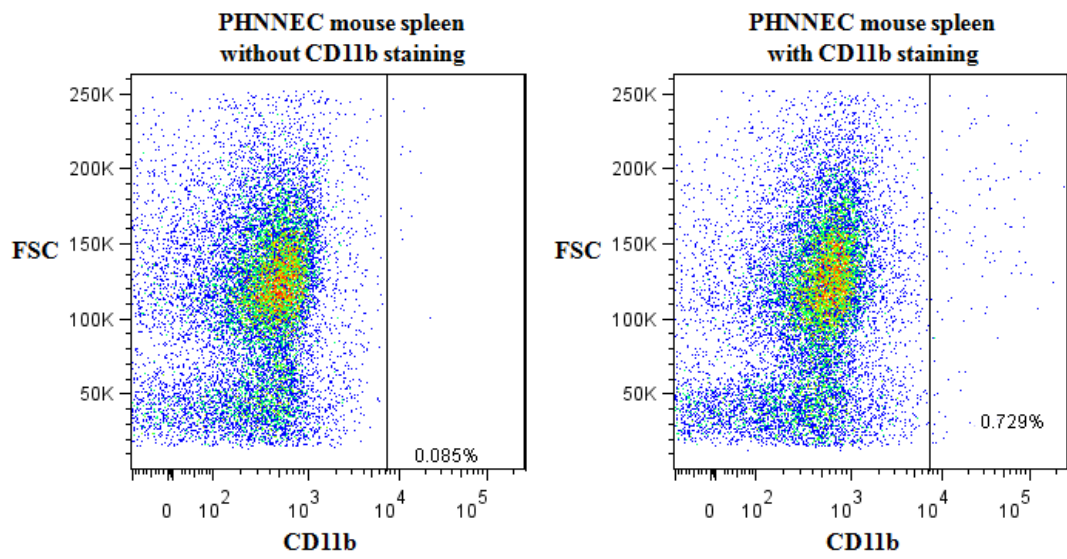
Figure 62. Less than 1% CD11b+ macrophage existing in PHNNEC mouse spleen.

FUTURE DIRECTIONS

The mechanism of hemoglobin's importance for reticulocyte survival remains to be answered. This issue can be divided into two aspects. First, the hemoglobin's importance may come from its quantity that is expressed in erythroid cells. In wild type definitive erythroid cells, globin genes are expressed from 4 alleles and 8 genes (four α globin genes and four β globin genes). In this study, I specifically expressed mCherry and mCherry tagged myoglobin in Hb Null erythroid cells from one single β^{major} globin gene promoter. In wild type mice, the ratio of β^{major} to β^{minor} is about 4 to 1[6,134]. Thus, the amount of mCherry or mCherry tagged myoglobin synthesized may only be about 20% of the total globin chains synthesized in wild type erythroid cells. However, so far there have been no studies focusing on the influence of different amount of hemoglobin on erythroid development. Heterozygous α ($\alpha^{0/+}$ $\beta^{+/+}$) or β ($\alpha^{0/0}$ $\beta^{0/+}$) knockout mice can survive and produce mature red blood cells, but homozygous α ($\alpha^{0/0}$ $\beta^{+/+}$) or β ($\alpha^{+/+}$ $\beta^{0/0}$) knockout mice die too early in uteri to study definitive erythroid cells[54,56]. Doubly heterozygous α and β knockout mice ($\alpha^{0/+}$ $\beta^{0/+}$) develop very normal without obvious hemoglobin reduction[105]. So we cannot rule out the possibility that if the expression of mCherry, or myoglobin, or some other proteins is increased to a similar level of hemoglobin in wild type erythroid cells, Hb Null reticulocytes could be rescued. Second, the importance of hemoglobin for reticulocyte survival may rely on some unique structural property of the individual α globin chain, β globin chain, or hemoglobin

125

tetramer itself. Broad inactions between hemoglobin and the cytoskeleton[17,20,21,26] could play a critical role in the maturation or ripening of the reticulocyte in the bone marrow before its release to the peripheral blood.

To explore the above issues, I proposed the following experiments:

1. Experimentally determine how much globin chain synthesis is required to rescue Hb Null reticulocytes from cell death. For these studies I would establish ES cell lines from embryos with the following α and β globin genotypes: $\alpha^{0/+}\beta^{0/0}$, $\alpha^{+/+}\beta^{0/0}$, $\alpha^{0/0}\beta^{+/0}$ and $\alpha^{0/0}\beta^{+/+}$. Label these ES cell lines with EGFP and/or mCherry, produce chimeric mice, and track ES cell derived erythroid cell development in chimeras. As discussed on above, mice with genotypes of $\alpha^{0/+}\beta^{0/+}$, $\alpha^{0/+}\beta^{+/+}$, $\alpha^{+/+}\beta^{0/+}$ can survive and produce mature red cells. These additional ES cell lines and chimeric mice will enable us to understand whether α chains, β chains, or α and β tetramers are important for reticulocyte survival, and how much of these proteins are needed.

2. Experimentally determine if high levels of a non-hemoglobin protein is able to rescue Hb Null reticulocytes from premature death. For these studies I will use a recombinant lentiviral vector designed for high level erythroid specific expression to deliver various transgenes to Hb Null ES cells. I have generated lentiviral vectors (pSRL18 and pSRL24, Figure 64) that contain the human β globin LCR sequences [DNase I hypersensitive sites (HS) 4, 3, 2] upstream of a human β globin gene promoter with different multiple cloning sites (MCS) for inserting transgenes of interest followed by the 3' part of the human β globin gene (exon2/IVS2/exon3/3'UTR/pA) for transcriptional termination and splicing

(Figure 63). A variety of protein coding sequences can be inserted into the MCS. To test the efficiency of these vectors, I inserted the mCherry coding sequence into the MCS of the pSRL18 lenti-vector (pSRL29), and lentiviruses were produced by co-infection of lenti-vector, packaging plasmid pCMV-dR8.91and envelope plasmid pMD.G into 293T cells as previously described[135]. I infected MEL cells with pSRL29 lentiviruses, and found about 8~10% cells were mCherry positive after 48~72 hours terminal differentiation induced by 2% DMSO (Figures 64, 65). I also infected wild type C57BL/6J mouse bone marrow cells with pSRL29 lentiviruses and transplanted them into lethally irradiated C57BL/6J mice. FACS analysis of these transplanted mice showed that mCherry was specifically expressed in red cells (Figure 66). These data demonstrate that these lentiviral vectors can be used to deliver proteins of interest into Hb Null erythroid cells. However, I found the infection efficiency of lentivirus for mouse bone marrow cells was much lower than that for human cells, and as shown in Figure 66, less than 1% blood cells were mCherry positive. This problem can be avoided by infecting Hb Null ES cells with lentiviruses and subcloning of the infected ES cells so that 100% of the starting Hb Null cells will have the lentiviral transgenes in exactly the same genomic locations. ES colonies with different copy number of lentivirus can then be used to generate Hb Null chimeric mice. Using this lentiviral transgenesis system, we can test whether non-hemoglobin proteins and how much of these proteins can rescue Hb Null reticulocytes. So far, I have generated actin (pSRL19), albumin (pSRL25), mouse β^{major} globin (pSRL21),

mouse α2 globin (pSRL22), and human myoglobin (pSRL26) lentiviruses to test in this system.

Another interesting question for future study is why erythroid development in heme exporter-FLVCR knockout mice was blocked at the proerythroblast stage due to the toxicity of excess free heme, which is inconsistent with my results in Hb Null chimeric and transplanted mice. Since FLVCR is highly expressed in macrophages, and elevated free heme in macrophages can cause cell death and lead to anemia, as exemplified in HO-1 knockout mice, it is possible that the phenotype of FLVCR knockout erythroid cells is an indirect effect resulting from compromised macrophages. To test this hypothesis, I propose to generate mCherry and/or EGFP labeled FLVCR knockout chimeric mice and study their erythroid development in the background of normal erythroblastic islands with normal macrophages in the chimeric bone marrow. If FLVCR knockout erythroid cells are still blocked at proerythroblast stage, it implies FLVCR is more important than hemoglobin for controlling the free heme level at the CFU-E to proerythroblast stages. Additionally, since FLVCR is not expressed in erythroid cells beyond the proerythroblast stage, tagging FLVCR with a fluorescence protein could enable the prospective isolation of BFU-Es and/or CFU-Es. If FLVCR knockout erythroid cells develop normally in chimeric mouse, it will suggest that the impairment in erythroid development in FLVCR knockout mice is an indirect effect of FLVCR deficiency instead of its direct effect in erythroid cells.
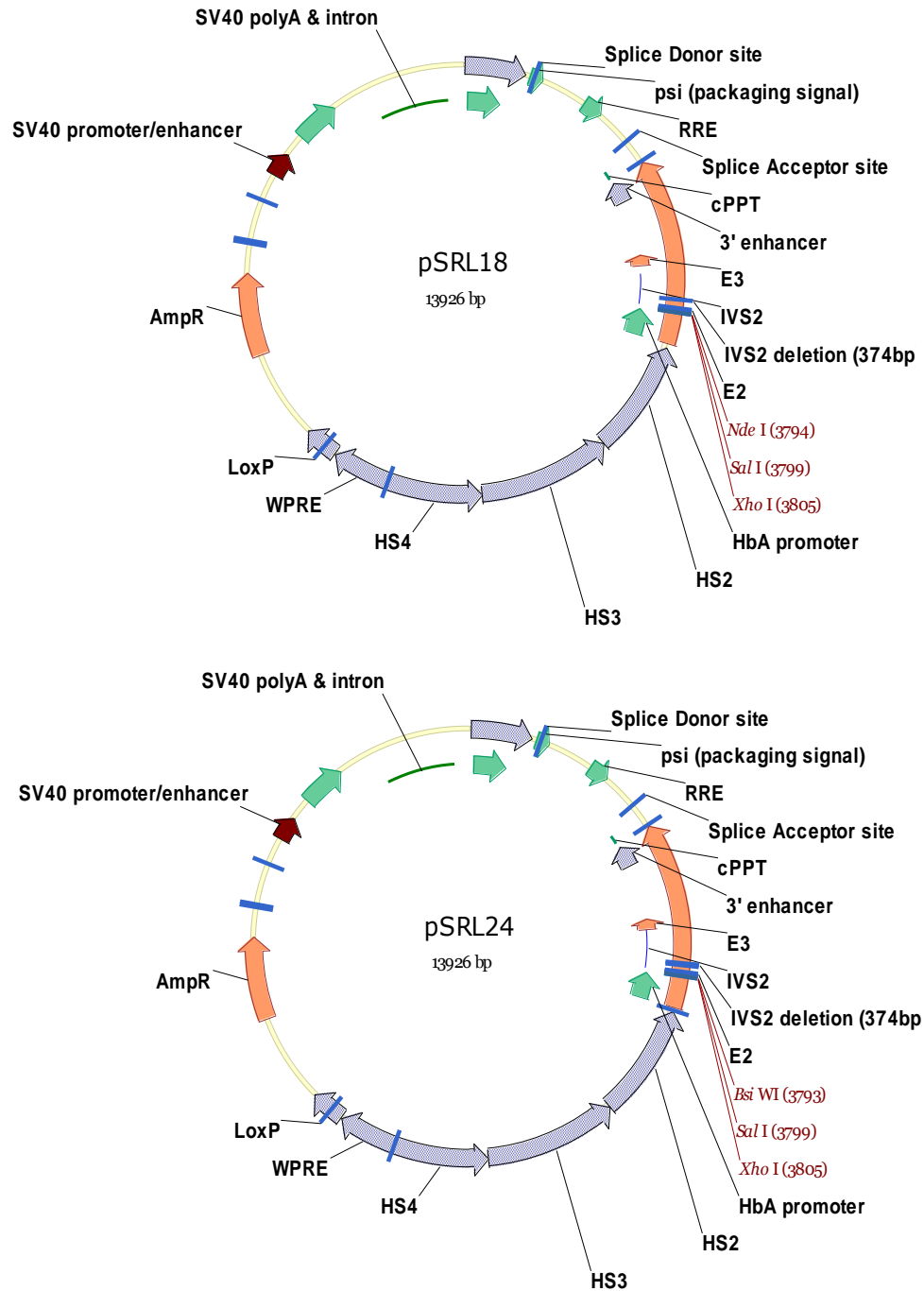
Figure 63. Erythroid specific lenti-vectors containing multiple cloning sites. pSRL18 contains *Nde*I, *Sal*I and *Xho*I cloning sites downstream of HbA promoter. pSRL24 contains *Bsi* WI, *Sal*I and *Xho*I cloning sites downstream of HbA promoter.
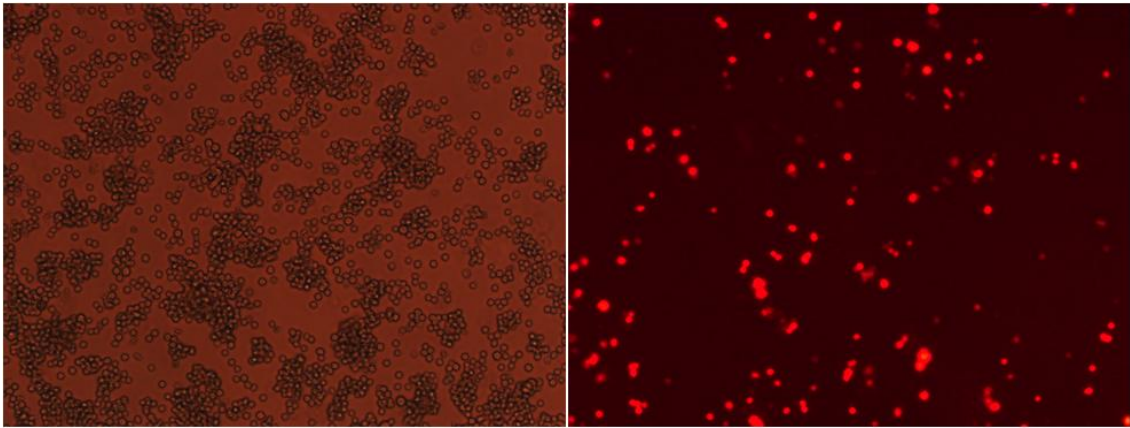
Figure 64. Fluorescence picture of mCherry-lentivirus (pSRL29) infected MEL cells after 48 hours terminal differentiation. Left: bright field. Right: red fluorescence. Objective: ×10.
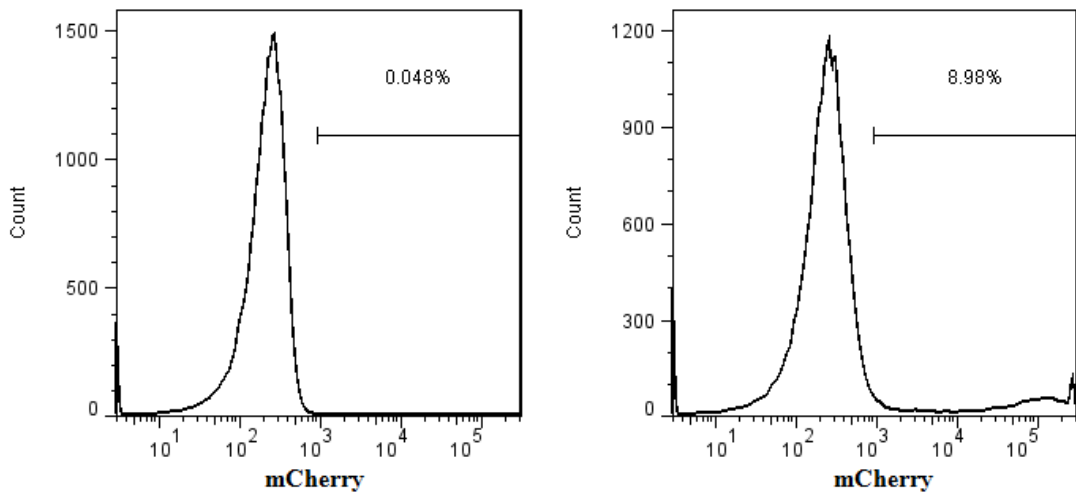
Figure 65. FACS analysis of mCherry-lentivirus (pSRL29) infected MEL cells after 72 hours terminal differentiation.
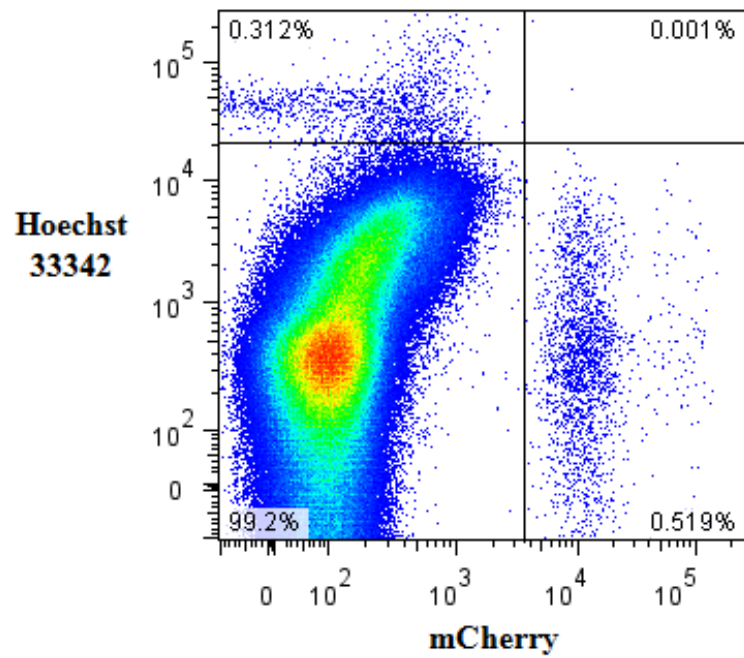
Figure 66. FACS analysis of blood cells from mice transplanted with mCherry-lentivirus (pSRL29) infected bone marrow cells.

EXPERIMENTAL PROCEDURES AND MATERIALS

Generation of Hb Null ES cells:

Hb Null ES cells were generated according to the procedure described by Evans and Kaufman[136]. Briefly, knockout-transgenic HbA mice were bred with knockout-transgenic HbS mice (Figure 8), and E4.5 mouse blastocysts were flushed out from uteri and cultured on irradiation-inactivated mouse primary embryonic fibroblast feeder layers in ES cell media. Inner cell mass outgrowths were picked, dissociated, and expanded after 5 or 6 days. ES cells were genotyped by PCR (Table 3). Chromosomes of ES cell lines were counted[137], and the ones having 40 chromosomes were used for experiments.

Table 3 Primers for genotyping Hb Null ES cells

Gene	Primer Name	Primer Sequence	PCR Product
HbA transgene	LCR F	gcaatattcttcaggcacatgga	414 bp
	HbA R	gtttagccagggaccgtttcag	
HbS transgene	LCR F	gcaatattcttcaggcacatgga	328 bp
	HbS R	aattctggcttatcggaggcaag	
mouse α globin locus	mouse α F	tcttcttgcctcagcctacca	wild type α globin allele: 308bp
	mouse α WT R	tcctctttgtccactgtctcctc	
	mouse α KO R	tcagcagcctctgttccacata	α globin knockout allele: 211bp
mouse β globin locus	mouse β F	aggagattcatccatgcactcaaa	wild type β globin allele: 292bp
	mouse β WT R	aatcaggcttcggtgatgacaag	
	mouse β KO R	tgtggtttccaaatgtgtcagtttc	β globin knockout allele: 169bp

Chromosome counting:

70% confluent ES cells in 10cm dish were incubated with 2µg/ml Vinblastine Sulfate (Sigma, St. Louis, MO) in 10ml ES cell media for 4 hours. Cells were dissociated by trypsin, resuspended in 10ml hypotonic solution containing 0.01M sodium citrate and 0.03M potassium chloride, and incubated at 37°C for 20 minutes. Cells were then spun down and resupsended in 5ml fixative solution containing 25% glacial acetic acid and 75%methanol for three times. After final fixation, cells were dropped from a two-meter distance onto glass slides. Slides were dried, and stained by DipQuick solutions. ES cell clones with a minimum 70% of spreads containing 40 chromosomes are acceptable.

Constructs:

Generation of EGFP-EKLF (pSRL34) construct: mouse EKLF BAC DNA[138] was transferred into *E. coli* strain SW102[139] by electroporation. A pgk/Hygro-Kan fragment flanked by Loxp was amplified from a HA-EKLF-TAP plasmid[138] by PCR and targeted into EKLF intron 1 (GenBank Accession NO. AF019074.1: between 3424 and 3425) of EKLF BAC (Figure 15) in SW102 by homologous recombination selected by kanamycin (pSRL30). A sequence of EGFP (without stop codon) plus GGA GGT GGA (three glycin codons) was inserted into EKLF BAC (containing Loxp-pgk/Hygro-Kan-Loxp) before EKLF ATG start codon (Figure 15) by galK positive and counter selection[139] (pSRL32). The final EGFP-EKLF construct pSRL34 containing 5.8 kb 5' and 3.6 kb 3' homologous targeting sequences was rescued from the modified EGFP-EKLF BAC (pSRL32) by a gap-repair (GR) plasmid[138]. *Not*Ⅰ-linearized pSRL34 targeting constructs were electroporated into V6.5 wild type and Hb Null ES cells selected by hygromycin B.

Targeted colonies were screened by 5', 3' and TK PCR (Figures 16, 23). Selection markers were deleted by transiently expressing Cre recombinase (pCAGGS-nlsCre plasmid, a gift from Dr. Nagy Lab)[140] in targeted positive ES clones (Figure 16).

Generation of mCherry construct (pSRL11): A BAC clone containing mouse β hemoglobin locus was isolated from a 129 mouse strain genome library. Mouse β hemoglobin BAC was electroporated into *E.coli* strain SW102. A 14.5 kb fragment of BAC sequence from a point in mouse β^{major} IVS2 to a point in mouse β^{minor} exon2 (GenBank Accession NO. X14061.1, 39374-53836) was replaced by pgk/Hygro-Kan PCR fragment by homologous recombination selected by kanamycin (pSRL1). A 1017 bp fragment of pSRL1 from β^{major} start codon ATG to a point in mouse β^{major} IVS2 (GenBank Accession NO. X14061.1, 38339-39355) was replaced by galK gene (pSRL2). The galK gene plus the left β^{major} IVS2 (GenBank Accession NO. X14061.1, 39356-39373) in pSRL2 was then replaced by mCherry coding sequence plus TAA stop codon by galK counter selection (pSRL5). mCherry sequence was PCR-amplified from the mCherry-C1 plasmid (a gift from Dr. Jei-Hwa Yu). The final construct pSRL11 containing 6.8 kb 5' and 7 kb 3' homologous targeting sequences was rescued from the pSRL5 BAC by the GR plasmid (Figure 29). *Not* I -linearized pSRL11 targeting constructs were electroporated into EGFP-EKLF Hb Null ES cells selected by hygromycin B. Targeted colonies were screened by 5', 3' and TK PCR (Figure 30). Selection markers were deleted by transiently expressing Cre recombinase in targeted positive ES clones (Figure 29).

Generation of mCherry-human myoglobin construct (pSRL12): human myoglobin with stop codon TAG (PCR-amplified from a human myoglobin cDNA clone-Origene

SC116773) was inserted into the mCherry-C1 plasmid between *Bgl* II and *EcoR* I sites (pSRL6). mCherry-linker (TCC GGA CTC AGA TCT, coding for Ser-Gly-Leu-Arg-Ser)-human myoglobin cassette was PCR-amplified from pSRL6 and then used to replace the sequence of galK gene plus the left β^{major} IVS2 (GenBank Accession NO. X14061.1, 39356-39373) in pSRL2 by homologous recombination (pSRL7). The final construct pSRL12 containing 6.8 kb 5' and 7 kb 3' homologous targeting sequences was rescued from the pSRL7 BAC by the GR plasmid (Figure 53). *Not* I -linearized pSRL12 targeting constructs were electroporated into EGFP-EKLF Hb Null ES cells selected by hygromycin B. Targeted colonies were screened by 5', 3' and TK PCR (Figure 54). Selection markers were deleted by transiently expressing Cre recombinase in targeted positive ES clones (Figure 53).

Gene targeting in ES cells and production of chimeras:

ES cells were grown on irradiation-inactivated mouse primary embryonic fibroblast feeder layers in ES cell media containing Dulbecco modification of Eagle medium (1 X DMEM), 16.7% fetal bovine serum (Invitrogen, Carlsbad, CA), 1 X nucleosides (Millipore, Billerica, MA), 2 mM L-glutamine, 1 X nonessential amino acids, 100 I.U./mL penicillin, 100 µg/mL streptomycin (Mediatech, Manassas, VA), 0.1 mM β-mercaptoethanol (Sigma). Leukemia inhibitory factor (LIF) was added that had been produced from COS-7 cells transfected with LIF-expressing plasmid pC106R [141]. *Not* I -linearized constructs were electroporated (Gene Pulser Xcell electroporation system, Bio-Rad, Hercules, CA; voltage: 450V, capacitance: 250µF, resistance: ∞, cuvette: 4mm) into ES cells, and hygromycin B (120 µg/ml) and ganciclovir (1 mM) was added to the

ES medium 36 h after electroporation and replenished every other day until colonies were picked. After selection, DNA from drug-resistant ES cell colonies was screened by PCR (Figures 16, 23, 30, 54) to identify the homologous recombinants. Cre plasmids were electroporated into recombinant colonies, and marker-deleted colonies were screen by PCR (Figures 16, 23, 30, 54). Chimeric mice were produced by injecting the targeted ES cells into 3.5 day C57BL/6J (The Jackson Laboratory, Bar Harbor, ME) blastocysts that were then transferred into the uteri of outbred CD1 (Charles River Laboratories, Wilmington, MA) pseudopregnant recipient mice. Germline transmission of EGFP-EKLF targeting was achieved by breeding wild type V6.5 male chimeras with C57BL/6J female mice. All procedures were approved by the University of Alabama at Birmingham's Institutional Animal Care and Use Committee.

Table 4 Primers for screening targeted colonies

Primer Name	Primer Sequence	PCR
F1	gcagcagcagtagtttcatcc	EGFP-EKLF targeting, 5'PCR
R1	gtaggtcagggtggtcacga	(Figures 15, 16, 23)
F2	tcgccttctatcgccttcttg	EGFP-EKLF targeting, 3'PCR
R2	agggtcacctagtgcttcca	(Figures 15, 16, 23)
F3	taacaatgggcatgccttatgccg	TK gene PCR
R3	accgtattggcaagtagcccgtaa	(Figures 15, 16, 23, 29, 30, 53, 54)
F4	ctgcccgacaaccactacct	EGFP-EKLF targeting after selection marker deleted, 3'PCR (Figures 15, 16, 23)
F5	aatagtgtttgtgctgttcctccac	mCherry targeting, 5'PCR
R4	acccttggtcaccttcagc	(Figures 29, 30, 53)
F6	cagagcttggttgacggcaatttcg	mCherry targeting, 3'PCR
R5	tgagctccGgaggtacccagg	(Figures 29, 30)
F7	cggcgagttcatctacaagg	mCherry targeting after selection marker deleted, 3'PCR (Figures 29, 30)
R6	tctctgggtgacccttaaagagc	mCherry-human myoglobin targeting 5'PCR (Figures 53, 54)

Flow cytometry:

Ter119 antibody conjugated with Allophycocyanin (APC) or phycoerythrin (PE) (1:200 dilution), CD71-Biotin (1:200 dilution), Streptavidin-PECy7 (1:200 dilution), and Annexin V-PE Apoptosis Detection Kit were bought from BD pharmingen. CD44-Biotin (1:200 dilution) was bought from eBioscience. Freshly isolated cells were incubated with antibodies on ice in DPBS/0.5%BSA with 5% mouse serum for 30 minutes. Streptavidin-PECy7 was added after washing out CD71-Biotin and resuspending cells. To exclude dead cells, cells were incubated with 7AAD (BD pharmingen, San Diego, CA) or Sytox Blue on (Invitrogen) on ice for 15 minutes. For nucleus staining, cells were incubated with Hoechst 33342 or Dyecycle Violet (Invitrogen) at room temperature for 15 minutes. For reticulocyte detection, cells were incubated with Thiazole Orange (0.1 µg/ml) (Sigma) at room temperature for 15 minutes. For ROS detection, cells were incubated in 500µl DPBS/0.5%BSA with RedoxSensor Red CC (2 µm) or Dihydroethidium (10 µm) (Invitrogen) at room temperature for 10 minutes. Antibodies and dyes were added as indicated dilutions or as per the manufacturers' protocol. Cells were washed one time by 1ml DPBS/0.5%BSA before applying to FACS machines. For heme and iron measurements, cells were suspended and incubated only in DPBS for sorting. Cells were analyzed or sorted by the following flow cytometers: MoFlo (with 405nm, 488nm and tunable-dye lasers, Cytomation, Fort Collins, CO) from UAB Flow Cytometry and Sorting Facility; BD FACSAria (with 405nm, 488nm and 633nm lasers) and BD LSRII (with 405nm, 488nm, 360nm and 633nm lasers) from UAB Center for AIDS Research (CFAR) Flow Cytometry Core; BD FACSVantageSE (with 360nm, 488nm and 632nm lasers) and BD LSRII (with 405nm, 488nm, 532nm and 633nm lasers) from UAB

Arthritis and Musculoskeletal Center (AMC) Flow Cytometry Core Facility; BD FACSCalibur (with 488nm and 635nm lasers) from Dr. Tim M. Townes lab.

Quantitative Realtime RT-PCR:

Cell RNA was isolated by TRIzoL LS (Invitrogen), and treated with TURBO DNA-free^{TM} Kit (Ambion, Austin, TX). cDNA was generated using the High Capacity cDNA Archive Kit (Applied Biosystems, Foster City, CA). All procedures were followed according to the manufacturers' instructions. Realtime PCR reactions contained SYBRR GreenER^{TM} qPCR SuperMix for ABI PRISMR (Invitrogen), 500 nM primers, and 5 ~ 10 ng cDNA, in a 20 μl total volume. Reactions were run on a 7900HT Real-Time PCR System (Applied Biosystems) with 40 cycles of 95 ℃ for 15 sec and 60 ℃ for 1 min. Sequences of primers and probes used are listed in Table 5 and Table 6. Experiments of each reaction were performed in triplicate with a 384-well optical plate, and the standard error of the mean (S.E.M.) from three samples is calculated for Figure 58.

Table 5 Primers for Realtime PCR analysis of ES-EP culture

Primer Name	Primer Sequence	Gene
Beta actin F	ccaaccgtgaaaagatgacc	Beta actin
Beta actin R	accagaggcatacagggaca	
mouse β globin F	gctgctggttgtctacccttg	Mouse β globin
mouse β globin R	cccatgatagcagaggcagag	
mouse α globin F	agctgaagccctggaaaggat	Mouse α globin
mouse α globin R	gccgtggcttacatcaaagtg	
mouse βh1 F	ggtacttgtgggacagagcattg	Mouse βh1 globin
mouse βh1 R	ccaaggaattcaccccagag	
mouse εy F	atcaccagcaacctcccagac	Mouse εy globin
mouse εy R	tactccacaggccattgatgag	
EKLF F	acactggacatcgtcccttc	EKLF
EKLF R	tgtgcaggatcactcagagg	
GypA F	cgtgatggcagggattatcg	Glycophorin A
GypA R	tgttgtcaccaccctcagga	
EpoR F	cgagctacctcccactccac	
EpoR R	atgccagaatcggacaccac	Erythropoietin receptor
Gata1 F	cctatggcaagacggcactc	GATA 1
Gata1 R	ttgctcttcccttcctggtc	
Tal1 F	tccgtaaagactgctctgga	Tal1
Tal1 R	tgtgctgggtgtagaacaca	
Gata2 F	tgggtggaacatactcttgg	GATA 2

Gata2 R	caggaggaagtgggtctctt	
NF-E2 F	atcaccatcgtcaaatctgc	NF-E2
NF-E2 R	ggctgagaagggtacagagg	
c-mpl F	cctctcatctacgaagtgtgga	c-mpl
c-mpl R	agccagtgtgttctcaattgtt	
GPIIb F	tcacaatgctggtgagtgtg	CD41
GPIIb R	tgtttggattctggctgttc	
CEBPα F	ccatgtggtaggagacagagac	CEBPα
CEBPα R	ggcgacatacagtacacacaag	
IL3Rα F	gtgacagacgcctgagaact	IL3Rα
IL3Rα R	ggaatccacgcactttattg	
GATA3 F	ttatcaagcccaagcgaag	GATA3
GATA3 R	attagcgttcctcctccaga	
PAX5 F	cagtcacagcatagtgtctacagg	PAX5
PAX5 R	gccactgatggagtatgagg	
IL7R F	ccctccactcctttcctcta	IL7 receptor
IL7R R	ccagagtttggcagcaag	
VE-Cadherin F	aggtgacaggtcatagagcaag	VE-Cadherin
VE-Cadherin R	tctttctggtgagtgggttaga	
flk1 F	ttggcaaatacaacccttca	flk1
flk1 R	cgcattcagtcaccaatacc	
Bra F	acattatgaagccaaggacaga	Brachyury
Bra R	gaccctacctagcaaaggactc	

Table 6 Primers for Realtime PCR analysis of genes regulating heme and iron

Primer Name	Primer Sequence	Gene
EF1α F	gatggaaagtcacccgcaaa	EF1
EF1α R	caggggcttgtcagttggac	
ALAS1 F	ggctgtgttggaggatacatt	ALAS1
ALAS1 R	caaggaggtggtgaagatga	
ALAS2 F	atttgggcataagcagacac	ALAS2
ALAS2 R	cagctccatgattcttcagg	
Ppox F	attggccgcaagttatcatc	Protoporphyrinogen oxidase
Ppox R	aagatcgcaccatctgatcc	
Fech F	agaagagaagcgaggtggtc	Ferrochelatase
Fech R	ttgtggacagtggctcctac	
hmox1 F	gaagggtcaggtgtccaga	Heme oxygenase 1
hmox1 R	tggtacaaggaagccatcac	
hmox2 F	cccaattctacctgtttgagc	Heme oxygenase 2
hmox2 R	aggtccaaggcattcattct	
FLVCR1 F	aacctcgggtacatcatcgt	FLVCR1
FLVCR1 R	ctccacagcaaactcaaagc	
HRI F	gctcgtctccttactggaaca	HRI
HRI R	gcagccccatcttgataaaa	
FPN1A F	tgctgttgttgtttgcctta	Ferroportin-FPN1A
FPN1A R	acagccttatgccgaaagac	

FPN1B F	tggagtttcaatgtttaggatcac	Ferroportin-FPN1B
FPN1B R	ttgtcaggtttgtcaacacttc	
MFN F	gagcactccatcatgtaccc	Mitoferrin
MFN R	ctctgcatccgtgtcttcac	
MFN2 F	aagtcgtcaagcagaggatg	Mitoferrin 2
MFN2 R	cactgcccgaacacagtc	
Fth1 F	tggagttgtatgcctcctacg	Ferritin-Fth1
Fth1 R	ttcagagccacatcatctcg	

ES-EP culture:

ES-EP cells were generated according to the paper by S. Carotta et al [67] with some modification.

Briefly, ES cells were first differentiated into embryoid body (EB) in EB medium for 7~8 days. EB medium contains IMDM (Invitrogen), 2 mM L-glutamine, 100 I.U./mL penicillin and 100 μg/mL streptomycin, 15% fetal bovine serum, 1% methylcellulose (Sigma), 50 μg/mL ascorbic acid (Sigma), 300 μg/mL iron-saturated human transferrin (Sigma), 5% protein-free hybridoma medium (PFHM-II; Invitrogen) and 4×10^{-4}M monothioglycerol (MTG, Sigma).

At day 7 or 8 differentiation, EBs were harvested by centrifugation and then dissociated by 0.25% Trypsin (Mediatech). Single EB cells were put into erythroid progenitor (EP) medium at a concentration of 2×10^6/mL. EP medium contains StemPro34 plus nutrient supplement (Invitrogen), 2 mM L-glutamine, 1% methylcellulose, 2 U/mL human recombinant erythropoietin (Epoetin Alfa, Amgen Inc, Thousand Oaks, CA), 100 ng/mL murine recombinant stem cell factor (SCF, R&D Systems, Minneapolis, MN), 10^{-6}M dexamethasone (Sigma), and 40 ng/mL human insulin-like growth factor 1 (IGF-1; Promega, Madison, WI). Cell density was maintained at 2~4 $\times 10^6$ cells/mL, and medium was changed at an interval of 1 ~2 days. After 6~8 days, the culture contains pure erythroid progenitors.

For terminal differentiation of ES-EP cells, ES-EPs were collected by centrifuging over Ficoll (lymphocyte separation medium, Mediatech) to remove dead and differentiated cells, and then seeded into terminal differentiation medium, which contains StemPro34

plus nutrient supplement, 2 mM L-glutamine, 1% methylcellulose, 10 U/mL Epo, 10 ng/mL insulin (HumulinR, Eli Lilly and Company, Indianapolis, IN), 1×10^{-6}M of the glucocorticoid receptor antagonist RU 486 (Sigma) and 1mg/mL iron-saturated human transferrin. ES-EP cells were analyzed by FACS before terminal differentiation, and 48 and 72 hours after terminal differentiation (Figure 13).

Bone marrow, spleen and fetal liver sample preparations:

Bone marrow was flushed out from tibias and femurs by 26G syringe. Spleen was pushed through a 70 µm strainer by a plunger. Fetal liver (E11.5 or E12.5) was pipetted up and down by 1ml tips. Bone marrow chunks, spleen and fetal liver pieces were drawn into and pushed out of 26G syringe to make single cells in DPBS/0.5% BSA.

Cytospin:

Single cells were centrifuged onto slides for 4 minutes for 500 rpm (Cytospin 3, Thermo Scientific Shandon, Pittsburgh, PA).

DipQuick stain:

Cytospin or blood smear slides were air dried, and stained with DipQuick solution 1, 2 and 3 for 30 seconds for each and washed by deionized water briefly. Slides were sealed with cover slips using Cytoseal XYL Xylene Based Mounting Medium (Fisher Scientific, Pittsburgh, PA). Images were acquired using 100x objective lens and visible light with an Olympus AX70 microscope (Center Valley, PA) and a Carl Aeiss Axiocam HR digital camera (Thornwood, NY).

Irradiation and transplantation:

One week before irradiation, the recipient mice (C57BL/6J male, 8 weeks) were given acidified water. Mice were irradiated for two doses of 6 Gy with an interval of 4 hours using X-RAD 320 irradiator (Precision X-Ray, North Branford, CT) at a rate of 1 Gy/min. Irradiated mice were fed with antibiotic water for one week. 24 hours after irradiation, mice were transplanted with sorted CD45.1+ and EGFP+ cells by retro-orbital injection (10^6 cells per mouse). Mice were maintained in accordance with guidelines of the University of Alabama at Birmingham's Institutional Animal Care and Use Committee.

Tissue section and staining:

Tissues were fixed in 75% ethanol/10% formalin solution, embedded in paraffin, sectioned, and stained with hematoxylin-eosin by standard methods at the UAB Comparative Pathology Laboratory (CPL). Liver iron was stained by Prussian Blue and counterstained with nuclear fast red.

Electron microscopy:

Transmission electron microscopy was performed at the UAB High Resolution Imaging Facility. In brief, bone marrow and spleen chunks was fixed in buffered glutaraldehyde, post-fixed in osmium tetroxide, and embedded in Epon 812. Sections were post-stained with uranyl acetate and lead citrate, and viewed with a Tecnai T12 Spirit TWIN electron microscope (FEI Company, Hillboro, OR) at 80kv. Images were captured with an AMT XR60B digital camera (Advanced Microscopy Techniques, Danvers, MA).

Fluorescence image:

Cytospin of dissociated cells were fixed by 4% paraformaldehyde for 10 minutes and washed by PBS. Coverslips were mounted using ProLong Gold antifade reagent (Invitrogen) as instructed and sealed by nail polish. Fluorescence images were obtained using a Zeiss LSM 710 Confocal Microscope (Carl Zeiss MicroImaging, LLC, Thornwood, NY) provided by the High Resolution Imaging Facility at the University of Alabama at Birmingham.

Lentivirus:

pSRL18 and pSRL24 lenti-vectors (Figure 63) were generated from a human β^{AS3} lenti-vector pDL118[135] by deleting β^{AS3} exon1, IVS1 and 185 bp of exon2, and introducing MCS after human HbA promoter. Lentiviruses were produced as previously described [135]. Briefly, 20μg lenti-vector, 5μg envelope plasmid pMD.G and 15μg packaging plasmid pCMV-dR8.91 were used to transfect 2.5×10^6 293T cells grown on 10cm dishes in DMEM medium with 10% FBS. Transfection medium was replaced to DMEM/F12 without phenol red (Invitrogen) containing 2% FBS after 14 to 16 hours transfection. Viral containing supernatant was collected after additional 24 hours incubation. The virus was concentrated by centrifugation at 26 000 rpm for 90 minutes at 8 ℃ using an SW-28 rotor (Beckman, Palo Alto, CA) and resuspended in StemPro34 plus nutrient supplement (Invitrogen). Viruses were used immediately or stored at -80 ℃.

Heme content measurement:

Total heme level in cells was measured according to the method described by S. SASSA[142]. Briefly, EGFP and Ter119 double positive cells were sorted from Hb Null

EGFP-EKLF chimeric mouse bone marrow and were also sorted from wild type EGFP-EKLF/EKLF mouse bone marrow. Sorted cells were resuspended in 10ul DPBS, added with 500ul 2M oxalic acid and boiled at 100°C for 30 minutes. The fluorescence intensity of samples was measured by a Cary Eclipse Fluorescence spectrophotometer (Varian, Walnut Creek, CA). The excitation wavelength was at 400nm, and the emission wavelength was at 655nm. Sorted cells in 500μl 2M oxalic acid without boiling were used as a control. The heme level was calculated by comparing the 655nm fluorescence intensity of samples with a standard curve made by hemin solutions.

LIST OF REFERENCES

1.   Haar JL, Ackerman GA. A phase and electron microscopic study of vasculogenesis and erythropoiesis in the yolk sac of the mouse. Anat Rec. 1971;170:199-223.

2.   Palis J, Robertson S, Kennedy M, Wall C, Keller G. Development of erythroid and myeloid progenitors in the yolk sac and embryo proper of the mouse. Development. 1999;126:5073-5084.

3.   McGrath K, Palis J. Ontogeny of erythropoiesis in the mammalian embryo. Curr Top Dev Biol. 2008;82:1-22.

4.   Houssaint E. Differentiation of the mouse hepatic primordium. II. Extrinsic origin of the haemopoietic cell line. Cell Differ. 1981;10:243-252.

5.   Kingsley PD, Malik J, Fantauzzo KA, Palis J. Yolk sac-derived primitive erythroblasts enucleate during mammalian embryogenesis. Blood. 2004;104:19-25.

6.   Whitney JB, 3rd. Differential control of the synthesis of two hemoglobin beta chains in normal mice. Cell. 1977;12:863-871.

7.   Weaver S, Comer MB, Jahn CL, Hutchison CA, 3rd, Edgell MH. The adult beta-globin genes of the "single" type mouse C57BL. Cell. 1981;24:403-411.

8.   Stephenson JR, Axelrad AA, McLeod DL, Shreeve MM. Induction of colonies of hemoglobin-synthesizing cells by erythropoietin in vitro. Proc Natl Acad Sci U S A. 1971;68:1542-1546.

9.   Heath DS, Axelrad AA, McLeod DL, Shreeve MM. Separation of the erythropoietin-responsive progenitors BFU-E and CFU-E in mouse bone marrow by unit gravity sedimentation. Blood. 1976;47:777-792.

10.   Gregory CJ, Eaves AC. Human marrow cells capable of erythropoietic differentiation in vitro: definition of three erythroid colony responses. Blood. 1977;49:855-864.

11.   Gregory CJ, Eaves AC. Three stages of erythropoietic progenitor cell differentiation distinguished by a number of physical and biologic properties. Blood. 1978;51:527-537.

12.   Granick S, Levere RD. Heme Synthesis in Erythroid Cells. Prog Hematol. 1964;4:1-47.

13.   George Stamatoyannopoulos PWM, Roger M. Perlmutter, Harold Varmus. The Molecular Basis of Blood Diseases (ed 3rd Edition): W.B.Saunders; 2001.

14.   Mohandas N, Gallagher PG. Red cell membrane: past, present, and future. Blood. 2008;112:3939-3948.

15.   Bruce LJ, Beckmann R, Ribeiro ML, et al. A band 3-based macrocomplex of integral and peripheral proteins in the RBC membrane. Blood. 2003;101:4180-4188.

16.   Salomao M, Zhang X, Yang Y, et al. Protein 4.1R-dependent multiprotein complex: new insights into the structural organization of the red blood cell membrane. Proc Natl Acad Sci U S A. 2008;105:8026-8031.

17.   Eisinger J, Flores J, Salhany JM. Association of cytosol hemoglobin with the membrane in intact erythrocytes. Proc Natl Acad Sci U S A. 1982;79:408-412.

18.   Shaklai N, Abrahami H. The interaction of deoxyhemoglobin with the red cell membrane. Biochem Biophys Res Commun. 1980;95:1105-1112.

19.   Shaklai N, Sharma VS. Kinetic study of the interaction of oxy- and deoxyhemoglobins with the erythrocyte membrane. Proc Natl Acad Sci U S A. 1980;77:7147-7151.

20.   Liu SC, Palek J. Hemoglobin enhances the self-association of spectrin heterodimers in human erythrocytes. J Biol Chem. 1984;259:11556-11562.

21.   Lebbar I, Stetzkowski-Marden F, Mauffret O, Cassoly R. Interactions of actin and tubulin with human deoxyhemoglobin. Their possible occurrence within erythrocytes. Eur J Biochem. 1987;170:273-277.

22.   Kaul RK, Kohler H. Interaction of hemoglobin with band 3: a review. Klin Wochenschr. 1983;61:831-837.

23.   Schuck P, Schubert D. Band 3-hemoglobin associations. The band 3 tetramer is the oxyhemoglobin binding site. FEBS Lett. 1991;293:81-84.

24.   Salhany JM, Cordes KA, Sloan RL. Characterization of the pH dependence of hemoglobin binding to band 3. Evidence for a pH-dependent conformational change within the hemoglobin-band 3 complex. Biochim Biophys Acta. 1998;1371:107-113.

25.   Walder JA, Chatterjee R, Steck TL, et al. The interaction of hemoglobin with the cytoplasmic domain of band 3 of the human erythrocyte membrane. J Biol Chem. 1984;259:10238-10246.

26.   Chu H, Breite A, Ciraolo P, Franco RS, Low PS. Characterization of the deoxyhemoglobin binding site on human erythrocyte band 3: implications for O2 regulation of erythrocyte properties. Blood. 2008;111:932-938.

27.   Chen K, Liu J, Heck S, Chasis JA, An X, Mohandas N. Resolving the distinct stages in erythroid differentiation based on dynamic changes in membrane protein expression during erythropoiesis. Proc Natl Acad Sci U S A. 2009;106:17413-17418.

28.   Mel HC, Prenant M, Mohandas N. Reticulocyte motility and form: studies on maturation and classification. Blood. 1977;49:1001-1009.

29.   Koury ST, Koury MJ, Bondurant MC. Cytoskeletal distribution and function during the maturation and enucleation of mammalian erythroblasts. J Cell Biol. 1989;109:3005-3013.

30.   Chasis JA, Prenant M, Leung A, Mohandas N. Membrane assembly and remodeling during reticulocyte maturation. Blood. 1989;74:1112-1120.

31.   Waugh RE, Mantalaris A, Bauserman RG, Hwang WC, Wu JH. Membrane instability in late-stage erythropoiesis. Blood. 2001;97:1869-1875.

32.   Liu J, Guo X, Mohandas N, Chasis JA, An X. Membrane remodeling during reticulocyte maturation. Blood. 2010;115:2021-2027.

33.   Tahara T, Sun J, Nakanishi K, et al. Heme positively regulates the expression of beta-globin at the locus control region via the transcriptional factor Bach1 in erythroid cells. J Biol Chem. 2004;279:5480-5487.

34.   Chen JJ. Regulation of protein synthesis by the heme-regulated eIF2alpha kinase: relevance to anemias. Blood. 2007;109:2693-2699.

35.   Nakajima O, Takahashi S, Harigae H, et al. Heme deficiency in erythroid lineage causes differentiation arrest and cytoplasmic iron overload. Embo J. 1999;18:6282-6289.

36.   Magness ST, Maeda N, Brenner DA. An exon 10 deletion in the mouse ferrochelatase gene has a dominant-negative effect and causes mild protoporphyria. Blood. 2002;100:1470-1477.

37.   Kumar S, Bandyopadhyay U. Free heme toxicity and its detoxification systems in human. Toxicol Lett. 2005;157:175-188.

38.   Ponka P. Tissue-specific regulation of iron metabolism and heme synthesis: distinct control mechanisms in erythroid cells. Blood. 1997;89:1-25.

39.   Morse D, Choi AM. Heme oxygenase-1: from bench to bedside. Am J Respir Crit Care Med. 2005;172:660-670.

40.   Quigley JG, Yang Z, Worthington MT, et al. Identification of a human heme exporter that is essential for erythropoiesis. Cell. 2004;118:757-766.

41.   Neuwirt J, Ponka P, Borova J. Evidence for the presence of free and protein-bound nonhemoglobin heme in rabbit reticulocytes. Biochim Biophys Acta. 1972;264:235-244.

42.   Ponka P, Borova J, Neuwirt J. Accumulation of heme in mitochondria from rabbit reticulocytes with inhibited globin synthesis. Biochim Biophys Acta. 1973;304:715-718.

43.   Fujita H, Sassa S. The rapid and decremental change in haem oxygenase mRNA during erythroid differentiation of murine erythroleukaemia cells. Br J Haematol. 1989;73:557-560.

44.   Keel SB, Doty RT, Yang Z, et al. A heme export protein is required for red blood cell differentiation and iron homeostasis. Science. 2008;319:825-828.

45.   Draptchinskaia N, Gustavsson P, Andersson B, et al. The gene encoding ribosomal protein S19 is mutated in Diamond-Blackfan anaemia. Nat Genet. 1999;21:169-175.

46.   Gazda HT, Grabowska A, Merida-Long LB, et al. Ribosomal protein S24 gene is mutated in Diamond-Blackfan anemia. Am J Hum Genet. 2006;79:1110-1118.

47.   Cmejla R, Cmejlova J, Handrkova H, Petrak J, Pospisilova D. Ribosomal protein S17 gene (RPS17) is mutated in Diamond-Blackfan anemia. Hum Mutat. 2007;28:1178-1182.

48.   Narla A, Ebert BL. Ribosomopathies: human disorders of ribosome dysfunction. Blood. 2010;115:3196-3205.

49.   Muncie HL, Jr., Campbell J. Alpha and beta thalassemia. Am Fam Physician. 2009;80:339-344.

50.   Vichinsky EP. Alpha thalassemia major--new mutations, intrauterine management, and outcomes. Hematology Am Soc Hematol Educ Program. 2009:35-41.

51.   Schrier SL. Thalassemia: pathophysiology of red cell changes. Annu Rev Med. 1994;45:211-218.

52.   Rund D, Rachmilewitz E. Beta-thalassemia. N Engl J Med. 2005;353:1135-1146.

53.   Yang B, Kirby S, Lewis J, Detloff PJ, Maeda N, Smithies O. A mouse model for beta 0-thalassemia. Proc Natl Acad Sci U S A. 1995;92:11608-11612.

54.   Ciavatta DJ, Ryan TM, Farmer SC, Townes TM. Mouse model of human beta zero thalassemia: targeted deletion of the mouse beta maj- and beta min-globin genes in embryonic stem cells. Proc Natl Acad Sci U S A. 1995;92:9259-9263.

55.   Huo Y, McConnell SC, Liu SR, et al. Humanized Mouse Model of Cooley's Anemia. J Biol Chem. 2009;284:4889-4896.

56.   Paszty C, Mohandas N, Stevens ME, et al. Lethal alpha-thalassaemia created by gene targeting in mice and its genetic rescue. Nat Genet. 1995;11:33-39.

57.   Kingsley PD, Malik J, Emerson RL, et al. "Maturational" globin switching in primary primitive erythroid cells. Blood. 2006;107:1665-1672.

58.   Ryan TM, Ciavatta DJ, Townes TM. Knockout-transgenic mouse model of sickle cell disease. Science. 1997;278:873-876.

59.   Hu M, Krause D, Greaves M, et al. Multilineage gene expression precedes commitment in the hemopoietic system. Genes Dev. 1997;11:774-785.

60.   Miyamoto T, Iwasaki H, Reizis B, et al. Myeloid or lymphoid promiscuity as a critical step in hematopoietic lineage commitment. Dev Cell. 2002;3:137-147.

61.   Akashi K. Lineage promiscuity and plasticity in hematopoietic development. Ann N Y Acad Sci. 2005;1044:125-131.

62.   Socolovsky M, Nam H, Fleming MD, Haase VH, Brugnara C, Lodish HF. Ineffective erythropoiesis in Stat5a(-/-)5b(-/-) mice due to decreased survival of early erythroblasts. Blood. 2001;98:3261-3273.

63.   Zhang J, Socolovsky M, Gross AW, Lodish HF. Role of Ras signaling in erythroid differentiation of mouse fetal liver cells: functional analysis by a flow cytometry-based novel culture system. Blood. 2003;102:3938-3946.

64.   Shinar E, Rachmilewitz EA. Differences in the pathophysiology of hemolysis of alpha- and beta-thalassemic red blood cells. Ann N Y Acad Sci. 1990;612:118-126.

65.   Nagy A, Rossant J, Nagy R, Abramow-Newerly W, Roder JC. Derivation of completely cell culture-derived mice from early-passage embryonic stem cells. Proc Natl Acad Sci U S A. 1993;90:8424-8428.

66.   Poueymirou WT, Auerbach W, Frendewey D, et al. F0 generation mice fully derived from gene-targeted embryonic stem cells allowing immediate phenotypic analyses. Nat Biotechnol. 2007;25:91-99.

67.   Carotta S, Pilat S, Mairhofer A, et al. Directed differentiation and mass cultivation of pure erythroid progenitors from mouse embryonic stem cells. Blood. 2004;104:1873-1880.

68.   Keller G, Kennedy M, Papayannopoulou T, Wiles MV. Hematopoietic commitment during embryonic stem cell differentiation in culture. Mol Cell Biol. 1993;13:473-486.

69.   Kina T, Ikuta K, Takayama E, et al. The monoclonal antibody TER-119 recognizes a molecule associated with glycophorin A and specifically marks the late stages of murine erythroid lineage. Br J Haematol. 2000;109:280-287.

70.   Neildez-Nguyen TM, Wajcman H, Marden MC, et al. Human erythroid cells produced ex vivo at large scale differentiate into red blood cells in vivo. Nat Biotechnol. 2002;20:467-472.

71.   Loken MR, Shah VO, Dattilio KL, Civin CI. Flow cytometric analysis of human bone marrow: I. Normal erythroid development. Blood. 1987;69:255-263.

72.   Scheid MP, Triglia D. Further Description of the Ly-5 System. Immunogenetics. 1979;9:423-433.

73.   Miller IJ, Bieker JJ. A novel, erythroid cell-specific murine transcription factor that binds to the CACCC element and is related to the Kruppel family of nuclear proteins. Mol Cell Biol. 1993;13:2776-2786.

74.   Eggan K, Akutsu H, Loring J, et al. Hybrid vigor, fetal overgrowth, and viability of mice derived by nuclear cloning and tetraploid embryo complementation. Proc Natl Acad Sci U S A. 2001;98:6209-6214.

75.   Lohmann F, Bieker JJ. Activation of Eklf expression during hematopoiesis by Gata2 and Smad5 prior to erythroid commitment. Development. 2008;135:2071-2082.

76.   Shaner NC, Campbell RE, Steinbach PA, Giepmans BN, Palmer AE, Tsien RY. Improved monomeric red, orange and yellow fluorescent proteins derived from Discosoma sp. red fluorescent protein. Nat Biotechnol. 2004;22:1567-1572.

77.   Shaner NC, Steinbach PA, Tsien RY. A guide to choosing fluorescent proteins. Nat Methods. 2005;2:905-909.

78.   Koury MJ, Koury ST, Kopsombut P, Bondurant MC. In vitro maturation of nascent reticulocytes to erythrocytes. Blood. 2005;105:2168-2174.

79.   Kent G, Minick OT, Volini FI, Orfei E. Autophagic vacuoles in human red cells. Am J Pathol. 1966;48:831-857.

80.   Lagasse E, Connors H, Al-Dhalimy M, et al. Purified hematopoietic stem cells can differentiate into hepatocytes in vivo. Nat Med. 2000;6:1229-1234.

81.   Wittenberg JB, Wittenberg BA. Myoglobin function reassessed. J Exp Biol. 2003;206:2011-2020.

82.   Furuyama K, Kaneko K, Vargas PD. Heme as a magnificent molecule with multiple missions: heme determines its own fate and governs cellular homeostasis. Tohoku J Exp Med. 2007;213:1-16.

83.   Dailey HA, Fleming JE. Bovine ferrochelatase. Kinetic analysis of inhibition by N-methylprotoporphyrin, manganese, and heme. J Biol Chem. 1983;258:11453-11459.

84.   Poulson R, Polglase WJ. The enzymic conversion of protoporphyrinogen IX to protoporphyrin IX. Protoporphyrinogen oxidase activity in mitochondrial extracts of Saccharomyces cerevisiae. J Biol Chem. 1975;250:1269-1274.

85.   Rossi E, Attwood PV, Garcia-Webb P, Costin KA. Inhibition of human lymphocyte ferrochelatase activity by hemin. Biochim Biophys Acta. 1990;1038:375-381.

86.   Crosby JS, Lee K, London IM, Chen JJ. Erythroid expression of the heme-regulated eIF-2 alpha kinase. Mol Cell Biol. 1994;14:3906-3914.

87.   Shaw GC, Cope JJ, Li L, et al. Mitoferrin is essential for erythroid iron assimilation. Nature. 2006;440:96-100.

88.   Hentze MW, Muckenthaler MU, Galy B, Camaschella C. Two to tango: regulation of Mammalian iron metabolism. Cell. 2010;142:24-38.

89.   Zhang DL, Hughes RM, Ollivierre-Wilson H, Ghosh MC, Rouault TA. A ferroportin transcript that lacks an iron-responsive element enables duodenal and erythroid precursor cells to evade translational repression. Cell Metab. 2009;9:461-473.

90.   Ryter SW, Kim HP, Hoetzel A, et al. Mechanisms of cell death in oxidative stress. Antioxid Redox Signal. 2007;9:49-89.

91.   Gatidis S, Foller M, Lang F. Hemin-induced suicidal erythrocyte death. Ann Hematol. 2009;88:721-726.

92.   Schrier SL, Centis F, Verneris M, Ma L, Angelucci E. The role of oxidant injury in the pathophysiology of human thalassemias. Redox Rep. 2003;8:241-245.

93.   Lang KS, Roll B, Myssina S, et al. Enhanced erythrocyte apoptosis in sickle cell anemia, thalassemia and glucose-6-phosphate dehydrogenase deficiency. Cell Physiol Biochem. 2002;12:365-372.

94.   Chen CS, Gee KR. Redox-dependent trafficking of 2,3,4,5, 6-pentafluorodihydrotetramethylrosamine, a novel fluorogenic indicator of cellular oxidative activity. Free Radic Biol Med. 2000;28:1266-1278.

95.   Tanaka H, Matsumura I, Ezoe S, et al. E2F1 and c-Myc potentiate apoptosis through inhibition of NF-kappaB activity that facilitates MnSOD-mediated ROS elimination. Mol Cell. 2002;9:1017-1029.

96.   Carter WO, Narayanan PK, Robinson JP. Intracellular hydrogen peroxide and superoxide anion detection in endothelial cells. J Leukoc Biol. 1994;55:253-258.

97.   Rothe G, Valet G. Flow cytometric analysis of respiratory burst activity in phagocytes with hydroethidine and 2',7'-dichlorofluorescin. J Leukoc Biol. 1990;47:440-448.

98.   Hunefeld FL. Der Chemismus in der tierescher. Organization. Leipsic; 1840:160.

99.   Robb L, Lyons I, Li R, et al. Absence of yolk sac hematopoiesis from mice with a targeted disruption of the scl gene. Proc Natl Acad Sci U S A. 1995;92:7075-7079.

100.   Shivdasani RA, Mayer EL, Orkin SH. Absence of blood formation in mice lacking the T-cell leukaemia oncoprotein tal-1/SCL. Nature. 1995;373:432-434.

101.   Fujiwara Y, Browne CP, Cunniff K, Goff SC, Orkin SH. Arrested development of embryonic red cell precursors in mouse embryos lacking transcription factor GATA-1. Proc Natl Acad Sci U S A. 1996;93:12355-12358.

102.   Mucenski ML, McLain K, Kier AB, et al. A functional c-myb gene is required for normal murine fetal hepatic hematopoiesis. Cell. 1991;65:677-689.

103.   Wickramasinghe SN, Hughes M, Wasi P, Fucharoen S. Morphology and kinetics of erythropoiesis in haemoglobin H disease. Br J Haematol. 1981;49:185-188.

104.   Schrier SL, Rachmilewitz E, Mohandas N. Cellular and membrane properties of alpha and beta thalassemic erythrocytes are different: implication for differences in clinical manifestations. Blood. 1989;74:2194-2202.

105.   Voon HP, Wardan H, Vadolas J. Co-inheritance of alpha- and beta-thalassaemia in mice ameliorates thalassaemic phenotype. Blood Cells Mol Dis. 2007;39:184-188.

106.   Beauchemin H, Blouin MJ, Trudel M. Differential regulatory and compensatory responses in hematopoiesis/erythropoiesis in alpha- and beta-globin hemizygous mice. J Biol Chem. 2004;279:19471-19480.

107.   Pootrakul P, Sirankapracha P, Hemsorach S, et al. A correlation of erythrokinetics, ineffective erythropoiesis, and erythroid precursor apoptosis in thai patients with thalassemia. Blood. 2000;96:2606-2612.

108.   Papassotiriou I, Kanavakis E, Stamoulakatou A, Kattamis C. Tissue oxygenation in patients with hemoglobinopathy H. Pediatr Hematol Oncol. 1997;14:323-334.

109.   Benesch RE, Ranney HM, Benesch R, Smith GM. The chemistry of the Bohr effect. II. Some properties of hemoglobin H. J Biol Chem. 1961;236:2926-2929.

110.   Pevny L, Simon MC, Robertson E, et al. Erythroid differentiation in chimaeric mice blocked by a targeted mutation in the gene for transcription factor GATA-1. Nature. 1991;349:257-260.

111.   Simon MC, Pevny L, Wiles MV, Keller G, Costantini F, Orkin SH. Rescue of erythroid development in gene targeted GATA-1- mouse embryonic stem cells. Nat Genet. 1992;1:92-98.

112.   Levy JE, Jin O, Fujiwara Y, Kuo F, Andrews NC. Transferrin receptor is necessary for development of erythrocytes and the nervous system. Nat Genet. 1999;21:396-399.

113.   Rivella S, May C, Chadburn A, Riviere I, Sadelain M. A novel murine model of Cooley anemia and its rescue by lentiviral-mediated human beta-globin gene transfer. Blood. 2003;101:2932-2939.

114.   Na Nakorn T, Traver D, Weissman IL, Akashi K. Myeloerythroid-restricted progenitors are sufficient to confer radioprotection and provide the majority of day 8 CFU-S. J Clin Invest. 2002;109:1579-1585.

115.   Flygare J, Karlsson S. Diamond-Blackfan anemia: erythropoiesis lost in translation. Blood. 2007;109:3152-3154.

116.   Borsook H. The change of hemoglobin synthesis from minor to major in the course of erythroblast maturation. Ann N Y Acad Sci. 1968;149:416-422.

117.   Chasis JA, Mohandas N. Erythroblastic islands: niches for erythropoiesis. Blood. 2008;112:470-478.

118.   Kovtunovych G, Eckhaus MA, Ghosh MC, Ollivierre-Wilson H, Rouault TA. Dysfunction of the heme recycling system in heme oxygenase 1 deficient mice: effects on macrophage viability and tissue iron distribution. Blood. 2010.

119.   Sadahira Y, Mori M. Role of the macrophage in erythropoiesis. Pathol Int. 1999;49:841-848.

120.   Sadahira Y, Yasuda T, Yoshino T, et al. Impaired splenic erythropoiesis in phlebotomized mice injected with CL2MDP-liposome: an experimental model for studying the role of stromal macrophages in erythropoiesis. J Leukoc Biol. 2000;68:464-470.

121.   Sheftel AD, Kim SF, Ponka P. Non-heme induction of heme oxygenase-1 does not alter cellular iron metabolism. J Biol Chem. 2007;282:10480-10486.

122.   Harigae H, Nakajima O, Suwabe N, et al. Aberrant iron accumulation and oxidized status of erythroid-specific delta-aminolevulinate synthase (ALAS2)-deficient definitive erythroblasts. Blood. 2003;101:1188-1193.

123.   Mendel A, Santos D, Ponka P. Investigation of the role of heme oxygenase-1 in β-thalassemia pathophysiology. McGill Science Undergraduate Research Journal. 2009;4:20-24.

124.   Han AP, Fleming MD, Chen JJ. Heme-regulated eIF2alpha kinase modifies the phenotypic severity of murine models of erythropoietic protoporphyria and beta-thalassemia. J Clin Invest. 2005;115:1562-1570.

125.   Grayzel AI, Fuhr JE, London IM. Effects of inhibitors of protein synthesis on the synthesis of heme in rabbit reticulocytes. Biochem Biophys Res Commun. 1967;28:705-710.

126.   Tavassoli M, Crosby WH. Fate of the nucleus of the marrow erythroblast. Science. 1973;179:912-913.

127.   Lichtman MA, Santillo P. Red cell egress from the marrow: ? vis-a-tergo. Blood Cells. 1986;12:11-23.

128.   Tavassoli M. Red cell delivery and the function of the marrow-blood barrier: a review. Exp Hematol. 1978;6:257-269.

129.   Waugh RE, Sassi M. An in vitro model of erythroid egress in bone marrow. Blood. 1986;68:250-257.

130.   Weiss L. The structure of bone marrow. Functional interrelationships of vascular and hematopoietic compartments in experimental hemolytic anemia: an electron microscopic study. J Morphol. 1965;117:467-537.

131.   Leblond PF, LaCelle PL, Weed RI. Cellular deformability: a possible determinant of the normal release of maturing erythrocytes from the bone marrow. Blood. 1971;37:40-46.
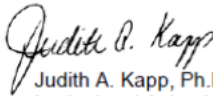
132.   Dintenfass L. Molecular and Rheological Considerations of the Red Cell Membrane in View of the Internal Fluidity of the Red Cell. Acta Haematol. 1964;32:299-313.

133.   Reinhart WH, Chien S. Roles of cell geometry and cellular viscosity in red cell passage through narrow pores. Am J Physiol. 1985;248:C473-479.

134.   Rovera G, Abramczuk J, Surrey S. The effect of hemin on the expression of beta globin genes in friend cells. FEBS Lett. 1977;81:366-370.

135.   Levasseur DN, Ryan TM, Pawlik KM, Townes TM. Correction of a mouse model of sickle cell disease: lentiviral/antisickling beta-globin gene transduction of unmobilized, purified hematopoietic stem cells. Blood. 2003;102:4312-4319.

136.   Evans MJ, Kaufman MH. Establishment in culture of pluripotential cells from mouse embryos. Nature. 1981;292:154-156.

137.   Nagy A, Gertsenstein M, Vintersten K, Behringer R. Manipulating the Mouse Embryo: A Laboratory Manual. Third Edition. p388-389. 2002.

138.   Zhou D, Ren JX, Ryan TM, Higgins NP, Townes TM. Rapid tagging of endogenous mouse genes by recombineering and ES cell complementation of tetraploid blastocysts. Nucleic Acids Res. 2004;32:e128.

139.   Warming S, Costantino N, Court DL, Jenkins NA, Copeland NG. Simple and highly efficient BAC recombineering using galK selection. Nucleic Acids Res. 2005;33:e36.

140.   Hardouin N, Nagy A. Gene-trap-based target site for cre-mediated transgenic insertion. Genesis. 2000;26:245-252.

141.   Koller BH, Kim HS, Latour AM, et al. Toward an animal model of cystic fibrosis: targeted interruption of exon 10 of the cystic fibrosis transmembrane regulator gene in embryonic stem cells. Proc Natl Acad Sci U S A. 1991;88:10730-10734.

142.   Sassa S. Sequential induction of heme pathway enzymes during erythroid differentiation of mouse Friend leukemia virus-infected cells. J Exp Med. 1976;143:305-315.

APPENDIX: IACUS APPROVAL FORM

THE UNIVERSITY OF ALABAMA AT BIRMINGHAM

Institutional Animal Care and Use Committee (IACUC)
NOTICE OF APPROVAL

DATE: June 4, 2010

TO: Ryan, Thomas M.
            KAUL 566A 0024
            996-2175

FROM: *Judith A. Kapp*
            Judith A. Kapp, Ph.D., Chair
            Institutional Animal Care and Use Committee

SUBJECT: Title: Cell Therapies for Cooley's Anemia
            Sponsor: NIH
            Animal Project Number: 100508769

On June 4, 2010, the University of Alabama at Birmingham Institutional Animal Care and Use Committee (IACUC) reviewed the animal use proposed in the above referenced application. It approved the use of the following species and numbers of animals:

Species	Use Category	Number in Category
Mice	C	137
Mice	B	602
Mice	A	3702

Animal use is scheduled for review one year from May 2010. Approval from the IACUC must be obtained before implementing any changes or modifications in the approved animal use.

Please keep this record for your files, and forward the attached letter to the appropriate granting agency.

Refer to Animal Protocol Number (APN) 100508769 when ordering animals or in any correspondence with the IACUC or Animal Resources Program (ARP) offices regarding this study. If you have concerns or questions regarding this notice, please call the IACUC office at 934-7692.